Visual Techniques for Geological Fieldwork Using Mobile Devices

Christian Kehl

Thesis for the degree of philosophiae doctor (PhD)
at the University of Bergen

2017

Date of defence: 06.10.2017

Figure 1: The major workflow outlined in this dissertation: by using visual techniques on mobile devices in the field, geologists can create digital outcrop interpretations on geological units(top). The outcrop itself can be transformed into a volumetric object (mid), and together with the interpretations also as gridded volumes (bottom). These are subsequently used as multiple point statistics training images for stochastic hydrocarbon reservoir modelling.

Preface

This dissertation has been submitted for the degree of philosophiae doctor (PhD) at the Faculty of Mathematics and Natural Sciences (Department of Earth Science) at the University of Bergen, Norway. The research presented in this thesis was conducted between October 2014 and April 2017 as part of the VOM2MPS project, funded by the FORCE consortium and the Research Council of Norway (RCN) (Petromaks 2 project 234111/E30) and under support of the "Sedimentary Architecture of Field Analogues" (SAFARI) phase III consortium (`www.safaridb.com`). Fieldwork and conference attendances at the International Society for Photogrammetry and Remote Sensing (ISPRS) congress, 3D NordOst workshops, and the 2nd Virtual Geoscience Conference (VGC) were funded by the referred parties, whereas the attendance at the American Association of Petroleum Geologists (AAPG) Annual Convention and Exhibition (ACE) 2016 was funded by the Statoil Akademia program. Further attendance at the EUROGEO conference 2015 and the International Supercomputing Conference (ISC) 2015 where covered by the candidate himself, which are not included in the VOM2MPS project.

The research is a collaborative study at Uni Research AS Centre for Integrated Petroleum Research (Uni Research AS CIPR, Norway), where the largest parts of the work was conducted, the University of Bergen (UiB, Norway), the University of Aberdeen (UoA, UK), the Technical University of Vienna (TU Vienna, Austria), the "Centre de Recherche et d'Enseignement de Géosciences de l'Environnement" (CEREGE, France) and the Université Aix-Marseille (AMU, France), where the candidate conducted research within an extensive visit during the final year of the PhD candidacy. Within this frame, the candidate was supervised by Dr. Simon John Buckley (Uni Research AS CIPR) as project leader and daily supervisor, Professor Robert Leslie Gawthorpe (University of Bergen) as department supervisor, Professor John Anthony Howell (University of Aberdeen, Department of Geology and Petroleum Geology) and Professor Ivan Viola (TU Vienna, Institute for Computer Graphics and Algorithms). The final part of the candidacy and research was supervised by Dr. Sophie Viseur (Sedimentary and Reservoir Systems, CEREGE, Aix-Marseille Université). Parts of the scientific education were covered during previous research appointments at the Technical University of Delft (TU Delft, the Netherlands) and the University of Amsterdam (UvA, the Netherlands) between March 2012 and October 2014.

This scientific paper-based thesis is separated into three main sections: the introduction to the topic, the submission-ready drafts and scientific articles (main section), and a final synthesis of the work in the form of a discussion. The appendices are to be taken into consideration as they give further insight for topics covered in the thesis, in particular the discussions. They contain the full version or, for brevity of the dissertation, extended summaries of published research related to the overall thesis

topic in form of academic articles, extended abstracts and presented research posters. This is in accordance with the doctoral dissertation style in Norway. The introduction provides academic- and application-driven motivations for the research topic and the formal background information, as well as a state-of-the-art technological overview. It defines the main research objectives and states the major research questions to be addressed by this dissertation. The second part contains two submission-ready paper drafts and four scientific papers that are published, in-press or submitted for publication to international, peer-reviewed journals. The final chapter discusses the research presented in the main articles, as well as the further scientific contributions towards the research topic given in the appendices, with respect to the major research questions. It presents technical, engineering and theoretic-scientific limitations experienced during the research, relates to further applications of the developed algorithms and computational approaches within the geosciences, and introduces some potential extensions and near-future developments that benefit from the conducted research in this thesis.

Contents

Acknowledgements

I would like to thank my supervisors Dr. Simon John Buckley, Prof. John Anthony Howell, Prof. Robert Leslie Gawthorpe and Prof. Ivan Viola for providing me with the opportunity of the Ph.D. studies leading up to this dissertation and for securing the candidacy funding for my regular income during that period.

Moreover, I am indebted to Dr. Jan Tveranger for his great introductions and geological explanations provided in form of formal courses (e.g. Advanced Petroleum Geology and Applied Reservoir Modelling) as well as informal office- and cigarette-break discussions. You always managed to target your explanations to the right level of understanding so that I was actually able to continuously build up knowledge from the given explanations. Furthermore, I want to thank you for inspiring me on cutting-edge and future topics in geology and energy, such as fault facies, CO_2 storage, geothermal energy, and the interesting discussions on future geomodelling techniques.

Although being commonly very distant in every aspect to the usual environment and mindset of the research institute and my environment in Norway, I had the privilege of some great companionship with my former Ph.D. candidate colleagues and office mates. I thus thank Christian Eide, Björn Nyberg, Luisa Zuluaga, Dongfang Qu, Alina Astrakova and Audun Libak for the discussion and sharing the "ups and downs" of Ph.D. candidacy and also, together with Benjamin Dolva, for the occasionally-occurring, pleasant after-work activities during my stay in Bergen. Your companionship and general advices were invaluable.

I'd also extend my gratitude for companionship to my Ph.D. colleagues from the SAFARI III project: Eva, Luca and James. The fieldwork time with you all in Whitby was exceptionally funny and a great experience. Eva - thank you for dragging me out of the North Sea when the tide swept my feet away! And I particularly appreciate the knowledge and opinion exchange with you, James, over e-mail. Our conversations laid the foundation for some of the future concepts explained in the discussion section of this thesis.

During my final year of candidacy, I stayed in Marseille (France), where I got to know many new, open-minded colleagues at CEREGE and AMU. I thank you all: Julia, Christophe, Justine, Dawin, Cécile, Johan, Juliette, Baptiste and the other colleagues at CEREGE. You let me, as an outsider and temporary visitor, into your group and invited me to the many social activities I have been missing for a long time. Having you as my colleagues made the end of my Ph.D. studies brighter – a pleasant, amazing experience. Et, enfin, je suis désolé – pardonnez-moi pour mon niveau limité de français. J'espère que le temps passé ensemble etait aussi agréable pour vous que pour moi.

A special thanks goes to Dr. Sophie Viseur for inviting me to Marseille, CEREGE and AMU. You invited me just as-is into the group and without any further precondition. You helped me organising my stay in France and handled problems asso-

ciated with the french administration system – stories best reminded by Goscinny and Uderzo's "Asterix Conquers Rome" and the way to obtain permits and official documents in France. You provided me with so much helpful guidance and supervision I could not have hoped for or anticipated beforehand. All the guidance and encouragement helped me find the way "back on the right track" for a fruitful, academic future. Your feedback on the structure and content of this dissertation have been insightful and essential to its quality improvement, as well as supportive in the understanding of details in geostatistical reservoir modelling. For all this, I am in debt and I hope for several future, great collaborations and shared projects. Merci beaucoup, pour tous!

This thesis is just the merit end of a considerably long journey within science that had its beginning back in March 2011. The path was all but straight, with some bends that I managed and some that I didn't, and with up's and down's ever since. It is therefore that I want to extend my gratitude to all the great mentors and supervisors that I had the privilege to meet and learn from over the years.

I thank Claus B. Madsen for inviting and welcoming me to Aalborg and integrating me into the VGIS group of 2011. I will always remember the honest and warm welcome I received from day 1 arriving in Aalborg. Although I left towards the Netherlands after the semester for the master thesis, I am glad that we maintain the contact over the years. I would be happy to come back once more to Aalborg in the future to rejuvenate the fine experience.

I also thank Olivier Hoes. In my academically hardest time at the TU Delft, you continued your support for my work and helped me to establish some new connections in the Netherlands after my unfortunate academic dismissal. I value your trust, your loyalty and the open expression of your opinion on science, research and life in the Netherlands.

Additionally, I thank Gerwin de Haan for providing me with the initial junior research position and the introduction to the scientific environment at Delft. I am sorry for some rather ungentle forms of criticism I initially offered. I think our collaboration would have worked out well in the end, would it not have been for the internal changes in 2012 and 2013.

I am indebted to Charl P. Botha and Daniel Francois Malan. The two of you provided me with the chance to come to Delft, work on my master thesis and greatly expand on my initially meagre knowledge of geometry. Although the academic "in's and out's" I learned from you formed my current research interests, it was your both' advices on how to manage work and still maintain a cheering and enjoyable character off-work that contributed most to my personal development. I was a slow learner in that department, and I still have some way to go to reach your "Zen-like" view on life, but I promise to do my best. What I value most of all is the mutual trust and friendship that emerged from our collaboration.

I further thank Ana Lucia Varbanescu for the collaboration and friendship that emerged from our shared research during my time at the Universiteit van Amsterdam. It was fortunate to be your student in the HPC course in Delft, having the possibility to meet people that share the passion for parallel- and GPU computing. I was also lucky to afterwards collaborate with you on the project with *Beeld & Geluid*. It's sad that I couldn't extend my stay at the time, but I hope we have the chance to "put our heads together" in the future once again. Your straight-forward advices on how to handle supervisors, research, critical academic situations and how to evaluate oneself only made

this dissertation possible.

Finally, I want to express my immense gratitude to my mentor, Prof. Dr. rer. nat. Herbert Litschke. Our collaboration that began in 2007 – with me as the young, graphics-interested undergraduate student – developed over the years into a trusted colleague relationship. There is not enough space in one thesis section to thank you for all the advices, support, the great lab-assistance jobs and the furthering of my personal- and academic development in detail. Therefore, I thank you for having been my mentor in the past and for your continuous support after all the years. I hope we will still have many opportunities to meet up in Wismar and exchange ideas on cutting-edge topics in graphics and computer vision in the future.

I also want to thank all my friends outside academia – in "the real world" – that supported me over all the years, including the past years' Ph.D. candidacies. I know that the past years were difficult because I was always "the friend who's never there (physically)" due to my habit of changing my country-of-living in a frequency other people change their smartphones or minor personal belongings. It hurts me as much as you all to not see you as often as we all wish, but I hope for plenty opportunity for giving back the trust, the unconditional support, the heartship in the near future. Specifically, I want to thank Christian, Rike, Nicole, Oxana, Christoph and Daniela, and all my dear German friends; Sergej, Kolya, Sasha, Timofey, Masha; Ana, Gabriel, Sourena, Stojan, Olga, Mihai, Noeska, Marjolein and all my dutch (and Holland-inhabiting) friends. I want to thank Mahelet Solomon and Muhterem Küçükönder for their many motivational words that built me up during struggling Ph.D. times in Bergen.

My final words of gratitude go to my family - Werner, Marianne, Beate and Andreas. Standing alone is sometimes too much of a fight and it is always good to know one is never truly alone. Family is the backbone that allows to withstand and prevail despite the overwhelming troubles at times. It's good to have family support, and I am happy to have you.

Abstract

Visual techniques in general and 3D visualisation in particular have seen considerable adoption within the last 30 years in the geosciences and geology. Techniques such as volume visualisation, for analysing subsurface processes, and photo-coloured LiDAR point-based rendering, to digitally explore rock exposures at the earth's surface, were applied within geology as one of the first adopting branches of science. A large amount of digital, geological surface- and volume data is nowadays available to desktop-based workflows for geological applications such as hydrocarbon reservoir exploration, groundwater modelling, CO_2 sequestration and, in the future, geothermal energy planning. On the other hand, the analysis and data collection during fieldwork has yet to embrace this "digital revolution": sedimentary logs, geological maps and stratigraphic sketches are still captured in each geologist's individual fieldbook, and physical rocks samples are still transported to the lab for subsequent analysis. Is this still necessary, or are there extended digital means of data collection and exploration in the field ? Are modern digital interpretation techniques accurate and intuitive enough to relevantly support fieldwork in geology and other geoscience disciplines ? This dissertation aims to address these questions and, by doing so, close the technological gap between geological fieldwork and office workflows in geology.

The emergence of mobile devices and their vast array of physical sensors, combined with touch-based user interfaces, high-resolution screens and digital cameras provide a possible digital platform that can be used by field geologists. Their ubiquitous availability increases the chances to adopt digital workflows in the field without additional, expensive equipment. The use of 3D data on mobile devices in the field is furthered by the availability of 3D digital outcrop models and the increasing ease of their acquisition. This dissertation assesses the prospects of adopting 3D visual techniques and mobile devices within field geology.

The research of this dissertation uses previously acquired and processed digital outcrop models in the form of textured surfaces from optical remote sensing and photogrammetry. The scientific papers in this thesis present visual techniques and algorithms to map outcrop photographs in the field directly onto the surface models. Automatic mapping allows the projection of photo interpretations of stratigraphy and sedimentary facies on the 3D textured surface while providing the domain expert with simple-to-use, intuitive tools for the photo interpretation itself. The developed visual approach, combining insight from all across the computer sciences dealing with visual information, merits into the mobile device *Geological Registration and Interpretation Toolset* (GRIT) app, which is assessed on an outcrop analogue study of the Saltwick Formation exposed at Whitby, North Yorkshire, UK. Although being applicable to a diversity of study scenarios within petroleum geology and the geosciences, the particular target application of the visual techniques is to easily provide field-based outcrop inter-

pretations for subsequent construction of training images for multiple point statistics reservoir modelling, as envisaged within the VOM2MPS project.

Despite the success and applicability of the visual approach, numerous drawbacks and probable future extensions are discussed in the thesis based on the conducted studies. Apart from elaborating on more obvious limitations originating from the use of mobile devices and their limited computing capabilities and sensor accuracies, a major contribution of this thesis is the careful analysis of conceptual drawbacks of established procedures in modelling, representing, constructing and disseminating the available surface geometry. A more mathematically-accurate geometric description of the underlying algebraic surfaces yields improvements and future applications unaddressed within the literature of geology and the computational geosciences to this date. Also, future extensions to the visual techniques proposed in this thesis allow for expanded analysis, 3D exploration and improved geological subsurface modelling in general.

Statement of Authorship

The author of the thesis hereby declares that this thesis has been written solely by himself and without supplementary tools other than indicated in-text explicitly, by reference or footnote. The author declares that all figures, sketches and other pictorial information have been obtained or created by the author, unless otherwise indicated.

This dissertation is a paper-based thesis, for which the main section is composed of the collection of published, accepted or submitted articles. For textural brevity, the author of the thesis and head author of the papers is just referred to as *the author*. All mobile device photographs have been exclusively collected by the author, which is thus not further mentioned separately per paper. Furthermore, the software development leading to this thesis' mobile application results has been exclusively conducted by the author, which represents the major time consumption and practical contribution of the dissertation. This commonly uncredited code provides basic software library extensions for graphical display and computer vision (i.e. OpenSceneGraph and OpenCV) on mobile devices, without which the state-of-the-art visual approach of this thesis would have not been possible. The software implementation to the research period covered in this dissertation has been influenced to a minor degree by Simon J. Buckley. The graphical user interface design has been influenced by feedback from related parties (i.e. supervisors and project collaborators).

Paper 1 (chapter 4) is published in the double-blind peer-reviewed International Annals of Photogrammetry and Remote Sensing (IAPRS). The ideas leading up to the paper are in its majority contributed by the author and Simon J. Buckley, and have been refined in collaboration with John A. Howell, Robert L. Gawthorpe, Ivan Viola and Sophie Viseur. The lidar data collection of the Mam Tor dataset was conducted by Benjamin Dolva and Simon J. Buckley. The interpretations were done by the author. The lidar data collection of Bryggen was conducted by Benjamin Dolva and Simon J. Buckley. The paper has been written solely by the author. It was internally reviewed by Simon J. Buckley, Ivan Viola and Robert L. Gawthorpe to a major degree and John A. Howell to a minor degree. The paper has further been presented at the ISPRS XXIII Congress 2016 in Prague and received the award for the best paper amongst young researchers within ISPRS Commission II.

Paper 2 (chapter 5) is published in the Photogrammetric Record (PHOR). The ideas leading to this paper's contribution are solely contributed to the author, and have been minorly refined by Simon J. Buckley. The lidar data of Mam Tor are equal to paper 1. The photographic dataset of the Devil's Lane Canyon has been collected by Simon J. Buckley. The paper has been solely written by the author. It was internally reviewed by Simon J. Buckley and Sophie Viseur to a major degree and by Ivan Viola to a minor degree.

Paper 3 (chapter 6) is submitted for publication in the Photogrammetric Record

(PHOR) Special Issue of the Virtual Geoscience Conference (VGC) 2016. The paper is only remotely related to the accompanying extended conference abstract, which is hence appended separately. Instead, it extends the ideas of paper 2. The ideas leading to the paper are contributed by the author to a major degree and by Simon J. Buckley through former discussions to a minor degree. It further includes and concludes commentary feedback on the software usability by James R. Mullins and John A. Howell. The lidar data of Mam Tor are equal to paper 1. The paper has been solely written by the author. It was internally reviewed by Simon J. Buckley and Sophie Viseur.

Paper 4 (chapter 7) is submitted for publication in the AGU Books Special Issue of the EGU 2016 conference track '3D digital geological models: from terrestrial outcrops to planetary surfaces'. It is only remotely related to the accompanying conference abstract, which is hence appended separately. Instead, it is based on a field study conducted in 2015 at the Whitby coastline within the VOM2MPS and SAFARI III project group. The authorship of the paper is explicitly stated as shared first authorship as both first authors, Christian Kehl and James R. Mullins, contributed with ideas, literature review, research and writing in equal parts to the paper. Additionally, John A. Howell provided input to the geological content of the paper. The lidar data at Whitby were collected by Benjamin Dolva. The sedimentary logs were created and supplement geological data were collected by James R. Mullins. The paper was internally reviewed by Robert L. Gawthorpe and John A. Howell.

The papers and contributions of the appendices were created by the authors indicated in the authorlist. A detailed summary of their singular contributions is not provided. Unless otherwise indicated, the digital outcrop-aimed papers utilize the previously mentioned datasets of Bryggen and Mam Tor. Additional contributions are indicated in the related acknowledgements. Paper D and E are VOM2MPS-unrelated papers (as subsequently indicated in the list of publications), but contribute to the understanding of some future research directions and discussion explanations in chapter 8. Academic affiliations may differ in these cases.

List of Publications

This dissertation is based on the following, peer-reviewed publications:

1. **Christian Kehl**, Simon J. Buckley, Robert L. Gawthorpe, Ivan Viola, John A. Howell, *Direct Image-to-Geometry Registration Using Mobile Sensor Data*, ISPRS Annals of Photogrammetry, Remote Sensing and Spatial Information Science III(1), pp. 121-128, 2016.

2. **Christian Kehl**, Simon J. Buckley, Sophie Viseur, Robert L. Gawthorpe, John A. Howell, *Automatic Illumination-Invariant Image-to-Geometry Registration in Outdoor Environments*, The Photogrammetric Record 32(158), 2017.

3. **Christian Kehl**, Simon J. Buckley, Sophie Viseur, Robert L. Gawthorpe, James R. Mullins, John A. Howell, *Mapping Field Photos to Textured Surface Meshes Directly on Mobile Devices*, The Photogrammetric Record, submitted under manuscript ID PHOR-2017-01-1115, 15 January 2017; in second review after minor initial review (first decision).

4. ***Christian Kehl***, *James R. Mullins*, Simon J. Buckley, John A. Howell, Robert L. Gawthorpe, *Interpretation and mapping of geological features using mobile devices in outcrop geology – A case study of the Saltwick Formation, North Yorkshire, UK*, AGU Books, submitted under manuscript ID 2016-Dec-CH-0583, 09 December 2016.

The following publications are also related to this dissertation, located in the appendix:

1. **Christian Kehl**, Simon J. Buckley, John A. Howell, *Image-to-Geometry Registration on Mobile Devices - An Algorithmic Assessment*, Proceedings of the 18th 3D NordOst, ISBN 978-3-942709-14-9, pp. 17-26, 2015. (*scientific paper*)

2. Simon J. Buckley, **Christian Kehl**, James R. Mullins, John A. Howell, *Interpretation and mapping of geological features using mobile devices for 3D outcrop modelling*, European Geoscience Union (EGU) - Geophysical Research Abstracts 18, p. 16784, 2016. (*abstract*)

3. James R. Mullins, John A. Howell, **Christian Kehl**, Simon J. Buckley, *Virtual Outcrop Models to Multiple Point Statistics: Improved Reservoir Modeling Supported by Digital Field Computing*, American Association of Petroleum Geologists (AAPG) Annual Conference and Exhibition (ACE), 2016. (*peer-reviewed extended abstract, poster*)

4. **Christian Kehl**, James R. Mullins, Simon J. Buckley, Robert L. Gawthorpe, John A. Howell, Ivan Viola, Sophie Viseur, *Geological Registration and Interpretation Toolbox (GRIT): A Visual and Interactive Approach for Geological Interpretation in the Field*, Proceedings of 2nd Virtual Geoscience Conference, pp. 59-60, 2016. (*peer-reviewed extended abstract*)

5. **Christian Kehl** and Simon J. Buckley, *Automatic Image-to-Geometry Registration in Varying Illumination Conditions using Local Descriptors*, Proceedings of the 19th 3D NordOst, ISBN 978-3-942709-16-3, pp. 151-160, 2016. (*scientific paper*)

6. **Christian Kehl**, Dongfang Qu, James R. Mullins, Simon J. Buckley, Sophie Viseur, John A. Howell, Robert L. Gawthorpe, *Exploring Volumetric Data Using Interactive Statistical Views*, Proceedings of the 19th 3D NordOst, ISBN 978-3-942709-16-3, pp. 7-16, 2016. (*scientific paper*)

The following scientific contributions (i.e. articles, extended abstracts and posters) are only indirectly related to the thesis topic, researched outside the VOM2MPS and SAFARI III project frame, published during this Ph.D. studies and are located in the appendices:

1. **Christian Kehl** and Ana Lucia Varbanescu, *Towards Distributed, Semi-Automatic Content-Based Visual Information Retrieval (CBVIR) of Massive Media Archives*, International Supercomputing Conference (ISC), 2016. (*peer-reviewed extended abstract, poster*)

2. **Christian Kehl**, *Disseminating Large-Scale Semantic 3D Landscape Models Using Open Visualisation Platforms*, European Journal of Geography 6(2), pp. 51-68, 2015.

I

Chapter 1

Introduction

This introduction aims to give an overview on the research topic and its background covered in this thesis, which focuses on the integration of computational methods, algorithms and digital-visual techniques in field geology. It puts the research into context of the VOM2MPS project and its aims, and the connection to the SAFARI project. Established and prevalent principles within the published literature are introduced, which is important to the understanding of the starting point and the research objectives addressed by the thesis. The multidisciplinary nature of the research is explained and ambiguous terminology, emerging from the synthesis of the different disciplines, is resolved.

Additionally, introductory state-of-the-art literature overviews on digital facies- and interpretation mapping, mobile technologies in 3D visual applications and geological fieldwork give the reader an overview of existing techniques, software systems, workflows and technologies which this thesis aims to extend. Subsequently, research challenges are deduced from the project objectives and the state-of-the-art of the available technology. The data acquisition is explained and the geological setting of the datasets used in this thesis is briefly introduced in a dedicated section. As a final point of the introduction, the storyline of the presented research is given that serves as a guideline for the detailed reading of the main chapters and appendices.

1.1 Motivation

The research outlined in the thesis is part of the wider project "VOM2MPS: From virtual outcrop models to multiple point statistics training images for improved reservoir modelling". Numerical geocelluar models are of high value for the prospect assessment of subsurface hydrocarbon reservoirs (such as oil and natural gas [189,247]) as they describe the geological formation of the prospect. They are built for a specific target of the assessment, such as the distribution of porous media, the influence of sandbody connectivity as well as structural features (e.g. fractures and faults) on the hydrocarbon fluid flow, near-well flow analysis or the assessment of injector well placement for enhanced oil recovery (EOR). More recently, they are also used in research for analysing deep fractures for geothermal energy generation or for assessing large-scale formations over long timescales as CO_2 storages [134, 222, 248]. In the short term future, it is likely be used for assessing sealing properties of potential hazardous mineral repositories. Fig. 1.1 shows an example of a geological model for the Saltwick Formation,

built based on an outcrop near the town of Whitby (see chaper 7 for more information). A typical geomodelling workflow is depicted in fig. 1.2, based on Ringrose and Bentley [247] and adapted towards a multiple point statistics modelling scenario covered in this research. In the hydrocarbon exploration scenario, the focus is more often on the actual geobody distribution than on fluid flow concerns, as little is known of the geology in exploratory areas.

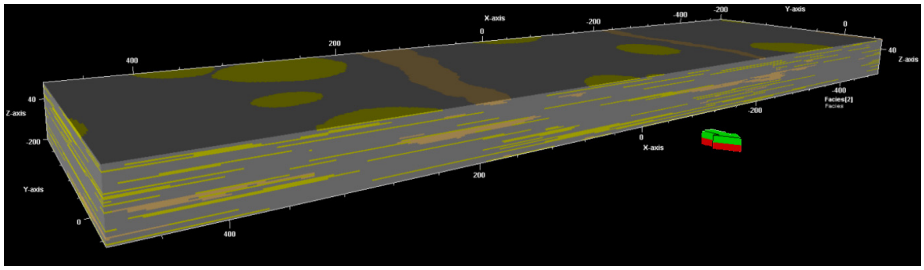

Figure 1.1: Illustration of a regular-gridded geocellular reservoir model of the Saltwick Formation, based on the Whitby cliff outcrop in chapter 7. Yellow areas depict crevasse splay, orange areas depict channel body facies and the grey surrounding represents the overburden.

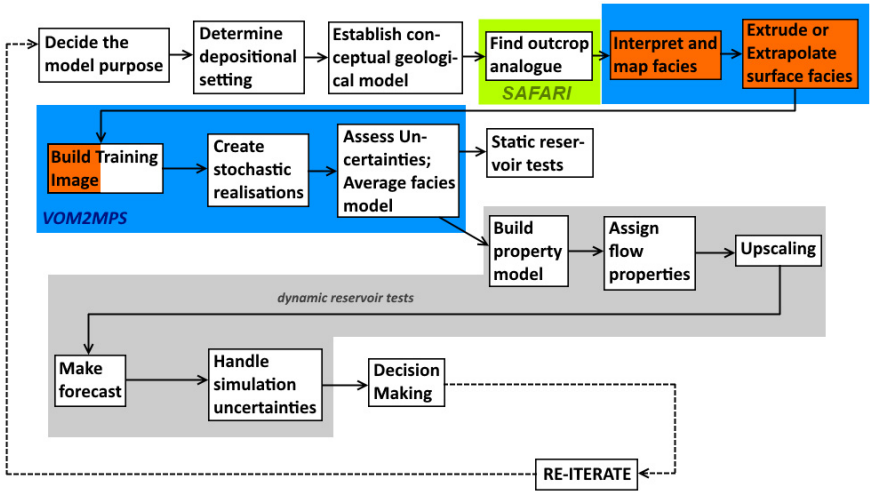

Figure 1.2: A simplified reservoir modelling workflow, modified from Ringrose and Bentley [247] to outcrop analogue studies using MPS.

Hydrocarbon reservoirs can be modelled by using characteristics and properties of rock exposure on the earth's surface. With the advance of computer technology over the past decades, in particular in 3D graphics thanks to the entertainment industry, these rock exposures are increasingly studied by digital means. Continuous improvements in remote sensing equipment makes such exposures digitally available to a larger audience in an increasing quantity. This digital, visual analysis distinctly depends on

knowledge from applied mathematics and computer sciences, as visible from the following sections in this thesis. The thesis focusses on making these analysis techniques for rock exposure (i.e. *digital outcrops*) available on modern, mobile devices to support fieldwork and geological reservoir modelling.

1.2 Related Work

1.2.1 Geostatistical reservoir modelling

Reservoir modelling utilizes knowledge, methods and tools from geostatistics to forecast the sedimentary layout, the lithological composition and the petrophysical properties of reservoirs.

A reservoir model is a 3D gridded, anisotropic, scalar value box (i.e. a scalar uniformal grid). Generally, constructing a reservoir model means to account for constraints introduced by primary data (i.e. *hard data*) and secondary data (i.e. *soft data*) during the scalar value (i.e. primary variable) prediction. Hard data are physical measurements of the target property, for example via wells, cores and sedimentary logs. A traditional example of soft data is trending functions defined by the modeller to describe geological constraints of shape and primary variable distribution based on the underpinning geological concept of a study area. They are also the means to express and incorporate geological expectations into the statistical modelling process. The distribution of the primary variable is constrained by the available, measured hard data, which can be realised with varying degrees of complexity depending on the specific modelling method. Applying hard data constraints to the model is termed *hard conditioning* or sometimes just *conditioning*.

Apart from the data conditioning and the distinction of predicting physically-continuous or discrete primary variables, there are further geostatistical principles to consider. The scale of the geological investigation controls the relationships and the fidelity of depositional elements and information to be included in the target model. The scale is a result of the target application case, as recently discussed and illustrated by Issautier et al. [134]. *Heterogeneity* is a modelling property related to the scale of the study and describes the variation detail between the modelled objects and facies. *Stationarity* is a key property of statistical methods which expresses that the joint probability (i.e. covariance) of data points depends on their relative position. It can hence be thought of as spatial dependency of the primary variable. Modelling methods essentially need to be non-stationary, meaning that the underlying statistical model (e.g. semivariogram, training image (TI) pattern) is valid as-is everywhere within the model. A recent discussion on the non-stationarity for object-based reservoir models is given by Allard et al. [6]. A final concept to consider, which is related to the data conditioning, is a trade-off between continuity and data resolution. As an example, seismic surveys provide a continuous description of the subsurface structure at the cost of per-sample (i.e. per-cell) resolution. On the other hand, sediment cores and well data provide (vertically) very high resolution information of the subsurface that is discontinuously sampled at sparse locations.

It is common practice for exploratory reservoirs to use stochastic simulations in the modelling process. Stochastic simulation procedures aim at generating several equi-

probable models that all fit the available hard data. The set of generated models corresponds to a representative sample of all possibilities, on which uncertainty analysis is performed [70, 110, 154, 189].

Several geostatistical methods are available for the task of indicator modelling. Pixel-based approaches predict the value of the primary variable from a continuous probability distribution function (PDF) on a per-cell basis individually. For models expressing physical quantities for fluid flow analysis, a prominent example of pixel-based modelling is sequential gaussian simulation (SGS) [71], while common methods for discrete indicator (e.g. facies) models include truncated gaussian simulation (TGS) [197]/plurigaussian simulation (PGS) and sequential indicator simulation (SIS) [71].

Object-based approaches distribute geometric shapes in 3D space which represent geological objects, such as channels, levees, crevasse splays [70] and point bars. The distribution itself, accommodating for geological adjacency rules, is controlled by their centroids (i.e. *marks*) and their relative positions, which are distributed in a Markov point process framework [282, 291]. Object-based modelling is well-known for applications in fluvial [118, 203] and fluvio-deltaic [70] depositional environments, such as for major reservoirs on the Norwegian Continental Shelf (NCS) [128]. Moreover, these approaches are conceptually accessible for geologists because it allows to easily and rapidly translate depositional concepts and knowledge into stochastic reservoir models.

Process-based approaches, in a strict interpretation of the concept, consider the forward modelling of geological processes. These approaches attempt to simulate the creation- or (de)formation of a geological environment and its constituting elements (e.g. stratigraphic layers, sedimentary geobodies and elements, structural objects of deformation) over time, as a results of geological processes (e.g. tectonics, deposition, erosion, aggradation and degradation). Available simulation approaches are physically based on Airy and Stokes wave theory [195, 196] or computational fluid dynamics (CFD) [124, 174] to model the sediment transport- and deposition processes for selected depositional environments (e.g. deltas, shorelines). FLUMY[1] is an approach to simulate the structure of complex meandering channel environments in 3D [185]. Process-based models represent the physically most accurate description of particular depositional environments.

Multiple point statistics (MPS) is a recent geostatistics simulation method that allows for an easy incorporation of measured data and a more faithful interpolation of unknown data locations that follows geological, conceptual constraints [247]. The method represents an attempt to merge pixel-based and object-based approaches. Pixel-based approaches uses a bivariate (i.e. point-to-point, two-point) data conditioning of a statistical model (e.g. *semivariogram*). MPS takes, in contrast to pixel-based approaches, training images as the basis for modelling. A TI is a 2D- or 3D gridded model (i.e. a scalar pixel- or voxel image) [283], similar to the target geomodel, which depicts joint probability, data patterns and local relationships between cells [114, 284]. In practice, unconditioned object-based models are often used as TIs for MPS [285, 286]. Alternatively, process-based models [59, 134, 205], high–resolution seismics [284], modern analogues [14, 60, 184], existing reservoir models [132] and computed tomography (CT)-

[1] FLUMY - Modèles génétiques de réservoirs chenalisés méandriformes - `www.geosciences.mines-paristech.fr/en/organization/presentation-of-the-group-2/main-projects/flumy?set_language=en`

scans of sediment cores [60] can be utilised as sources for MPS TIs. After providing a MPS algorithm with training images, the algorithm proceeds in a random walk [284] within the boundaries of the target model to populate cells with values based on the TI patterns. Therefore, at any given time, the target model contains cells that are to be evaluated and cells that have already been evaluated. When assessing a specific empty cell along the random walk, the neighbourhood of that cell represents the constraint pattern for the TI look-up. A collection of candidate patterns fitting the constraint are found in the TI, and the representative indicator amongst the candidates is chosen for filling the empty cell. The further the MPS simulation progresses with populating the target grid, the more constrained the TI look-up process is and the more deterministic each cell evaluation becomes. The process is illustrated in fig. 1.3 as a process flow, which is explained in detail in the original literature of the MPS method [114, 283, 284, 287]. The random walk-based grid population allows generating an arbitrary number of equiprobable resulting geomodels.

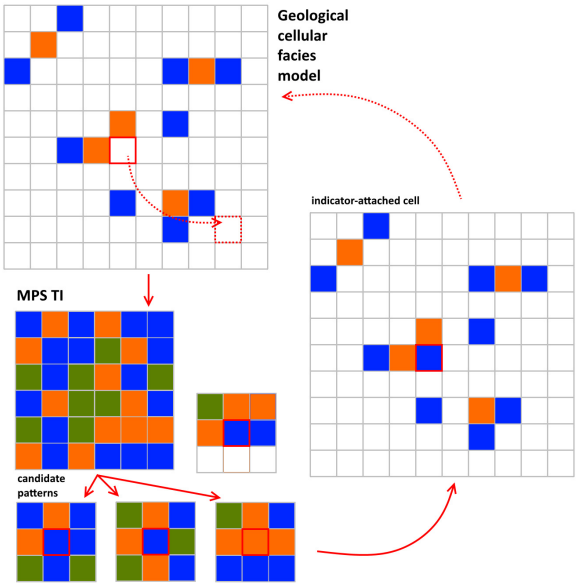

Figure 1.3: Illustration of the facies indicator population process using the MPS method.

A plethora of classifications and orders between the existing modelling techniques is available in the literature. Koltermann and Gorelick provide an original classification of the methods, mainly distinguishing between process-imitating and structure-imitating methods [154]. Ringrose and Bentley provide an alternative distinction between pixel-based, object-based and texture- (or: pattern) based methods [247]. Perrin et al. distinct between data-driven and concept-driven approaches for reservoir modelling [230]. The existing literature lacks consistency in the classification and the driving terminology. The reader is invited to select a terminology most appropriate to the specific application case. The terminology and classification in this thesis is most in-line with Ringrose and Bentley [247].

The major focus of the VOM2MPS project is to use outcrop analogues for MPS TI population, as previously proposed by several authors [125, 126, 232].

1.2.2 Digital outcrops

Outcrops are ”visible exposures of bedrock or ancient superficial deposits on earth’s surface“ [131]. They allow studying the structure and processes of geological formations, which are usually hidden beneath the earth’s surface, directly at the surface. Outcrop analogues are outcrops that share common properties or sediment deposition processes with the target subsurface geological formation [130]. As part of the SAFARI project, the constraint of outcrops for VOM2MPS is the sedimentary depositional architecture. It refers to the observation that geological formations from the same deposition environment share common architectural features. They are therefore related to one another, but the surface outcrop is easier to study and delivers geological information at a higher resolution than is obtainable from direct subsurface measurements, such as high-resolution seismics. Outcrops give more insight to the heterogeneity of a formation (as a result of the high-resolution observation), which has implications on some parts of the modelling workflow (e.g. upscaling, flow simulation, static reservoir tests).

A digital outcrop model (DOM) is a digital representation of the naturally occurring outcrop. It consist of a geometric representation of the outcrop’s shape and optionally a radiometric component of the colour from the visible light spectum. The digital representation can be a coloured point set [15, 127, 244, 246, 312], a digital elevation model (DEM) with photos attached as textures [138, 199] or textured surface models as triangulated irregular networks (TINs) [40, 129]. Examples of the different representations are shown in fig. 1.4(a) to 1.4(c). The adequate form of representation is dependent on the specific application cases. Procedures for the acquisition of DOMs are outlined in section 1.2.3.

(a) (b) (c)

Figure 1.4: The different types of digital outcrop model representations: points, DEMs and TINs (composed of multiple distinct sections, highlighted by the diverging colour codes).

The DOM is, within outcrop studies, the basis on which geological interpretations are created digitally. The interpretations themselves can be used to derive geobody statistics for object-based modelling [84, 88, 165, 252], where the resulting geocellular model is then taken as MPS TI. Other approaches make more direct use of the DOM by importing the point set-delineated facies into a reservoir modelling software package

such as Petrel, RMS or GoCAD to derive geocellular facies indicators for a TI. In this dissertation, the modelling workflow of Enge et al. [88] is taken as a starting point for proposed modelling extensions, meaning that the DOMs used in this work are textured surface models on which subsequent interpretations are performed. The geological interpretations, in terms of stratigraphy, structural layout, as well as sedimentary layout and composition via sedimentary facies, adheres to pre-defined classification schemes [203]. The adopted classification for the depositional architecture and depositional elements in this thesis follows the SAFARI standard [79, 130][2], although comparable outcrop databases with varying classifications have also previously been published [58, 304].

1.2.3 Acquisition of digital outcrop models

DOMs can be acquired in various ways. Xu et al. [316] and Bellian et al. [15, 16] introduced digital outcrop models for geological studies using terrestrial laser scanning (TLS) without photo attachment. The scanning itself was originally a time-consuming operation and supported limited scanning range setups, which has improved in recent years due to technical advances in manufacturing and miniaturization. The TLS acquisition is still very expensive and demands labour-intense postprocessing. The physical access of an outcrop study location to obtain an optimal surface model is also problematic in some cases. Further details on TLS acquisition challenges are provided by Buckey et al. [37] and Hodgetts et al. [125].

Early studies [199] used coarse-resolution, satellite-derived DEMs for outcrop studies via Google Earth or ArcGIS, which circumvents the physical access issue at the expense of the available model's accuracy. More recent studies use aerial [165]- and terrestrial [37, 125, 130, 239, 244] light detection and range (lidar), or a combination of both [246], for the DOM acquisition. In the combined acquisition cases, aerial methods fill in the data gaps of terrestrial lidar (i.e. TLS) that occur due to aforementioned scanning issues (e.g. outcrop access, scanning shadows, acquisition time). An expensive method of data collection remains Heli-lidar [36, 296], which allows capturing very large sections of outcrop terrain in a short amount of time from optimal scanning positions in a relatively high level of detail.

Current trends in the acquisition of DOMs are the photogrammetric reconstruction via structure from motion (SfM) from image collections [53] and the use of unmanned aerial vehicles (UAVs) [72] (i.e. *drones*) as cost-efficient, flexible and logistically simple alternative to Heli-lidar. Conducting UAV surveys has been complicated recently by the introduction of new legislative and administrative frameworks. The development is facilitated by precise and efficient multi-view point reconstruction algorithms [100, 101, 277], intuitive user interfaces [108, 314] and a general increase in computing power. The introduction of full-waveform lidar in previous years potentially presents a technical alternative to time-consuming manual laser postprocessing (e.g. vegetation removal). In the future, it is envisaged to capture DOMs using ubiquitously-available mobile devices, which is discussed in further detail in this dissertation.

The datasets used within this dissertation are DOMs structured as triangular polygonal soups as explained in section 1.3. They were acquired within the SAFARI pro-

[2] the SAFARI classification standard - `https://safaridb.com/#/standard`

ject according to previously-established workflows [35, 37, 40]. SAFARI is a database approach for the collection of hard and soft data for hydrocarbon reservoir modelling outcrop analogues, made available through a web portal (fig. 1.5). The research presented in this thesis makes use of previously interpreted DOMs [83, 87, 221, 250], where applicable.

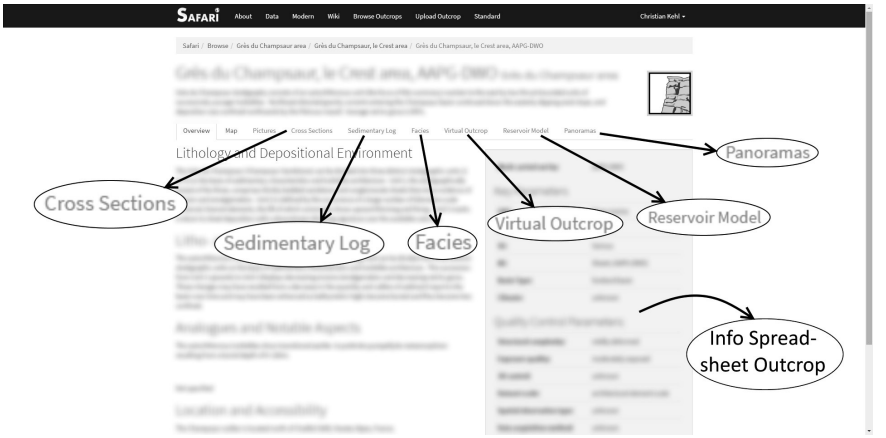

Figure 1.5: Image of a SAFARI database entry and the diversity of provided data options available to project members.

The utilised instrument for the data acquisition of digital outcrops is a Riegl VZ-1000 TLS, mounted with a Nikon D800E digital single lens reflex (DSLR) camera for the photo texturing. The DSLR lens configuration varies between the datasets (50-80 mm Nikkor prime lenses). As for the mobile technology and development, two devices were consistently used during the research studies: a Google Nexus 5 smartphone with an 8 megapixels camera and a NVIDIA Shield tablet (5 megapixels camera).

Sima [273] illustrated a de-facto standard workflow for DOM acquistion, as presented in fig. 1.6: First, a point set is recorded via TLS from a studied outcrop. Then, the DSLR photos are accurately registered to the point set, potentially by accurate camera mounting based on com-measurement of reflectors that are placed within the scene. Next, the point set is stripped from noisy point outliers and disturbing vegetation covering the outcrop. The clean point set is then triangulated into a polygonal mesh using PolyWorks Modeler[3]. Holes in the polygonal model, occurring due to scanning shadows and the vegetation removal, are closed with a combination of automatic and interactive (i.e. human-guided) procedures. The resulting polygonal surfaces are subsequently textured using optimal, semi-automatic texturing approaches by Sima et al. [272, 274, 276]. In a final post-processing step, geologists determine the regions of interest so that the surface model is pruned accordingly.

For the mobile device studies, the following workflow has been established, illustrated in fig. 1.7: Photos are primarily acquired using the Nexus 5 smartphone (unless indicated otherwise within the study) due to its higher resolution camera compared to

[3]InnovMetric PolyWorks - `http://www.innovmetric.com/en/products/polyworks-modeler`

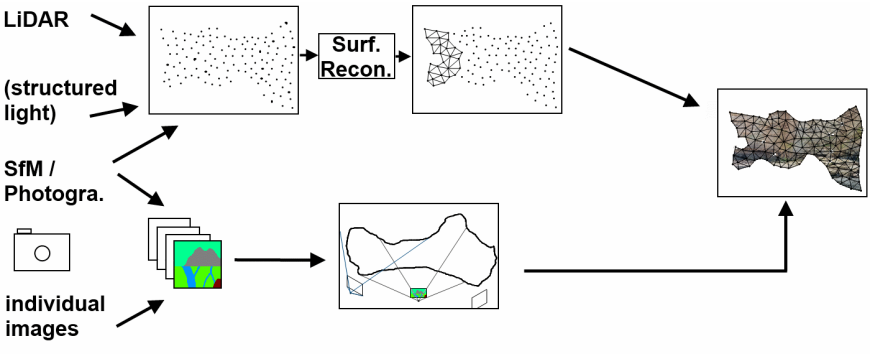

Figure 1.6: Illustrative process workflow for the construction of digital outcrops.

available tablets. Photo acquisition can be done with the NVIDIA tablet, but the behaviour of the standard Android camera interface differs between the devices, leading to issues with lens focussing with the NVIDIA device. More details on the problem's reasons can be found by the working principle of the "Frankencamera"[4] [1,175], which is the governing photo acquisition principle within Android. In addition to the visual consistency and high quality of photos, the smartphone also drains less battery than comparable tablets during constant photo acquisition. Subsequently, the photos and project files are shared with the tablet via cloud storage services (e.g. Google Drive), on which the 3D data reside.

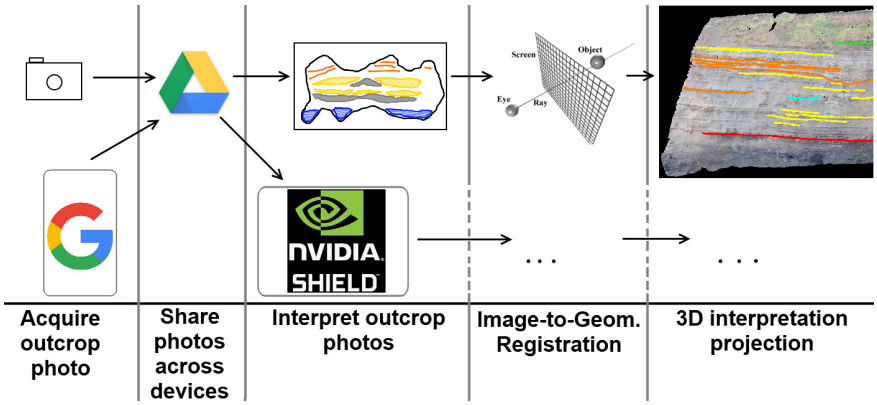

Figure 1.7: Illustrative process workflow for image acquisition, processing and mapping to surface geometry on mobile devices.

[4]The "Frankencamera" in computational photography - `http://graphics.stanford.edu/projects/camera-2.0/`

1.3 Multidisciplinary research & terminology

The research presented in this dissertation covers the disciplines of computer graphics, geomatics, computer vision, computational geosciences and various branches within the geosciences. It incorporates knowledge from the domains of discrete- and computational geometry, applied mathematics and virtual/augmented reality, and takes inspiration from machine learning and artificial intelligence (AI). Developing a research strategy to cover the mentioned disciplines, providing usable insight and tools as a research result, and still make particular scientific contributions to a specific discipline is not trivial. The diversity of this thesis' contribution is illustrated in fig. 1.8, where the position and attribution of the minor fields can be debated.

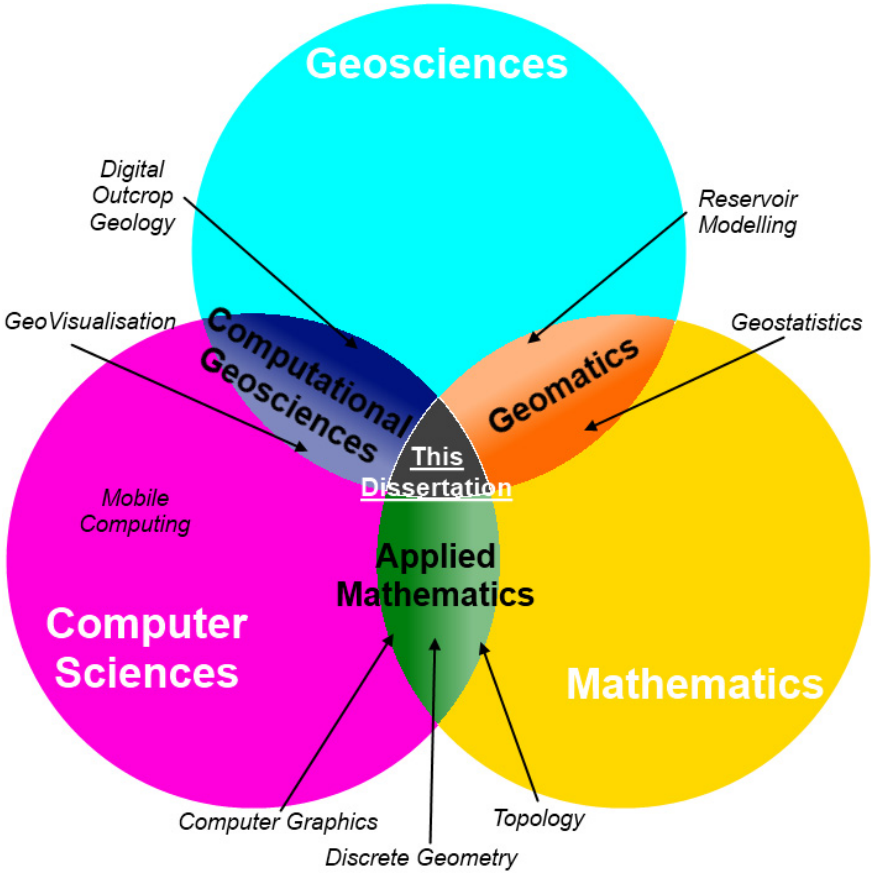

Figure 1.8: Contribution of the diverse scientific disciplines to this dissertation.

Due to this multidisciplinary nature, several terminology conflicts arise from the different perspectives and founding concepts between the constituting disciplines and domains. Therefore, we subsequently address the terminological differences and resolve existing ambiguities for a consistent definition within this thesis. While some terminologies are easily explained by a simple definition, some more abstract concepts

are explained in-text. Acronyms such as computer graphics (CG), computer-generated imagery (CGI), computer vision (CV), virtual reality (VR) and augmented reality (AR) are consistent across the following chapters. Further terms target specific application domain concepts and essential details, which need to be clarified for the understanding of the thesis. They also attempt to resolve common misconceptions about terms addressed in this dissertation.

1.3.1 Terminology and concepts within geology

The creation of geological models is the target application for the methods and techniques developed here. In this context of geological, volumetric cellular modelling in subsequent chapters, the term of **object** refers to geological heterogeneous units within the model, which is represented by the same indicator attributes for the constituting cells.

Stratigraphy

The concept of stratigraphy is key to the geological observation of outcrops. It is an abstract concept referring to different specific expressions. In sedimentology, stratigraphy generally refers to the layered succession of rock (*strata*) observable in outcrops, the processes that led to the layering, and the major information used to distinct the individual layers. Boggs describes the strata (i.e. rock *beds*) as "tabular or lenticular layers of sedimentary rock that have lithological, textural or structural unity that *clearly distinguishes them* from stata below and above" ([23], p. 65). Although already referring to the different types of stratigraphy, the major points are that (a) each strata is distinct in one or more aspects to its environment, (b) stratification is the process or scheme that organises the layer distinction (i.e. it formalises the coherent aspect of distinction), and (c) stratification is a vertically-oriented concept, with the exception that structural changes may tilt or fold the previously vertical organisation into different orientations.

Biostratigraphy distinguishes the layered rock succession by their biological content and the distribution of fossils in various geological formations [23]. Biological content refers in this context to roots and fossils enclosed in the rock succession. The evolution of organisms allows a time-based ordering and dating of a studied succession. Moreover, based on paleontological knowledge it is possible to attribute a given strata with a depositional environment (e.g. deep marine, shallow marine, terrestrial), which simplifies further sedimentological studies of the depositional architecture.

Lithostratigraphy describes the strata on the basis of their physical rock composition, such as mineral composition, their optical properties (e.g. colour) and grain attributes (e.g. size and order). Observing and documenting lithostratigraphy is for some cases very simple to conduct (e.g. on outcrops with diverging minerology and colourful reflection patters), but gets increasingly difficult with thin sediment layers or carbonate rocks, which often provide little visual information for their distinction.

Chronostratigraphy distinguishes the rock layers based on their geological age. This can be done by interpreting the layers and reconstructing the structural history of a formation to the time of its deposition, or by measuring the rock via geochronometry [23].

Facies

Facies is an abstract concept that is flexibly used within geology. The available literature is fuzzy with respect to a consistent definition of the term. There are different definitions targeting different rock properties, e.g. sedimentary facies, fault facies, diagenetic facies. This thesis, in its majority, treats sedimentary facies. A. Coe provides a definition of sedimentary facies, applicable to our case, which also extends to the design and development of visualisation techniques for sedimentology. She defines sedimentary facies as rock bodies with similar composition, texture fossils and sedimentary structures that represent a particular process or depositional condition ([57], p.127). This also reflects the interpretation and classification aim of structures originating from similar depositional processes [204] used within SAFARI [79]. Alternative declarations are provided by Middleton et al. [206]. Fig. 1.9 illustrates the difference between *objects* and *facies* with respect to geomodelling.

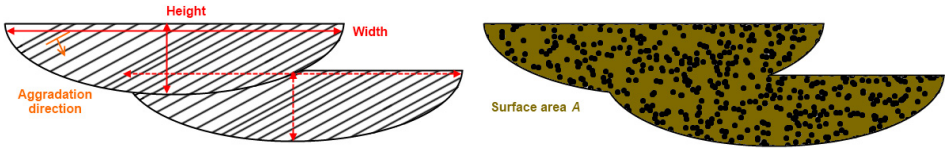

(a) Object Mapping (b) Facies Mapping

Figure 1.9: Illustration of the difference between object- and facies mapping on the example of two channel cross-sections that exhibit the same lithological composition.

Facies mapping is not only used for sedimentological cases. Recent developments lead to the development of fault facies to describe finer heterogeneous features, such as lenticular fault cores and deformation bands, within fault zones [34,97,294]. This fault facies description finds its application in the improved description of fault zones within reservoirs, which are still predominantly modelled as impenetrable or homogeneously-transmissive planar rock displacements. This way of modelling contradicts field observations of fault zones, which are highly heterogeneous. Recent studies [91, 240, 241] have shown improvements in flow predictions when replacing a planar-modelling fault with a volumetric fault facies description of the fault zone.

Conclusion for geological visualisation

Rey provides a good distinction between stratigraphic- and facies concepts [245]. In technical terms, the characteristic properties of segmented sedimentary facies and stratigraphy can be expressed by an indicator function for each surface element of a DOM $f(x) \in \mathbb{N} \quad \forall x \in V \cup T$, where V denotes the set of vertices and T denotes the set of triangles of a DOM. In this case, the described attribute can delineate rock regions, composition fluctuations, sediment depositional elements and the background fill material (which is referred to as *overburden* in subsurface reservoirs). In terms of visualisation, the indicators represent categories and the facies themselves are hence spatially-bound areas associated to a category. The spatially-bound area can be also represented by closed geometry surfaces at the outcrop and an attached indictor, hence

a 2D- or 3D object with a scalar attribute. The facies mapping is a result of geological observation and interpretation that is based on the following visual criteria:

- rock hue (colour) and saturation
- texture- and surface irregularities, such as cleavage and fossils
- ridges and scratches

”Texture” in this context relates to the fine-grained surface shape and roughness and not, as in the rest of this dissertation, to the mapped images on surface geometry. Sedimentary facies, although visually similar to depositional elements, are not the same as depositional elements (i.e. objects) as the former only describes areas of similar lithology while the latter describes the full element geometry that potentially encloses multiple facies. This distinction can be seen on the example outcrop photo interpretation by Johnston et al. in fig. 1.10 [136].

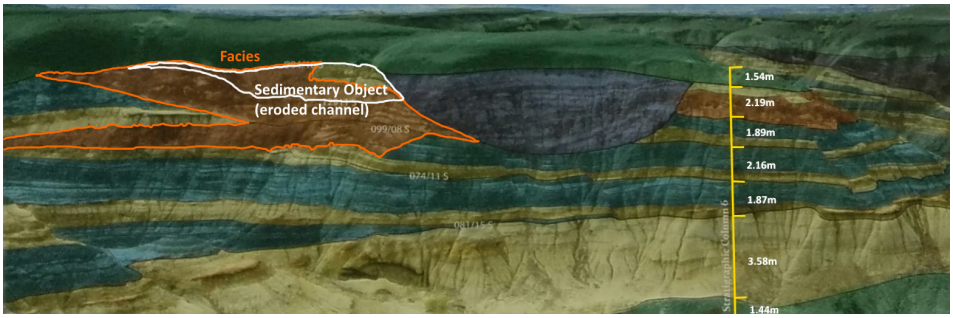

Figure 1.10: Example of a visual depiction of facies mapping of sedimentary features (e.g. muddy-normal point bars); annotated; modified from Johnston et al. [136]

1.3.2 Terminology for geometry

- **Point Set Surfaces (PSS)** are essentially point-based (i.e. vertex-only) representations for approximating and displaying the shape of an object [5]. It means that the whole surface shape of an object S is represented by a set of (theoretically infinitely-small) points $p \in V(S) \quad \forall p \in \mathbb{R}^3$, which makes the term synonymous with **point sets** and **point clouds**. This form of representation only works practically as each point, for its graphical representation, in its digital form has a minimum extent which allows it to be displayed [31]. The actual shape approximation and illusion of a surface is made possible by (a) a locally high sampling of the surface, so that the high amount of points after rasterisation by CG creates the illusion of a closed surface, or (b) by graphically rasterizing each point as an oriented disc (i.e. *splat* [172, 257]) where the varying disc sizes create the illusion of a close surface [31]. In the latter, the geometric representation, which is the definition used in this dissertation, is not a set of oriented discs but an attributed PSS (i.e. attribute function per point), $f(p) \in \mathbb{R} \quad \forall p \in V(S)$, in which the

attribute, based on actual surface properties (e.g. curvature, local feature size [8]) or acquisition properties (e.g. light reflectance for lidar or disparity for structured light), determines the extents of the disc (i.e. radius for circles; major axes lengths or radius-eccentricity information for ellipses). A drawback of PSS is the conceptual absence of the notion of connectivity and neighbourhood, although k-nearest neighbour approximations are often used in practice to express neighbourhood and connectivity.

- **Digital Surface Models (DSM)** are digital, discrete curved planar surfaces or a collective set of such surfaces. DSMs include the notion of curves, bends and deformations on the geometry. This is especially advantageous for **digital terrain models (DTMs)** (i.e. discrete surface representations for describing topography and terrains) that include steep elevation changes, overhang geometry or generally complex shape deformations to be represented. The terminologies, meaning and means of representation of DSMs and DTMs differ considerably from this geometry-focussed definition in geomatics application domains (e.g. geographic information systems (GIS), photogrammetry, remote sensing).

- **Triangulated Irregular Networks (TINs)** are a subcategory of DSMs , where the surface S consists of a vertex set $v \in V(S) \quad \forall v \in \mathbb{R}^3$ and a triangle set $t \in T \quad \forall t = \{v_n, v_{n+1}, v_{n+2}\}$, $S = \{V, T\}$. The term *irregular* hereby refers to the vertex sample being explicitly non-uniformal and the triangle shape being possibly anisotropic. As it is organised as a *network*, the surface itself is a *mesh*, hence $\mathcal{M} = S; \mathcal{M} = \{V, T\}$. This notation is equivalent to triangular surface meshes within CG, and thus both terms are used interchangeably in this thesis. It is important to note that the underlying triangulation is consistent across the whole shape of the object described by the discrete surface.

- **Polygonal soups** is a set of unstructured triangles or mixed triangulated polygons [115] with unfavourable geometric properties, being inconsistently oriented, potentially non-manifold, containing holes and self intersections, and are "mathematically ill-defined" [315]. A formal notation does not exists within the literature because the unfavourable mathematical properties. A polygonal soup, for the purpose of this thesis, is essentially a subcategory of DSMs but not equivalent to TINs. It consists of a vertex set $v \in V(S) \quad \forall v \in \mathbb{R}^3$ and a surface description, which can be a mix of triangles, triangle strips- or fans, quads and arbitrary polygons. Therefore, the underlying triangulation (if existent) is not consistent or continuous across the object's shape described by the discrete surface. Casual literature also refers to such surfaces as "polygonal zoos".

- **Reconstruction**, which hereby always relates to reconstruction of geometric shape, refers to the process of constructing a discrete, analytic or algebraic surface geometry for a set of vertices V, commonly organised in a three-dimensional euclidean space [17]. We further distinguish between (triangular) surface reconstruction and (tetrahedral) volume reconstruction. The specific reconstruction of a discrete surface of triangles from V is termed **triangulation**. A plethora of well-known 3D triangulation algorithms have been proposed in the literature, including but not limited to Delaunay triangulation [68], α-shapes [52, 81], median

least-square (MLS) surfaces [5, 76], ball pivoting [18], Power Crust [9], poisson surfaces [143] and Cocone [73, 74].

1.3.3 Terminology within computer graphics & visualisation

- In the context of surface geometry (e.g. DOMs), the term "**object**" refers to the actual object described by a given surface model. For example, the object refers to the digital representation of the rock face, stored as sets of vertices and triangles on a device, when rendering a DOM.

- The **interpretation** of geological segments (i.e. strata annd facies) has formerly been explained. The terms "interpretation" and "**annotation**" are used interchangeably in the thesis, as both terms are used within graphics and geosciences for describing the digital process of delineating semantic areas of objects.

- **Computer Graphics (CG)** is the process of converting data (be it user-generated content or measured data) into a digital, visual (i.e. graphical) representation that can be consistently displayed on graphical output devices (e.g. screens, projectors or integrated projection devices, such as head-up/head-mounted displays). The scientific branch of computer graphics covers topics such as graphical representation (e.g. imaging and geometry), animation and rendering (i.e. light transport reconstruction in virtual environments) and overlaps with branches of geometry and topology in mathematics (see content structuring in available base literature [308]).

- **Computer-Generated Imagery (CGI)** refers to artificial images created by means of computer graphics (i.e. rendering three-dimensional virtual environments). More strictly, it refers to a continuous animation (may it be predefined or interactive) of rendered images. It is hence a product of computer graphics by animating a rendered sequence of images based on (prevalently three-dimensional) geometric- and image content. Detailed information are available in the literature [4, 308].

- **Rendering**, in the context of this thesis, refers to the process of generating a (synthetic) image from the available data (i.e. surface geometry and textures) within a virtual scene by means of CG and displaying the result on screen or storing it as an image on the device. In practical terms, it maps to the process of traversing a given render pipeline [152] with the available graphical information towards the target pixel buffer.

- **Visualisation** is a larger discipline within the computer sciences, strongly connected to CG. There is a prevalent misconception observable within the (computational) geosciences that uses the terms of "rendering" and "visualisation" interchangeably. Munzner defines that "computer-based visualization systems provide visual representations of data intended *to help people carry out tasks more efficiently*" [213]. These tasks typically comprise actions such as exploration, analysis, presentation and illustration. From this taxonomy, it is evident that rendering a DOM for the purpose of viewing and navigating the data alone only covers

the task of data presentation and that, in order to actually "visualise" outcrop information, further operations need to be facilitated by a visual approach that solve specific tasks. Visualization is also generally used to quickly communicate information – not only in static images to present results or illustrate thought concepts, but also in terms of animation to sketch a process, an evolution or a story of thoughts.

- Computer graphics and visualisation research traditionally deals with topics of modelling [214], rendering [19, 112] and representing [151] **terrain**, as well as perceptually efficiently communicating its properties [80]. Available techniques and terminology are applied and extended where possible within this research for DOM applications.

- **Stereoscopic rendering** refers to the technique of rendering 3D scenes in a way so that the render target (e.g. display, image file) is split for visual information delivered to each eye individually. Together with a perceptual composition technique and stereoscopic display device, the observer of the 3D scene is presented with illusion of seeing "three-dimensionally". The split of visual information is currently possible by (a) rendering and displaying the 3D scene in full resolution for each eye individually in a split-screen setup, (b) intermixing the two individual, vertically half-resolution output images into one image (i.e. decomposition by interlacing) and directing the half-image information by polarisation to each eye separately (composition), (c) reserving for the intermixing half-resolution image per eye each a separate colour band (i.e. anaglyphic composition and decompisition), or (d) rendering the full-resolution image for each eye in an interleaving sequence with an elevated (e.g. doubled) display refresh rate (e.g. shutter technology). More information on the related technology is available in the literature [117].

- **Virtual Reality (VR)** refers to approaches of connecting the human sensor- and actor channels for a 3D virtual scene to digital devices that allow for an immersive experience of the virtual world. Within VR, replacing the view of 2D projections of the 3D scene on-screen with a stereoscopic rendering approach is only a part of the technology. Natural, three-dimensional user interaction with the virtual world is equally essential to VR [99]. The sensor replacement ideally covers more than just the visual sense (e.g. audio, touch and balance). In contrast to **augmented reality (AR)**, the goal is to immerse the user in a virtual scene that can be supplemented by real-world information (e.g. background imagery for horizon). The goal of AR, on the other hand, is to supplement the view and perception of the real-world with digital information of a correlated virtual scene. Also, the general focus in AR is to *augment* the senses of the user instead of replacing them with digitally analogous devices.

1.3.4 Terminology between computer vision and geomatics

Computer Vision (CV) is the process of gaining insight and deduce data from imagery content. It can be thought of as the reverse process of CG in terms of base information and target result. The research goal in computer vision is to gain an understanding of

human perception and the principles of the human-visual system, and deduce formal rules, expressed in mathematical terms, of visual perception principles to, in the end, replicate that in a computerized process. Due to the duality with computer graphics (shown in fig. 1.11), many terms and principles of both disciplines are shared and interchangeably applicable. Computer Vision draws upon major concepts and knowledge from machine learning and pattern recognition to gain an understanding of the human-visual processes. Major branches within computer vision are the 3D point reconstruction of objects and scenes from images, the computerized evaluation of objects (e.g. manufactured tools) and their behaviour (e.g. object interaction in image sequences), the estimation of position, orientation and/or motion of objects (meticulously covered within this thesis), the reconstruction of flawed, incomplete, split or sparsely described image information (covering topics from image interpolation to super-resolution and panoramic imaging) and the development of computerized instruments for doing so (including devices ranging from photo cameras to scanners for structured-light and electromagnetic waves outside the human-visual spectrum). A high terminology ambiguity exists between Photogrammetry & Remote Sensing (a, see [113, 156]) and Computer Vision (b, see [93]), while this dissertation, in general, advocates the use of Computer Vision terminology.

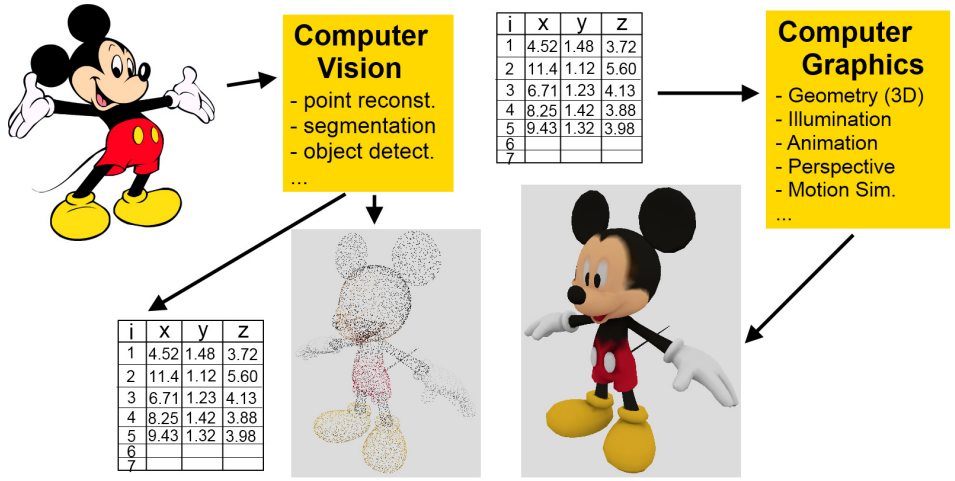

(a) Computer Vision (b) Computer Graphics

Figure 1.11: Visual differentiation between CG and CV.

An essential topic in this thesis is the registration of image information to provided surface geometry. Therefore, a mapping function (i.e. **surface paramterization**) needs to be determined that links the 2D space of the image and the 3D space that embeds the surface. The computation of such parameterization is referred to as **exterior orientation estimation** (photogrammetry) or **pose estimation** (CV). The difference in the naming convention relates to the different origins of the disciplines: photogrammetry originally used the related maths to compute camera orientations of pictures taken by aerial photography to a given surface [113]. Thus, the focus is on the external ori-

entation of the camera. In CV, the related techniques where used to find a "pose" (position and rotational transformation) of an object's surface so that its rendered image resembles a given photo to which it is compared. In the current literature, the names of the techniques are often used interchangeably as they are dual to one another. Another equivalent term from CV is the estimation of **external camera parameters**, which is semantically closer to photogrammetry. It refers to the connection between the imaging plane's position and orientation within the camera coordinate system (internal parameters) and within an arbitrary external coordinate system (external parameters). Irrespective of the terminology, each estimation produces the same result: a local parameterization of the 2D image space and the 3D space embedding the geometry. The full process is further referred to as **image-to-geometry registration**.

Digital Elevation Models (DEM) describe (a) 2D representations (e.g. images) with scalar attribute values to express surface elevation (i.e. *height maps* on a 2D grid), or (b) 2D uniformal grids with 3D vertices, where the vertex dimension along the surface normal direction expresses altitude variations (i.e. elevations). DEMs do not allow for complex shapes where two laterally overlapping vertices differ in their elevation. In practice, DEMs are a simple representation for terrestrial or planetary surfaces. The condition of applying DEMs as a geometric representation for such objects strongly varies with the representation scale, as these objects potentially include *complex* shape variations at small scales that are simplified at larger scales. The DEM representation originated as computational simplification in the years of 1978-1981, due to the limited computing capabilities of former PC hardware. It has limited value as mathematical concept, particularly in comparison to the general notation of DSMs. DEMs have been notably adopted in geomatics- and geoscience application domains (such as GIS) as major representation for topographic information due to their conceptual- and computational simplicity.

1.3.5 Concluding remarks on multidisciplinary terminology

In conclusion of this section, it becomes apparent that the differences in terminology, viewpoints and mathematical foundations between the related scientific disciplines is a major impedance to the ongoing inter-/multidisciplinary research in digital outcrop geology. Overcoming the terminology barriers in discussions amongst researchers of different domains, as well as in the coherent public communication of the research results, is one of the major practical challenges experienced during the preceding research period. For more information on specific details, knowledge foundations and the related terminology, the interested reader is referred to the following literature:

- Computational Geometry: implementation-specifics and practical notation see [225]; for terminology clarification and principle knowledge, consult [66], [121], [25] and [17]
- Photogrammetry: see [113, 156, 183, 200]
- Computer Vision: subdivided in specifics in single-view [242] and multi-view [120] geometry (i.e. shape) reconstruction; for general terminology, consult [93]; for introduction to principles outside scene reconstruction, see [210, 228]; for implementation details, see [142]

- Computer Graphics: for theory and algorithms, consult [308] and [193]; for implementation details, see [215], [152] and [4]
- Visualisation: visualisation design, see [213]; most relevant subdomains within visualisation for digital outcrop geology are scientific visualisation [119], information visualisation [281] and visual analytics [150]

1.4 State-of-the-art in mobile computing

Mobile devices are nowadays ubiquitously available to most people. Their comparably small form factor makes them ideal for field application. Furthermore, the computational capabilities and the available software packages have spawned a rapidly increasing appearance of new software ("apps") for various purposes on mobile devices. That said, a persisting, practical problem within mobile computing is the difference between the mobile platforms - namely Google Android, Windows 10 mobile and Apple's iOS. Apps developed for one platform are not interchangeable between platforms and cross-platform development is (as in desktop environments for UNIX, Windows and MacOS) a time-consuming and costly engineering endeavour, rarely achieved within research environments.

Computational capabilities of mobile devices have rapidly increased over the past decade. From the simple capabilities of phone calls, text messaging and occasional internet use with compact mobile phones (from around the year 2005), current mobile devices (i.e. "smart devices") facilitate a range of applications previously exclusive to personal computers and laptops. This holds particularly true for the (visual) analysis and presentation of content in 3D. The steep improvements in hardware and software technology for these compact devices is mainly attributed to the entertainment industry for its wide popular applicability.

1.4.1 Techniques in 2D–3D graphics

A first hint of the impressive computational capabilities of modern mobile devices can be gained when considering current image drawing, sketching and processing applications. Apps like Autodesk Sketchbook[5] and NVIDIA Dabbler[6] provide a rich set of tools for sketching, drawing and stylised painting of raster- and vector graphics, condensing the knowledge gained from decades of stylised painting research known as *image synthesis and analogies* [123, 164, 178] and *image quilting* [82, 309, 318] (see fig. 1.12). These techniques recently merited in the *BeCasso* app for Apple's iOS that combines photography with stylised, intuitive and quick editing capabilities [261]. Image editing apps make optimal use of the provided hardware platform, using multiple processors and GPU computing to deliver the graphical high fidelity and the related complex image calculations in realtime.

The use of 3D graphics on mobile devices is further shown by the various, available mobile 3D games. In some cases, full-scale games that were graphically state-of-the-art on commodity computers a decade ago (e.g. Star Wars[7]: desktop version 2003, mobile

[5] Autodesk Sketchbook - `https://www.sketchbook.com`

[6] NVIDIA Dabbler - `https://play.google.com/store/apps/details?id=com.nvidia.watercolor`

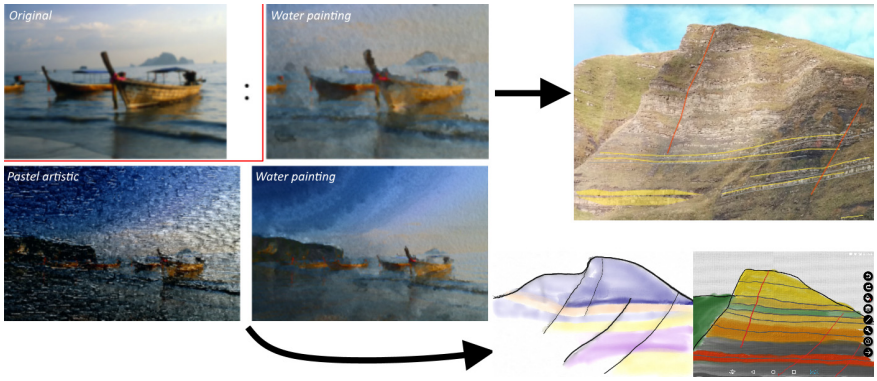

Figure 1.12: Stylised rendering as a prime example of how fundamental research in texture- and image synthesis (left, taken from Hertzmann et al. [123]) translated into smart tools for stylistic painting that can be used for geological mapping in the field on mobile devices (right, created via NVIDIA Dabbler).

version 2015) are already available on pocket-scale mobile devices. This shows the true potential of the hardware platform, which can be further utilised for geological 3D data. More serious applications that make use of the 3D graphics capabilities recently emerged within the domain of cultural heritage. Rodríguez et al. presented a mobile render system called "HuMoRS" for very large triangular meshes [253], demonstrated on cultural heritage case studies. HuMoRS demands WiFi connectivity as an online render system. García et al. presented a system for Point-based rendering (PBR) running natively and without WiFi connection on mobile devices [102]. The most recent addition in this line of 3D render systems on mobile devices has been presented by Ponchio and Dellepiane from the MeshLab development team [236]. All the mentioned systems are technically built upon WebGL or another form of OpenGL Embedded Systems (ES) [211]. A continuing research challenges that relates to this dissertation is the development of suitable, intuitive, "smart" 3D-space user interaction on limited screen space hardware, as recently addressed by multiple research groups (see [192,234,317]). The most-recent overview on mobile graphics research is provided by Agus et al. [2].

With respect to CG, VR and AR, the community has seen the emergence of novel, entirely unexpected instruments. One of the technologies is Google Cardboard VR. Cardboard allows to physically wrap a Google smartphone into a cheap, carton-based envelope equipped with a multi-stage lens system. Along with the visual line-of-sight separation come smartphone-exclusive CGI applications that render 3D scenes in ways that facilitate stereoscopic viewing. Example usage is show in fig. 1.13(a). Even more applicable to real-world applications is AR, realisable via Google Glass technology in fig. 1.13(b), which allows to project a heads-up display (HUD) on the glasses to give auxiliary information about the objects in view. The continuation of the technology is currently stalled, but smaller companies pick up the idea by Google and continue the development – both in case of Cardboard VR and Glass AR.

[7]Star Wars Knights of the Old Republic - mobile version `https://play.google.com/store/apps/details?id=com.aspyr.swkotor`

(a) User in Cardboard VR experience, ©Google

(b) view of the Glass AR device, ©Google

Figure 1.13: Technology examples of mobile device-based VR and AR technology, developed by Google.

1.4.2 Applications for geological fieldwork

Currently available mobile device applications within geology and the geosciences focus on three key areas:

1. geo-mapping and GIS
2. measurement and sedimentary logging
3. information documentations (e.g. ”the digital fieldbook“)

The first category covers the most matured applications on mobile devices, such as Google Maps[8] and Open Street Map (OSM)[9] for general geospatial mapping. Both systems can import global navigation satellite system (GNSS)-recorded positional data, track a user's position on the map and allow offline (i.e. non-WiFi connected) orientation in the field. Moreover, the development of applications for geological mapping to learn about local geology and track geological formations is increasingly popular. These applications are commonly provided by national agencies for geological mapping and geodesy, such as *iGeology*[10] by the British Geological Survey (BGS) for the UK and *InfoGeol*[11] by the Bureau de Recherches Géologiques et Minières (BRGM) for France, as shown in fig. 1.14.

Within the second category, various tools for measuring and logging geospatial and geological information are available, often derived from existing compass applications. Weng et al. initially presented with *GeoTools* [310] an application for position recording as well as measuring strike/dip of bedding planes and trend/plunge of folds, combined with the possibility to attach photo- and audio material to the measurements. Ferster and Coops formalised the requirements to such applications for a geoscience audience [92]. Rocklogger[12] is a more recent application that provides equal functionalities, as do numerous other apps freely available in the respective app

[8] Google Maps - `maps.google.com`

[9] Open Street Map (OSM) - `www.openstreetmap.org`

[10] BGS iGeology - `http://www.bgs.ac.uk/igeology/`

[11] BRGM InfoGeol - `http://www.brgm.fr/production-scientifique/donnees-services-numeriques/infogeol-acces-mobile-donnees-geologiques`

stores. Meek et al. recently presented a technically sophisticated app to collect 3D, georeferenced point measurements at large distances using mobile device photos and an underlying DEM. More applicable to the theme of this research investigation are apps for sedimentary logging, as initially shown by Wolniewicz via SedMob [313]. A more tangible stratigraphic logging application used within chapter 7 is Endeeper's Strataledge[13] (fig. 1.14), which provides a clean and yet complete interfaces for litho- and biostratigraphical logging.

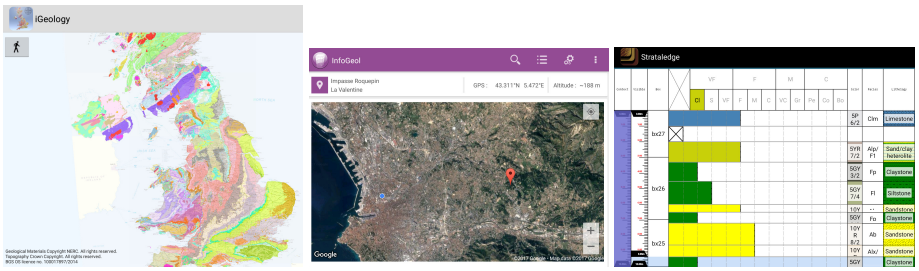

(a) (b) (c)

Figure 1.14: While apps such as iGeology and InfoGeol (a & b) provide contextural geological information in the field, sedimentary logging apps such as Strataledge (right) allow digital acquisition of geological information, relaxing the need for post-fieldwork digitisation.

The third, and at this stage final category encompasses applications that combine geospatial base maps with the integration of geological meta information and multimedia content. In addition, apps that aim to provide a digital replacement for "pen-and-paper" field methods equally contribute to this category of applications. Vivoni and Camilli presented and early application that aims to provide such "digital fieldbook" capabilities for the environmental geosciences [303]. Two similar, popular applications aiming for a "digital fieldbook" scenario are SIGMAmobile and MAPIT. SIGMAmobile [141] facilitates data logging, geological mapping, data querying and map visualisation via an ArcGIS interface. MAPIT [64] is an application that facilitates a similar range of tasks. Both are loosely related to the mobile approach within this thesis as they use outdoor laptops (i.e. "rugged tablet PCs") as computational base, constrained by the well-known limits of equipment weight and power consumption as well as special, non-ubiquitous devices. Clegg et al. provide an comprehensive overview of such technologies [56]. A modern, more extensive digitial fieldbook app was recently presented by Camp and Wheaton [45]. An established application that aims at fieldbook-replacement within geology is Midland Valley's FieldMove[14], which provides elaborate capabilities for field measurements, geo-referenced photo collections and note-keeping.

The listed geological apps demonstrate the usefulness of mobile devices and their potential within fieldwork. On the other hand, the capabilities that modern mobile

[12]RockGecko's Rocklogger - `http://rockgecko.com/about/`

[13]Endeeper Strataledge - `http://www.endeeper.com/` and `https://play.google.com/store/apps/details?id=com.endeeper.strataledge`

[14]Midland Valley FieldMove - `http://www.mve.com/digital-mapping`

devices facilitate are significantly underused when comparing the available geological tools and apps with the ”cutting edge“ of that mobile computing technology, as previously demonstrated for 2D–3D graphics (section 1.4.1). In addition to the previous three key categories of mobile apps within the geosciences, we envisage that two further categories emerge from current research efforts:

1. digitally immersive, interactive fieldwork
2. virtual fieldtrips

Multi-view geometry (from CV) and SfM (from photogrammetry) for reconstructing 3D point set surfaces are the possible on-spot, mobile 3D data acquisition techniques in the field. They can be adopted in various geoscience application scenarios ranging from monitoring glaciers, oceans and shorelines to the acquistion of digital outcrop models, as discussed in section 1.2.3. Moreover, the technology has recently been demonstrated to work under water, for the purpose of digital archaeology [297]. This photogrammetric reconstruction of coloured 3D point sets is demonstrated by Tanskanen et al. [290] on Android mobile devices using CV technology. A similar approach is proposed by Garro et al. [104]. Drawbacks of the technology are still persistent. Moreover, the software prototypes are not freely available, which is problematic for testing the techniques for geological field environments. Furthermore, based on collaborative discussions, computational stability problems of multi-view geometry methods emerge when reconstructing large-scale, wide-angle 3D point sets from outdoor landscape photographs.

Project Tango [109], introduced in 2016, made a public impact when showcasing large-scale indoor environment reconstruction in realtime on Android devices. Project Tango uses simultaneous localisation and mapping (SLAM) (see [90] for technical information) for the reconstruction. SLAM is known for having issues in outdoor reconstruction and tracking due to drastically changing illumination conditions in image sequences and the technique's reliance on temporal image consistency. A robust approach for photogrammetric reconstruction of outdoor environments has been published by Fritsch and Syll [98], which is designed as an online system with required WiFi connectivity.

A general issue with available, non-commercial software for 3D reconstruction is their availability. Software as demonstrated by Fritsch and Syll or Tanskanen et al. perform very well under the stated technical conditions and deliver high-quality results, but the software is badly maintained after its initial development and is subsequently removed from the rapidly-developing mobile market. A short survey on SfM software within Google's app store ”Play Store” to date of this dissertation (March 2017) yielded no available, listed applications for 3D reconstruction. Further ways of software distribution for mobile devices are uncommon, which leads to the conclusion that the above-mentioned software is not operational anymore.

The techniques most related to the chosen research direction in the main chapters, and also contributing to this new category of ”immersive fieldwork app“, are the annotation and interpretation of 3D-registered images on 3D surface models using mobile devices. Approaches that support this goal emerge from the domains of AR and VR. A pioneering application for mobile, immersive terrain visualisation was presented in 2003 by ”Pocket Panorama“, targeting outdoor laptops as the basic

computation platform [116]. Moreover, the fundamental technique of feature-based image-to-geometry registration from CV has recently been used to map images and image-based interpretations on existing 3D surface models within the geosciences. An exhaustive body of literature exists on the topic of image-to-geometry registration [50, 62, 63, 105, 106, 146, 219, 235, 289], which is continuously referred to in this dissertation, and which shall be considered for questions on technical details. Kröhnert [159] applies the technique for providing a waterline tracking interface in a public-participation (or Volunteered Geographic Information (VGI)) application for urban flooding early warning and response.

The use of mobile devices and 3D interpretation is an increasing trend within geology and the geosciences. Viseur et al. presented a prototypical approach for DOM interpretation directly in 3D [302] (fig. 1.15) using the commercial "Unity3D" software for loading and presenting the 3D surface models of outcrops. The authors stress the importance of smart interaction on small-screen mobile devices. In this respect, smart motion constraints have to be developed and tested in a fluent interplay with geoscientists in order provide an actually valuable mobile system for DOM interpretation. An additional challenge within geology is the use of this technology outdoors under comparatively less comfortable conditions than cultural heritage model exploration or 3D entertainment indoors.

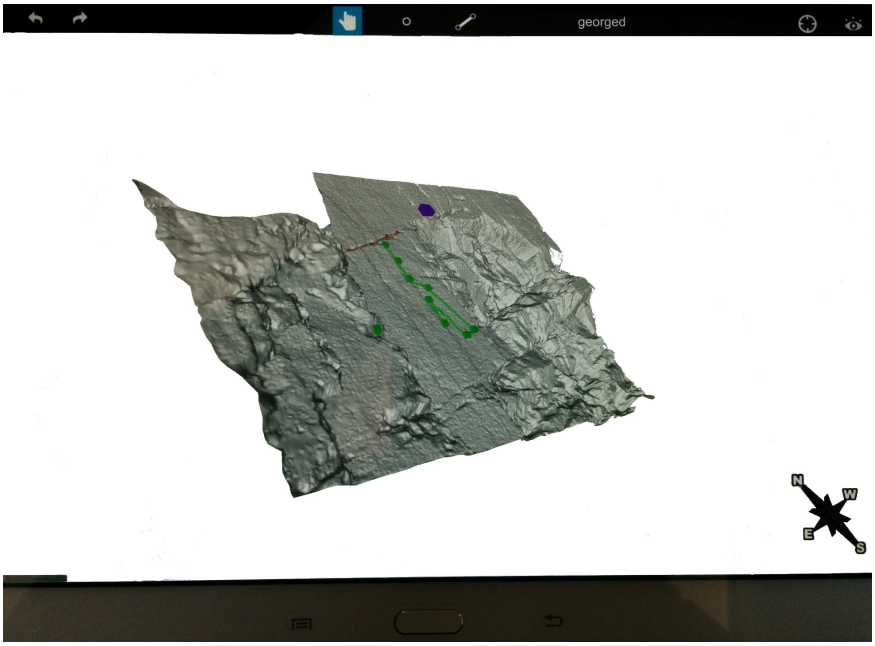

Figure 1.15: Mobile device screenshot of the "Outcrop" app [302] with data from a heavily-fractured carbonate outcrop.

Extensively using mobile device 3D technology for geological field applications has originally been envisaged by McCaffrey et al. [199]. The benefits of DOMs in the field are manifold. The technology allows for digitally consistent work between field- and

office-based geological work. DOM applications in the field facilitate easy and fast integration of field observations and interpretations into existing reservoir modelling software. The time-consuming effort of digitizing pen-and-paper documents henceforth become oblivious. Also, taking digital outcrops to the field allows to work at real scales with 3D information, in contrast to common maps, paper sketches and outcrop photo panel interpretations. A good DOM application ideally allows structural analysis, such as horizon surface interpolation or the creation of fracture stereonets, directly in the field and away from the office desk. Even more so, some observations can only be seen and documented in the field, in particular when considering carbonate outcrops. As a result, such immersive 3D applications potentially prevent overlooking crucial field information and subsequently repeat the fieldwork.

The second, new category of virtual fieldtrips has also been envisaged by McCaffrey et al. [198]. The related article introduces the idea on five example case studies that lend themselves for the purpose of virtual fieldtrips. *Virtual fieldtrips* themselves are the idea to present consistent DOM field studies to a large audience in a (potentially shared) virtual environment and communicate key insights of the study. It may also be possible for the audience to interact and modify the content (i.e. the interpretations and mapped facies) interactively in a subsequent step. From the author's perspective of this thesis, the virtual fieldtrip scenario deserves a separate category. Virtual fieldtrips certainly include the techniques and approaches described for immersive digital fieldwork, but moreover questions of how to visually communicate the insights in an easily-understandable manner and how to organise the shared interactive experience go further than what is previously presented. In terms of visual communication, visualisation approaches presented in the GeoIllustrator project that targets geological storytelling [180, 181] can provide inspiration and input when presenting outcrop studies in a guided manner to a fieldtrip audience. In terms of sharing the interactive, visual experience of the fieldtrip, collaborative interaction and visualisation approaches [145] can be extended to manage multi-user input, annotation and modification.

1.4.3 Implications and conclusions

One can deduce some principle requirements and challenges covered in this thesis based on the technological overview. The technical development needs to consider the restrictions of outdoor field environments. Henceforth, techniques that have theoretical limitations when being extended from indoor laboratory case studies to outdoor environments are not considered relevant for further analysis (e.g. SLAM). The following specification constraints apply to mobile, immersive interpretation field applications:

- **Interpretations in 3D**: A plethora of possibilities already exist for doing 2D interpretations on outcrop image content. Utilising DOMs in 3D is a prime requirement because of the additional benefit of scale, consistency, interactivity and ease of desktop integration to reservoir modelling.
- **Independency of WiFi reception**: Field work locations can be very remote. Some outcrop studies inside densely-populated countries (e.g. Gresse-en-Vercors study in France by Richet et al. [246], Big Rock Quarry in the U.S. by Olariu et al. [224]) can potentially utilise WiFi in the field. Field studies in remote environments (e.g. Svalbard archipelagos, Norway by Senger et al. [265], Book

Cliffs in Utah, U.S [85, 251], Tanqua Karoo basin in South Africa [127]) can lack WiFi reception. A sophisticated mobile device digital outcrop geology application should operate undisturbed even in these remote areas. Therefore, the employed techniques for rendering, 3D projection and 3D surface reconstruction need to run exclusively and natively on the mobile device without internet access.

- **Energy-efficient operability**: A large constraint of mobile devices is the limited battery capacity. This can be extended to a given limit by external batteries, but a mobile device application that targets field geology use needs to be designed in an energy-aware manner. This goal includes measures to only use techniques on-demand that require the use of energy-draining mobile components, such as physical sensors, network connectivity, multiple central processing unit (CPU) cores or graphics processing unit (GPU) procedures. An extended energy budget can also be used by the geologist to raise the screen luminance of the device for improved visibility.

- **Simple interaction**: Conducting fieldwork also always has a physical component, so that the target user base of the mobile device application is expected to not devote their full attention constantly to the device. In order to facilitate a smooth integration into field workflows, the target application needs to offer a simple and intuitive interaction scheme that engages the geologist to do his interpretations digitally. In the end, the goal is to provide the geologist with a superior digital alternative to paper-based interpretation and sketching.

- **Desktop interoperability**: one of the largest advantages of digital procedures is the removal of digitization after the fieldwork for subsequent modelling scenarios. This demands that the data of the mobile device are provided in an obviously interoperable fashion that indicates the user which data are to be imported in which desktop modelling system. If such indicators and matching data formats are not provided by the mobile device application, it is expected that the geologist will adopt a paper-based workflow, as one of the major digital advantages is not fulfilled.

Two prospective research directions are emerging from the technical review, which translate to different conceptual research challenges:

1. Interpreting geological structures directly in 3D on the outcrop surface model: The approach is inspired by the ”Outcrop“ application by Viseur et al. [302]. The major challenge is to find a tangible interaction scheme, preferably executable single-handedly. Such schemes potentially make optimal use of mobile motion sensors to ease the surface model navigation. Also, energy-efficient rendering patterns are necessarily investigated in this case, as the whole interaction and workflow is tied to 3D graphics.

2. Interpreting outcrop images captured by the mobile device, and subsequently projecting the interpretations on the 3D surface model (on demand): In this case, the application also facilitates non-3D use, which is advantageous in terms of energy efficiency. Furthermore, interacting and drawing on 2D images is trivial and their rendering onto images is natively facilitated in an energy-efficient way by mobile

platforms. In order to provide the envisaged, added value of DOMs in the field, the structures need to be projected into 3D. The projection can extend features-based registration techniques as given by Cavelius et al. [50], Gauglitz et al. [106], Sweeney et al. [289] and Nuernberger et al. [219]. For real-world scenarios, the registration of images under radiometric variance and changing illumination conditions is a fundamental challenge in the domains of photogrammetry and computer vision, which needs to be addressed. As before, mobile device location- and motion sensors can help to resolve the ambiguities arising from varying illumination.

1.5 Research statement

This dissertation focusses on the exploration of visual techniques, operating on DOMs, that facilitate the geological interpretation and analysis of outcrops in the field via mobile devices. The exploration of visual techniques refers in this context to the design, development, extension and application of mathematical and computational models and algorithms from the domains of vision, graphics and interactive systems. These explored visual approaches are to be used on mobile device platforms to support geological fieldwork. The proposed workflows, frameworks and visual techniques should allow a quick transition in the field from physical observations to digitised interpretations and concepts. The techniques further aim to narrow the gap between field-based geological observation and measurement collection, and the office-based geological workflow around observation digitisation, DOM interpretation and MPS TI generation. Considering the goals and the proposed, visual methodology, the dissertation represents a bridge between the existing mathematical-computational knowledge, its implementation in algorithms of visual disciplines within computer science, and their concrete application to tasks and challenges within petroleum geology. From this goal, we derive our main research question:

How can visual techniques, made available on mobile devices, support and improve geological fieldwork ?

In order to answer this question within an algorithmic approach, one can expect to encounter a number of primary research challenges, which shall be addressed by the proposed visual approach. These challenges, initially stated as such early project description, are summarizes as follows:

- Optimise and present optically-acquired, digital 3D geometry with 2D textures (i.e. DOMs derived from lidar, photogrammetry or SfM) and stratigraphic interpretations on limited-performance, mobile devices.
- capture and co-register generically-positioned, geo-referenced outcrop images with available DOM surface geometries, using on-board cameras, motion- and orientation sensors.
- provide intuitive, humanly-abstracted user interfaces that support stratigraphic interpretation.

1.6 Datasets

This study covers four different study locations, of which three are digital outcrops. For algorithmic testing and method verification, an urban TLS dataset was obtained from Bryggen. The dataset is used in an initial conference paper (see appendix A). Bryggen is a late-medieval building complex of the former Hanseatic League, located on the harbour of Bergen (Norway). Its original purpose of a trading post has been nowadays replaced by restaurants, bars and shops for traditional, Norwegian goods. The dataset is taken for algorithmic testing and verification because of its geometric simplicity and its photogrammetric potential, containing a lot of salient features in images and on the surface due to the straight, wooden architecture. An overview image (fig. 1.16), taken from appendix A, shows the textured surface model and a respective photo of the study area.

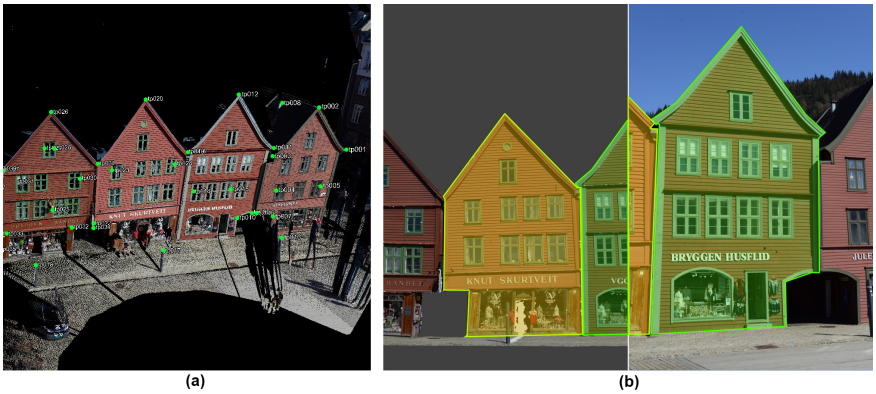

Figure 1.16: The textured surface model of Bryggen (Bergen, Norway) and its related mobile device photo. The coloured outlines segment the different units of the building complex.

The outcrops covered in this dissertation are (1) Mam Tor (UK), (2) the southern Whitby Cliff section (UK), and (3) the outcrop park of Brimham Rocks (UK). Their geological setting is briefly introduced. All outcrops covered in this thesis are of siliciclastic composition.

Mam Tor is a turbidite outcrop in the Peak District, Derbyshire, United Kingdom. It is a cliff-shaped outcrop formation with mudstone-sandstone interbedding. The outcrop has been recently used to study multi-story channel sandstone configurations in turbidites [280]. Its geology was covered by early DOM studies for improved petroleum recovery (Pringle et al. [237]). Traditionally, Mam Tor is studied by environmental geologists to improve the understanding of landslide processes [305], which the outcrop is subject to and which presently shape and deform the outcrop. Fig. 1.17, adapted from chapter 4, shows its location, an exemplary rendering and a collection of field photos. The model contains two sections with an overall amount of 34.51 million vertices and 11.5 million polygonal sets.

The outcrop at the Whitby cliff section is part of the mid-Jurassic Ravenscar group [209], located south of the town of Whitby (North Yorkshire, UK). The Saltwick formation in the Ravenscar group is the study focus of chapter 7. It is a fluvio-deltaic out-

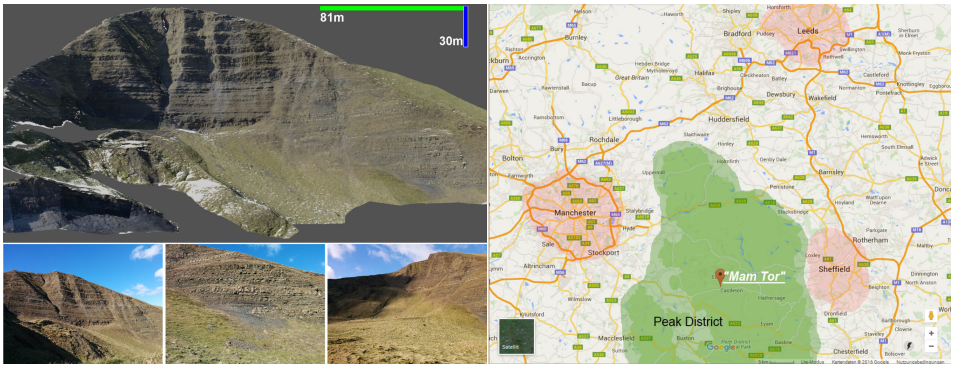

Figure 1.17: Map location, rendered image and photos of Mam Tor (Derbyshire, UK).

crop formation overlain by the Eller Beck, Cloughton, Scarborough and Scalby Formations [122,209]. Fig. 1.18 shows the outcrop and its location on a local geological map. The DOM of the Whitby cliff is separated into four sections with an overall amount of 2.01 million vertices and 3.74 million polygonal sets.

Brimham Rocks is a ”Nation Trust“-managed area of outcrops in North Yorkshire, UK. The DOM, its geographic location and a selected set of example photos from mobile devices is shown in fig. 1.19. The outcrop, geologically member of the Millstone Grit series of the Kinderscout Group [279] of lower carboniferous sediments, is composed of sandstone due to fluvio-deltaic deposition [278]. Channel cross-bedding is visible on several of the pillar-shaped rock sections (i.e. *tors*), shown in fig. 1.20. The local geology is well studied and a wide body of literature and interpretation data of the outcrop and the depositional environment is available [133, 307], with Soltan and Mountney [279] contributing the most recent studies based on DOM data in 3D. The geology is easily accessible and its good preservation proved advantageous for the presented technical experiments. Its digital representation is built from sixteen sections covering an overall amount of 15.16 million vertices and 5.05 million polygonal sets.

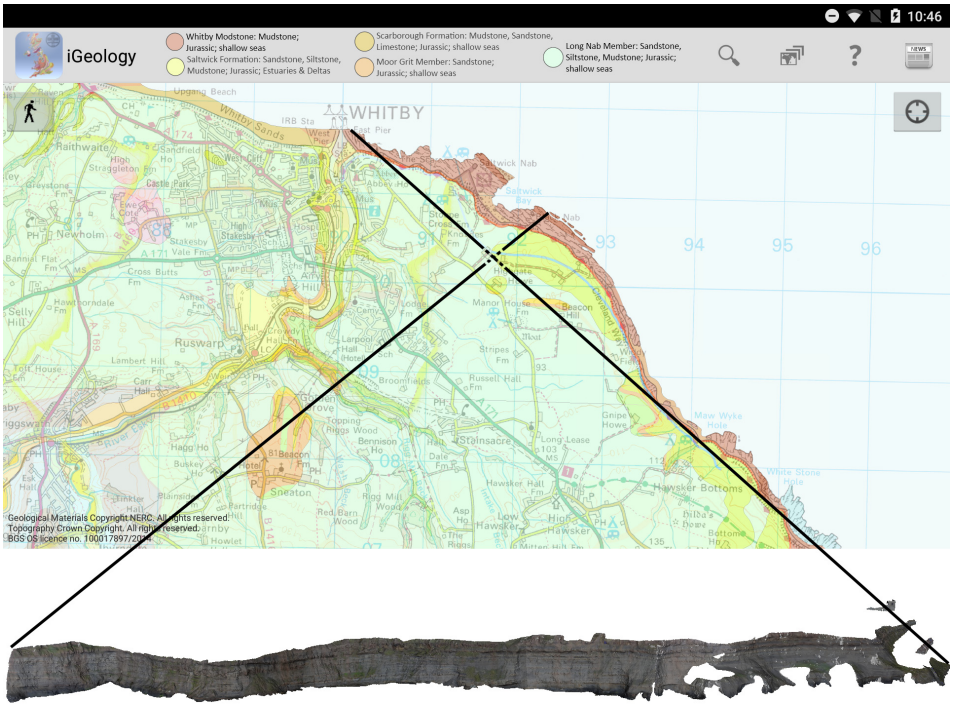

Figure 1.18: Map location and rendered image of the Whitby cliff section (North Yorkshire, UK).

Figure 1.19: Map location, aerial image overview, rendered image and photos of Brimham Rocks (North Yorkshire, UK).

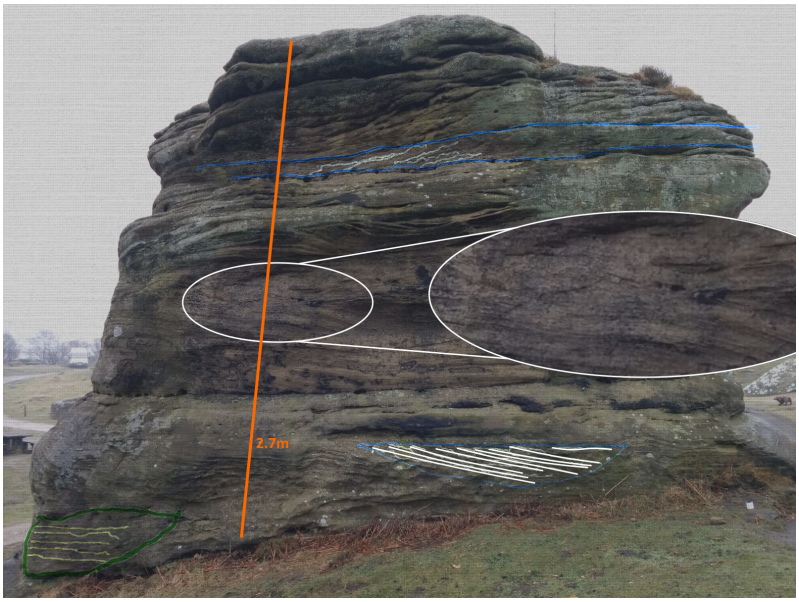

Figure 1.20: Cross-channel bedding, easily traceable on some of the pillar-shaped outcrop sections (i.e. *tors*) at Brimham Rocks.

1.7 Dissertation structure

This dissertation has a paper-based format, summarizing the research conducted over the three year research period by including the resulting academic journal publication as main sections. Because of the interdisciplinary nature of the research, this section attempts to provide a storyline by which the papers are connected.

First of all, the main section starts by introducing a mathematically consistent formulation and notation of DOM surfaces (chapter 2) that diverges from currently established knowledge within the literature, which is very unspecific and informal on that subject. The novel formulation includes concepts for texture mapping and volume geometry reconstruction, which subsequent chapters make use of. Subsequently, and based on the novel notation, currently available approaches of digital outcrop interpretations are revised and classified into a scheme that provides and overview of distinct methodologies and their applications (chapter 3). The discussion at the end of the thesis draws from the hereby introduced concepts and distinctions. Then, novel techniques developed during the research period are presented.

The original research idea is to map outcrop photos to the textured surfaces of DOMs. The photos can be subsequently interpreted in form of line segments and polygonally bound areas that represent (sedimentary) facies. On basis of the image-to-geometry registration, the interpretation structures can then be projected on the surface model to obtain accurate 3D vertex coordinates for the 2D polygons. The connectivity is not influenced by the projection operation. This workflow is described by the paper of Kehl et al. in chapter 4.

A major obstacle encountered within the initial approach are the inherent challenges of changing illumination and other environmental effects on the image-to-geometry registration, which is referred to as *radiometric variance* within images. The variance and differences refer in this case to the comparison of the rendered image (i.e. *synthetic image*) of the DOM and the captured outcrop photos. While the illumination within the photos changes, the DOM and its photo-texture is acquired once within the given frame of environmental conditions during the acquisition. The model is thus subsequently unchanged and stored as static object within the SAFARI database. Existing and novel techniques are assessed by Kehl et al. in chapter 5 to account for the radiometric variance in real-world outdoor case studies.

While novel feature-based image registration techniques account favourably for radiometric variance, as seen in chapter 5, a simpler approach is to assess the influence of common image processing techniques. These techniques potentially allow the application domain users to interactively influence the registration result and thus achieved an improved accuracy when working with the 3D-mapped data. They can also partially be automated. This image processing influence is assessed in the conference paper by Kehl et al. in appendix B.

The image-to-geometry registration procedures have originally been assessed on commodity desktop workstations, utilising the mobile device sensor data. In appendix A, the assessed techniques are transferred onto mobile device hardware and assessed for their computational feasibility.

The results of the image processing assessment and the alternative feature-based registration allows for a certain degree of radiometric robustness, determined by user interaction. Because most prospect users in the application domain of field geology are

not equipped with the in-depth knowledge of the related, computer-scientific literature, the parameterization and influence of the procedure need to be translated in a domain expert-accessible manner. For this purpose, the geological mobile device application is extended by a registration framework for simplified user interaction and graphical feedback of the quality of the registration results, which is presented by Kehl et al. in chapter 6.

The algorithmic research then results in a real-world, geological case study of the Saltwick Formation, North Yorkshire coastline, UK. Hence, chapter 7 shows the application of the mobile device technology to a concrete scenario of MPS TI generation from DOM interpretations. The related study site is a potential outcrop analogue for hydrocarbon reservoirs of the Brent group in the North Sea.

Further algorithmic research on related visual techniques for digital outcrop geology is presented in appendix C to H. Their relation to digital outcrop geology and their impact on the thesis is outlined in an introductory preface of each paper and the dissertation discussion (chapter 8).

II

Chapter 2

Digital Outcrop Geometry: Formulation, Reconstruction and Applications via Discrete Geometry and Topology

Digital outcrop models (DOMs) are increasingly applied within the environmental geosciences and geology, with applications to mineral exploration and mining [255], hydrocarbon reservoir modelling [88] and CO_2 storage [33, 134]. They are used as digital and visual representations of surface geology found in nature. They digitally represent the geological exposure as a surface model.

The current formal definition of these surface models is adapted from early forms of discrete shape representations in computer graphics. This early notation allows for a quick adoption of simple rendering- and analysis principles in computer graphics, using existing and well-established graphics software interfaces such as OpenGL [152]. Apart from the rapid deprecation of practical computer graphics workflows, for example the replacement of fixed-functionality render pipelines by unified shaders in programmable pipelines [4], these simple formulations of surface geometry limit the validly-supported range of applications, in particular extensions of surface geometries to volume analysis. The increasing, rapid adoption of point set surface acquisition techniques, namely lidar and SfM, that deliver noisy surface samples of real objects in 3D leads to a variety of surface reconstruction methodologies that deliver mathematically ill-defined discrete surfaces. Precise surface reconstruction schemes with theoretical guarantees, such as Delaunay Triangulation [24] or α-shapes [81], often fail as not being robust to noise. Although the less rigorous reconstruction constraints are advantageous for applications that involve texture mapping from multiple vantage points, it comes at the expense of surface accuracy compared to the originally acquired surface sample while still preventing further volume extensions.

This chapter attempts to order and formalise the digital surface representation and surface reconstruction processes for DOMs by introducing clear notations for the diversity of prevalent surface representations. First, prevalent surface- and volume geometry representations available within the geosciences are presented. Then, the new notation is introduced to formalise the geometry. This formalisation then allows the development of geometrically accurate and mathematically well-defined surfaces reconstruction procedures from noisy-sampled point set surfaces, as subsequently demonstrated. The advantages for the registration of sparsely acquired supplementary im-

agery to a well-defined surface geometry are analysed and it is discussed how to incorporate existing image texture mapping approaches within digital outcrop geology into the novel, *exact mathematics*-dominated surface reconstruction scheme. A final case study on the Brimham Rocks outcrop (Yorkshire, UK) demonstrates how the mathematically rigorous formulation allows to construct tetrahedral volumetric meshes from the topographic surface geometries of original, noisy-sampled point set surfaces (e.g. acquired via SfM and lidar). This approach has previously not been explored, as most volume meshing methods are based on computer-aided design (CAD) principles of volume decomposition.

2.1 Existing Representations of Topographic Surfaces and Volumes within the Geosciences

The starting point of our investigation is triangular surface representations, commonly used for DOMs in particular and topography in general within the geosciences. The geometric representation can be supplemented with radiometric information. In the case of triangular surface models, this radiometric information is provided by attaching photo textures to the model. Textures can be used for providing coloured information for the surface (i.e. photo textures), but also for supplementing the model with electromagnetic information outside the visual spectrum (e.g. hyperspectral images as texture [163, 275]), and for artificially increasing the geometric fidelity of the model (e.g. parallax- and displacement mapping, see [215] and [4] for further information). Outside of triangular surfaces, the surface shape of objects acquired by remote sensing can be alternatively described by other means.

Point set surfaces [5] are prominent means of object shape representation, in particular in cases where the shape is the result of a light-probing device (e.g. lidar,measuring the the travel time or phase shift of light particles) or a photogrammetric procedure (e.g. SfM [277], being based on point correlations between images and the disparity computation of these points). This way of shape representation is used in systems and application scenarios of *Virtual Reality Geology Studio* (VRGS) [127, 244, 293, 312], GoCAD (for digital outcrops) [46, 188, 246, 301] and others [3, 103, 316]. These object surface representations are only "quasi-surface" geometries and models, as points without connectivity cannot describe surfaces. The illusion of a surface is only conveyed and possible due to the working principles of CGI and CG.

In early adoption of surface geometries for visual analysis, DEMs were popular in usage within the geosciences (e.g. digital outcrop geology [258, 299, 300]) via GIS software [138]. DEMs are an artificial concept originally proposed within CG [194], synonymous to height maps or height fields [94], for the purpose of simplified digital representation and the ease of implicit connectivity calculations. They are an artificial concept because they have no relevantly distinct definition compared to DTMs or digital surface models (DSMs): Let S be a surface composed of a grid-based set of quads Q connecting either (a) a vertex set $v \in V, v \in \mathbb{R}^2$ with a connected elevation-representative attribute function $f(v) = y, y \in \mathbb{R}$ (i.e. height map notation) or (b) a vertex set $v \in V, v \in \mathbb{R}^3$, where the surface normal-parallel coordinate is the elevation indicator (i.e. surface notation). In either case, $S = \{V, Q\}$ which holds equally true for other DSMs that

replace the quad set Q by a triangle set T. Specific to DEMs, for each lateral coordinate the elevation value is unique. For application domain experts, this appears not to be the case for DSMs, but the actual definition neglects an essential property: every surface can be curved and every consistently described curve can be trivially projected on a flat plane [17]. Within this consideration, the restriction of each lateral coordinate on a curved plane also holds true for displacement maps (equivalent to height maps (a)) on DSMs and, in general, curved surfaces. For the definition of a surface with coordinates in 3D (case (b)) and the DSMs themselves, the definition of elevation lacks purpose. In conclusion, for the following sections, DEMs are treated as artificial concepts of surface geometry and formulations and reconstruction procedures focus on the general description of DSMs.

DSM representations, also defined as DTMs or TINs, are more recently established as surface geometries for DOMs. They are applied in systems such as *Lidar Interpretation Mapping Environment* (LIME) [37] and VRGS, and are used in several geological studies [84, 208, 224, 252]. A triangular surface can be organised in terms of a piecewise-linear complex [121] or a polygonal soup [115], composed of 2D elements (i.e. triangles) within 3D space, and the differences between them impact geological applications.

Another popular method of reconstructing surface geometry is the use of methods originally conceived for sparse-data interpolation, such as kriging [157], Discrete Smooth Interpolation (DSI) [190, 191], Beziér curve and spline interpolation.

For the volumetric reconstruction of subsurface information, the geosciences traditionally favours actual modelling instead of reconstruction of the geological subsurface from outcrops. The most common approach is the modelling of cubic, gridded, uniformal, laterally isotropic and vertically anisotropic meshes (i.e. geocellular models) using the information from outcrop observations [88, 139]. It largely relies on the geology and less on surface-constrained geometry (in a strictly-mathematical sense).

The currently most precise and mathematically-accurate formal volume representations are sealed geological models, introduced by Caumon et al. [48, 49] and recently adapted to specific applications [47, 229, 255]. Mathematically, the construction of a sealed geological model, although different in methodological detail, shares the common idea of discrete volume construction by space partitioning and splitting with Delaunay- and Voronoï-based volume reconstruction approaches. Let $\mathcal{V}$ be a volume of tetrahedra $t \in \mathcal{T}, t = \{v_n, v_{n+1}, v_{n+2}, v_{n+3}\}$ connecting a set of vertices $v \in V, v \in \mathbb{R}^3$ fully occupying the 3D space it is embedded in. Then, the construction of volumetric objects is the result of a space partitioning by splitting tetrahedra along a user-defined intersection surface S, so that $t \in \mathcal{T}, t \cap S \longrightarrow \{t_1, t_2\} \in \mathcal{T}$, where one new element is part of the delineated volume model I enclosed by S ($t_1 \in I$) and the other is outside ($t_2 \ni I$). This method is also conceptual similar to one computer-aided design (CAD) approach for creating volumetric objects by removing excess material around it – an approach commonly used in mechanical manufacturing. For the purpose of this work, is has to be noted that this method only works iff strict mathematical criteria and constraints on the geometry of the encompassing surface (see [7, 24, 111, 201]) are met, which has to date not been shown with noisy-sampled digital outcrop data. Tetrahedral volume meshes are essential to physical and physics-based analysis within the geosciences. Examples are fluid flow analysis [78, 216], coupled thermal, hydraulic, mechanical and chemical (THMC) analysis [229, 255] and finite-element analysis (FEA) [49, 268]

for mechanical stresses, crack formation and material deformations, also outside the geosciences [28, 155].

2.2 Definitions of Dimensionality, Connectivity and Projectivity

For the deduction of the geometric notation and formulation, the geometric properties of dimensionality and algebraic genus of surfaces are of pivotal importance. Jones et al. formerly published a study on the data dimensionality within the geosciences [140], initiated by the term ”2.5D data“ for outcrop surface descriptions and its validity thereafter, which is taken as a starting point due to its deep discussion of the matter. By resolving the prevalent ambiguities on the existing concepts, a novel notation emerges. Subsequently, the introduction of the algebraic genus allows a clean distinction between the current discrete surface geometry descriptions in use, which completes the formulation.

Jones et al. discuss the following definition of dimensionality in the article's introduction: "Within the traditional mathematical framework based on Euclidean geometry [...], a single point has a topological dimension of zero. Similarly, a line or curve connecting two points is one-dimensional, a plane or surface is two-dimensional and a volume is three-dimensional" (Jones et al., [140], p. 354). It is therefore evident that the dimensionality of an object is defined by the dimensionality of its constituting elements (i.e. topology) and not the space the object is commonly embedded in, as each lower-dimensional object can be embedded in higher-dimensional spaces (subsequently explained via projectivity). This is the basic reason why data dimensionality based on the embedding space is wrong: such a definition is essentially arbitrary ([140], p.355), inconsistent and ambiguous in the presence of a correct and unambiguous definition (i.e. topology). The topological definition is the convention subsequently applied and advocated.

The arbitrary definition of the embedding space (i.e. the underlying euclidean coordinate system) is arguably resolvable by coordinate system mapping for point coordinates. The principle is explained with two 3D coordinate systems (eq. 2.1- 2.4). Let β_1 be the original coordinate system and β_2 the target system, P being the original point in β_1 to transform, $[u \quad v \quad w]$ being the major axes, and $[x \quad y \quad z]$ being the common 3D coordinate values. Then, the transformation is as follows:

$$\beta_1 = \begin{bmatrix} x_{u_1} & x_{v_1} & x_{w_1} \\ y_{u_1} & y_{v_1} & y_{w_1} \\ z_{u_1} & z_{v_1} & z_{w_1} \end{bmatrix} \tag{2.1}$$

$$\beta_2 = \begin{bmatrix} x_{u_2} & x_{v_2} & x_{w_2} \\ y_{u_2} & y_{v_2} & y_{w_2} \\ z_{u_2} & z_{v_2} & z_{w_2} \end{bmatrix} \tag{2.2}$$

$$P' \in \beta_2 = \beta_2 \beta_1^{-1} P \tag{2.3}$$

$$P' \in \beta_2 = \beta_2 P \tag{2.4}$$

The mapping of coordinate systems is a process – from one system into another. Therefore, the assumption is that β_1 and β_2 (a, eq. 2.3) share the same basic euclidean

space that needs a clear, absolute (i.e. independent; non-relative to another system) definition, or (b, eq. 2.4) are directly transformable (e.g. β_2 is dependent on β_1). Digital outcrop surfaces are georeferenced (which is an absolute reference), but in practice some lidar systems violate the independency criterion in their project coordinate systems (PCS), which can make it impossible to use the data in further analysis coherently and make statements on their dimensionality outside the original acquisition system. This raises the final issue on the coordinate systems: if the data are non-transformable between systems as they lack a valid coordinate system definition, it is not possible to say with certainty what the data dimensionality is, as the coordinates are arbitrary.

Another solution offered by Jones et al. is to define the data dimensionality based on the dataset as a whole: "For example, a data set is described as "1D" when the data collectively represent a line, even if the set is a zero-dimensional point" ([140], p.355). This allows a better definition, as the word "represents" includes the idea that the data is more than the collection of points, leading to the prevalent notation of *connectivity* to represent *topology*, which resolves the ambiguity.

Let S be an object only represented by its constituent data points p with dimensionality N:

$$p \in P \tag{2.5}$$

$$p \in \mathbb{R}^N \tag{2.6}$$

$$S = \{P\} \tag{2.7}$$

Then, the connectivity $\mathcal{C}$ can be expressed as empty set, or a zero-dimensional connectivity:

$$\mathcal{C} \in \mathbb{R}^0 = \emptyset \tag{2.8}$$

This extends the original notation (eq. 2.7) of the point set as follows:

$$S = \{\mathcal{C}, P\} = \{P, \mathcal{C}\} = \{P, \emptyset\} \tag{2.9}$$

Within this notation, the points p are (according to prevalent terminology in geometry [17, 225]) termed *vertices*, for which their dimensionality represents attributes (i.e. spatial for $N \leq 3$) referred to as *coordinates*. For geometry that fulfils eq. 2.9 (e.g. a cluster of points as a vertex set; point set surfaces), the positions represent the object itself and the dimensionality of the object refers to the dimensionality of the embedding coordinate system (i.e. *nD coordinates*). These objects are not surfaces and, in order to avoid verbal ambiguities, they can be termed "nD point sets/point geometry/samples".

If an object has connectivity, then the dimensionality of the topological structure defines the dimensionality of an object (i.e. lines = $1D$, surfaces and polygons = $2D$, volumes and polyhedra = $3D$, polytopes = nD). The dimensionality can be most simply determined by taking the respective simplest representative primitive (i.e. line segment in 1D, triangle in 2D, tetrahedron in 3D).

Adapting the multidimensional formulation to the common first four dimensions currently encountered within the geosciences, the connectivity set $\mathcal{C}$ is replaced by the specific simplex set (i.e. lines L, triangles T, tetrahedra $\mathcal{T}$). For the fourth dimension (and above), the polytope $\mathcal{C}$ needs to be specified explicitly. The resulting consistent triangular surface geometry notation is shown in eq 2.10.

$$S = \{T, V\}. \tag{2.10}$$

The last general property of geometry discussed here is *projectivity*. It clarifies the relationship between geometric space and geometric topology for the given cases, and explains why the selection of the embedding space as the dimensionality criterion is disadvantageous. Projectivity, in this respect, refers to the fact that *mD* geometry in *nD* space can be projected to an $(n-1)D$ space, without resulting in topological changes, as long as $n > m$. The information of the object is equal in both spaces. The reverse process of embedding an *mD* object in *nD* space for $m < n$ is common within geology, for example by embedding geological line data (e.g. cores, wells, borehole data) in the context of 3D space, together with other *lD* geometries (i.e. $m \leq l \leq n$) such as digital outcrop surfaces [140, 244, 312]. The fact illustrates the arbitrary notation of "2.5*D*", where $m = 2$ and $n = 3$: n can be any number higher than m without adding information to the data itself, resulting in the fact that $2.5D = 2D$.

2.3 Surface Geometry Formulations for Polygonal Soups and Piecewise Linear Complices

Based on the above notation and formulation, this section considers the specific issue of surface geometry for DOMs. A discrete surface geometry is the discrete approximation of a continuous, analytical surface. Due to its discretely-sampled and linear approximation, a given surface simplex is defined as piecewise-linear simplex (PLS), and a complex surface composed of simplices is a piecewise-linear complex (PLC) [121]. This only holds true iff the surface approximation is continuously defined. A discontinuous discrete surface is referred to as *polygonal soup* [115, 315]. From a geometric- and topological perspective every DOM is a composition of connected 2D planar faces of an object in 3D space (i.e. 2D geometry). This holds true for surfaces derived by height maps, or surfaces modelled by CAD-like processes (as PLC), or constructed from (optical) field instruments as polygonal soup. This mathematical rigour contrasts currently established, less consistent definition in the (computational) geosciences- and geomatics literature. In order to indicate that the work considers objects in 3D space and to provide a relation to the prevalent literature on the topic of digital outcrop geology, we refer to DOMs as "3D surface geometries" or "3D surface models". Volume models are, by the previous definition, "3D geometries", often termed *solid geometry* in application-domain literature.

Let a DOM be a triangular surface mesh according to eq. 2.10:

$$S = (T, V) \tag{2.11}$$

$$V \in \mathbb{R}^3 \tag{2.12}$$

For some combinatorial and morphological algorithms, it is advantageous to include a set of edges E in the definition, so that

$$S = (T, E, V) \tag{2.13}$$

$$\forall\, e \in E, e = \{i_0, i_1\} \in \mathbb{N}^2. \tag{2.14}$$

The geometric properties of the surface can vary depending on the method by which a DOM is obtained and processed to construct S. The surface model can be a collection of n manifold, curved PLCs (i.e. curvilinear surfaces) of geometric (i.e. algebraic) genus 1 [121][18], so that

$$S = \{S_0, ..., S_i\} \quad \forall i = [0, n] \tag{2.15}$$

$$S_i \in C^1. \tag{2.16}$$

Each constituting PLC S_i is a subset of its related orientable, topologically-closed C^2 manifold surface that adheres to strict Delaunay constraints (see [7, 24, 111, 201], also referred to as a "watertight surface"). An example of the construction of PLC DOMs from a dense, irregular point set into a closed surface with geometric guarantees is shown in fig. 2.1(a) to 2.1(d).

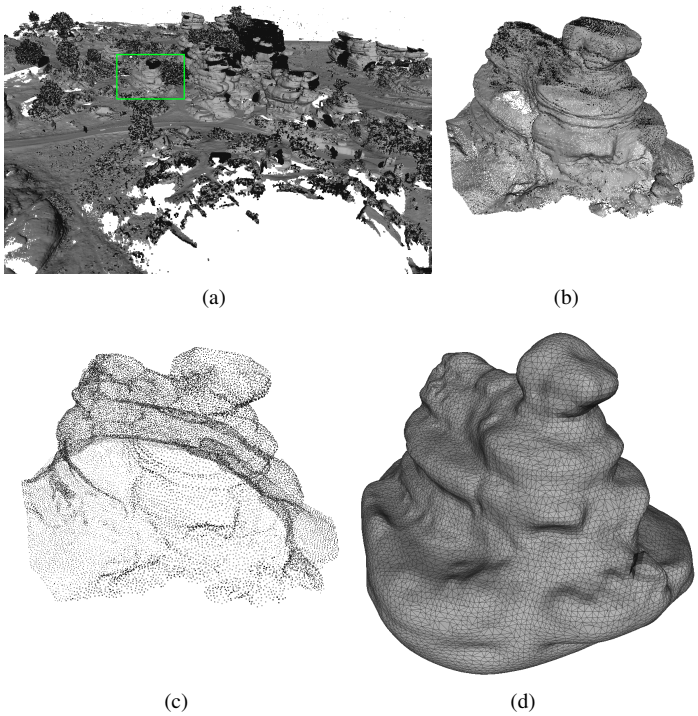

(a) (b) (c) (d)

Figure 2.1: Illustration of surface reconstruction process into piecewise linear complex from a point set acquired via TLS. A rock section (b) is extracted from the full-scale outcrop scan (a). An equidistant point subset is extracted via Poisson disk subsampling (c). Then, a Poisson surface reconstruction of a second-order manifold is created and existing, minor geometric inconsistencies are repaired to form a PLC surface with geometric guarantees, ready for subsequent volume processing (d).

[18] Simplified, condensed explanation of the genus property of algebraic curves - `https://www.encyclopediaofmath.org/`, topics of "Genus of a curve" and "Rational surfaces".

More prevalent within geology are less rigorous surface descriptions that can be obtained by simpler means of geometric processing and triangulation of algebraic, point-sampled surfaces. This merits in the formation of *polygonal soups*, which is a set of unstructured triangles or mixed triangulated polygons [115]. Formally, these models represent a collection of n potentially non-manifold surfaces without explicit genus, so that

$$S = \{S_0, ..., S_i\}. \tag{2.17}$$

The less rigorous formulation allows for more freedom in the application for splitting and subdividing S, as it does not need to adhere to geometric or topological constraints during the splitting. As a result, the surface patches of the splitting do not need to relate to separate orientable, manifold surfaces. This has advantages for applications that involve surface parameterization and texturing from arbitrary image sets, as is subsequently explained. The disadvantages of these models are their unfavourable geometric properties, being inconsistently oriented, potentially non-manifold, containing holes and self intersections, and are *mathematically ill-defined* [315]. Fig. 2.1(a) shows a larger area of the geological structure in fig. 2.1(b), which is subsequently modelled as a polygonal soup according to one of the prevalent workflows for digital outcrops [35] shown in fig. 2.2(a). Fig. 2.2(b) highlights the separate entities of the polygonal soup in a colour-coded representation, which correspond to different texture area explained in the following section (fig. 2.2(c)). These models contain four unfavourable geometric properties of polygonal soup surfaces, namely:

- inconsistent planar orientation (fig. 2.3)
- presence of non-manifold sections (in this case visible as *flakes* [153], fig. 2.4)
- triangulation discontinuity (fig. 2.5)
- formation of holes

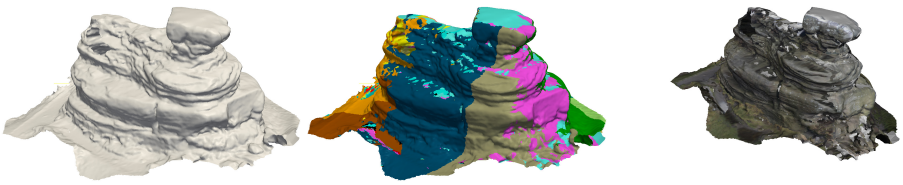

(a) (b) (c)

Figure 2.2: Illustration of a common DOM in form of a polygonal soup of triangle fans (a). The original point set is subsampled to triangular patches S_i (b), which are manually cleaned and gross errors corrected in a manual process. Still, several holes remain in the geometric representation (a). Each patch is subsequently textures with DSLR photos for a visually high-quality dataset (c) used in subsequent geological applications.

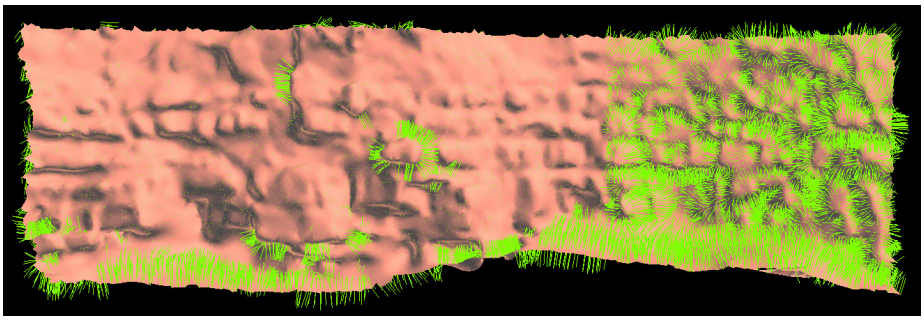

Figure 2.3: Orientation inconsistencies within a polygonal soup model, where the left-hand side of the model points away from the viewer in this image while the right-hand side points towards the viewer. The inconsistency is due to the arbitrary surface split, of which the separation boundary is clearly visible within the image.

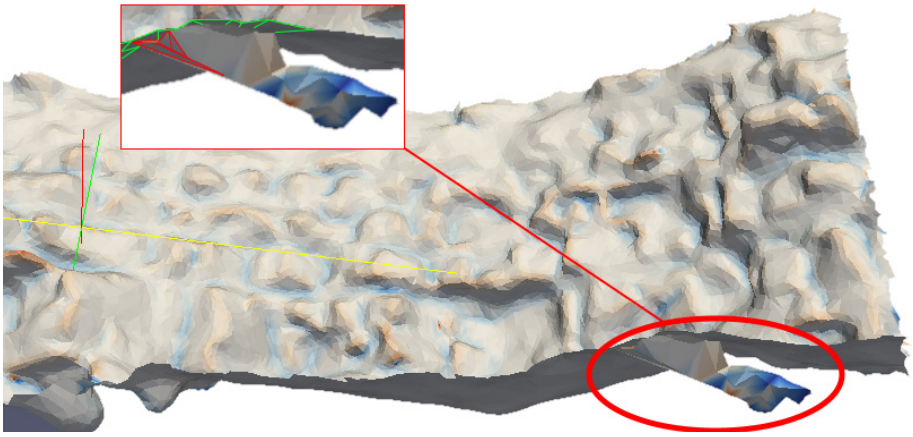

Figure 2.4: Topologically non-manifold geometry section of a polygonal soup model (same model as in fig. 2.3) from invalid triangulation. The triangulation in this case forms a flake to the local umbrella of the main geometry (see [153] for explanation of the terms). The main surface section and the flake (see inset) are topologically connected.

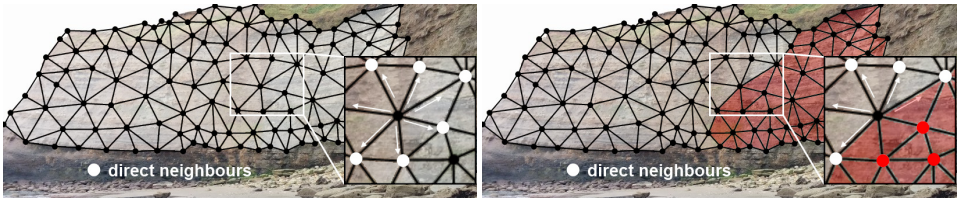

(a) piecewise-linear complex (PLC) (b) polygonal soup

Figure 2.5: Triangulation discontinuity of a polygonal soup surface, in contrast to continuous PLC representations. The discontinuity leads to two separate surfaces in one object. Extracted surface objects (e.g. via interpretation) at the discontinuity or defining a consistent manner of doing so is topologically undefined.

2.4 Image Registration and Local Parameterization of Textures

In order to simplify the local parameterization by reducing user input, it is suggested to transform a given surface geometry into an ortho-normal view for a respective photo camera external orientation and positions. Let $G_{3,4}$ be a cartesian, three-dimensional world coordinate system with positional information in matrix notation of which $G_{4,4}$ is the homogeneous affine transformation matrix. The studied surfaces (or surfaces patches) S_i are to be defined in this world coordinate system. Let $F_{4,4}$ further be a local, perspective camera coordinate system in its homogeneous, affine transformation matrix form, which is to be the ortho-normal basis for a subsequent image projection. Both systems are defined by their origin o and ortho-normal axis orientations, composed of horizontal (u), vertical (v) and normal (n) direction. A right-handed coordinate system, as common to most three-dimensional algebra notations in graphics, is taken as the basis for all 3D transformations. The task for the image registration is then to compute a transformation matrix $P_{4,3}^{-1}$ (and $P_{4,4}^{-1}$ as homogeneous transformation matrix) from $G_{3,4}$ to $F_{4,4}$, which is referred to as the *pose* and analogous to the external camera orientation $P_{3,4}$. The matrix layouts (eq. 2.18 to 2.23) is as follows, according to the notation above:

$$F_{4,4} = P_{4,3}^{-1}\, G_{3,4} \tag{2.18}$$

$$F_{4,4} = \begin{bmatrix} x_{u,f} & x_{v,f} & x_{n,f} & x_{o,f} \\ y_{u,f} & y_{v,f} & y_{n,f} & y_{o,f} \\ z_{u,f} & z_{v,f} & z_{n,f} & z_{o,f} \\ 0 & 0 & 0 & 1 \end{bmatrix} \tag{2.19}$$

$$G_{3,4} = \begin{bmatrix} x_{u,g} & x_{v,g} & x_{n,g} & x_{o,g} \\ y_{u,g} & y_{v,g} & y_{n,g} & y_{o,g} \\ z_{u,g} & z_{v,g} & z_{n,g} & z_{o,g} \end{bmatrix} \tag{2.20}$$

$$P_{3,4} = [R_{3,3}\ T_{3,1}] \tag{2.21}$$

$$C = -R^T\ T \tag{2.22}$$

$$P_{4,3}^{-1} = \begin{bmatrix} R_{1,1} & R_{2,1} & R_{3,1} \\ R_{1,2} & R_{2,2} & R_{3,2} \\ R_{1,3} & R_{2,3} & R_{3,3} \\ C_x & C_y & C_z \end{bmatrix} \tag{2.23}$$

The pose $P_{4,3}^{-1}$ is used as the model-view transformation matrix for all surface patches S_i. Subsequently, the surface information are projected on the related camera image plane using the internal camera orientation (referred to as $A_{3,3}$) as projection matrix (eq. 2.24, equal to computer vision notation in the literature [142]).

$$A_{3,3} = \begin{bmatrix} f_x & 0 & c_x \\ 0 & f_y & c_y \\ 0 & 0 & 1 \end{bmatrix} \tag{2.24}$$

In eq. 2.24, f_x and f_y are the vertical and horizontal focal length (where, in a perfect pinhole camera, $f_x = \frac{width}{height}\ f_y$), and c_x and c_y are the principal coordinates (i.e. centre coordinates) of the camera coordinate system. The overall transformation of surface vertex coordinates $V(S_i) \in \mathbb{R}^3$ to local camera coordinates $V'(S_i) \in \mathbb{R}^2$ is expressed in eq. 2.26, combining eq. 2.21 and 2.24 (in accordance with OpenCV, see `http://docs.opencv.org/2.4/modules/calib3d/doc/camera_calibration_and_3d_reconstruction.html`).

$$s\ m' = A\ [R|T]\ M' \tag{2.25}$$

$$s \begin{bmatrix} u \\ v \\ 1 \end{bmatrix} = \begin{bmatrix} f_x & 0 & c_x \\ 0 & f_y & c_y \\ 0 & 0 & 1 \end{bmatrix} \begin{bmatrix} R_{1,1} & R_{1,2} & R_{1,3} & T_x \\ R_{2,1} & R_{2,2} & R_{2,3} & T_y \\ R_{3,1} & R_{3,2} & R_{3,3} & T_z \end{bmatrix} \begin{bmatrix} X \\ Y \\ Z \\ 1 \end{bmatrix} \tag{2.26}$$

$$V'(S_i) = \begin{bmatrix} u \\ v \end{bmatrix}; V(S_i) = \begin{bmatrix} X \\ Y \\ Z \end{bmatrix} \tag{2.27}$$

In order to simplify the remainder of the local parameterization, the transformation via homogeneous coordinates for a camera is defined as follows (eq. 2.28):

$$G^{4,4} = A_{4,4}\ P_{4,4}^{-1} \tag{2.28}$$

For polygonal surface sets, there is a unique per-segment projection matrix for each segment, whereas each projection matrix is independent and does not span a continuous space across the surface S. Henceforth, the projection matrices contribute to matrix set $\mathcal{G}$ as follows:

$$\mathcal{G} = \{G_0^{4,4}, G_1^{4,4}, ..., G_i^{4,4}\} \quad \forall i = [0, N]. \tag{2.29}$$

Determining a fitting texture mapping can also generally expressed as follows:

$$V(S)' = G^{4,4}\ V(S) \tag{2.30}$$

A globally consistent mapping function $G^{4,4}$ does not exist for polygonal soups and noisy surfaces of natural objects, acquired by means of optical field instruments (e.g. laser, structured light), due to the lack of geometric control. Therefore, the acquired surface geometry is split into separate surface sets $S = \{S_0\ ...\ S_i\} \quad \forall (T, V) \in S$, where each surface mesh entity belongs to a specific image that allows a direct mapping. While vertices in V can be shared between meshes, the membership of each triangle $t_i \in T$ is mutually exclusive between mesh entities, so that

$$t_i \in T(S_i), t_i \ni T(S_j) \quad \forall i, j = [0, n], S_i \neq S_j. \tag{2.31}$$

As a result of this mesh splitting, each mesh entity has a separate, local parameterization for the 2D image mapping, so that

$$V(S_i) \in \mathbb{R}^3, V(S_i)' \in \mathbb{R}^2 \tag{2.32}$$

$$V(S_i)' = G_i^{4,4} V(S_i). \tag{2.33}$$

One set is added for completeness of the notation that contains all triangles without a valid local parameterization or a corresponding image texture, meaning that the mapping function equals the identity matrix:

$$V(S_n)' = G_n^{4,4} V(S_n) = V(S_n), G_n^{4,4} = I^{4,4} \tag{2.34}$$

The mapping can also be rewritten in form of a matrix operation $G_i^{4,4}$ relative to a specific vertex space of a mesh $V(S_i)$ and camera space $V(S_i)'$, resulting in

$$G_i^{4,4}(V(S_i), V(S_i)'). \tag{2.35}$$

This screen coordinate transformation is, for the given surface patches inside the camera space and its related image, equivalent to the local parameterization. A surface parametrization is required for texturing the surface with a set of images. The parameterization represents a coordinate system mapping from the surface vertices in 3D to the texture coordinates in 2D [176]. Subsequently, this original notation by Lévy is converted to the previously established notation for clarity.

Let S be a surface sample with coordinates (x,y,z), then there exists a mapping function $\mathcal{U}$ into local 2D space.

$$(x,y,z) \in S \longrightarrow \mathcal{U}(x,y,z) = \begin{pmatrix} \mathcal{U}_u(x,y,z) \\ \mathcal{U}_v(x,y,z) \end{pmatrix} \tag{2.36}$$

There exists an inverse function $\mathcal{X}$ for mapping coordinates from local space to geometric space $\mathbb{R}^2 \longrightarrow \mathbb{R}^3$, which is called *parameterisation*.

$$(u,v) \in \Omega \longrightarrow \mathcal{X}(u,v) = \mathcal{U}^{-1}(u,v) = \begin{bmatrix} x(u,v) \\ y(u,v) \\ z(u,v) \end{bmatrix} \tag{2.37}$$

This process maps to the previously presented notation as follows: $\mathcal{U}(x,y,z)$ is a piecewise linear function that does, in the end, a projective mapping $\mathbb{R}^3 \longrightarrow \mathbb{R}^2$. The basis of the mapping is the 3D input vertex set of surface S, so that

$$(x,y,z) \in V(S), V(S) \in \mathbb{R}^3. \tag{2.38}$$

The target output are image coordinates of a linear 2D image space $\mathcal{I} \in \mathbb{R}^2$. The mapping function is a linear, unconstrained projection without free, user-defined variables, and thus a projection matrix.

$$\mathcal{U}(x,y,z) = G^{4,4} \tag{2.39}$$

The resulting projection matrix $G_i^{4,4}$ for each surface patch S_i maps the respective vertex coordinates in $\mathbb{R}^3$ to image coordinates in $\mathbb{R}^2$.

$$V(S) \in V(S_i)\ \forall p, p' = (u,v)^T = G_i^{4,4}\ p \quad | \ (u,v) \in [0,1] \tag{2.40}$$

$$V(S_i) \ni V(S_j)\ \forall j \neq i \tag{2.41}$$

The parameterization is analogous for the colouring point set surfaces, with the difference being the absence of a triangle set S, the membership of the vertices in S being mutually exclusive to each parameterization set, and that the methods to obtain a projection matrix G differ between triangle meshes and point set surfaces.

Image-to-geometry registration methods aim at mapping arbitrary images $\mathbb{I} \in \mathbb{R}^2$ to the provided surface model segments of a DOM $S_i \in S$ by computing the local parameterizations $G_i^{4,4}(\mathbb{I}_i, V(S_i))$.

The adopted workflow for the mathematically-coherent surface reconstruction and a subsequent, globally-consistent texture mapping, which is proposed to be adopted in the future, is as follows:

1. C^1 or C^2 surface reconstruction by provably coherent triangulations (see [7, 24, 75, 267]
2. consistent surface parameterization (fundamentals [69,96,176], texture atlas parameterization [177], method for trivial per-triangle parameterization in MeshLab [233]; simple if triangulation is done properly)
3. texture mapping into a temporary space (e.g. parameterization of current polygonal sets), in order to provide a photo–geometry connection
4. parametric translation from temporary texture space to the consistent surface parameterization
5. final texture mapping into a texture atlas [233]

2.5 Tetrahedral Volume Reconstruction from Point-Sampled Surface Geometry - An Example from Brimham Rocks, North Yorkshire, UK

Brimham Rocks is particularly applicable to volumetric geology studies and also technical development aimed at volumetric DOM modelling. The individual rock sections are easily separable, which allows detailed volume modelling directly from the noisy lidar data on a technically feasible scale. Fig. 2.6 illustrates the volumetric modelling workflow applied for a prototypical case study: the specific section of interest is extracted from the overall lidar dataset. Vegetation, noise-related artefacts and other distorting scan elements are initially removed in an interactive procedure within dedicated, open source 3D point set software, such as MeshLab[19] [55, 243] or CloudCompare [20] [108]. Subsequently, a high-resolution C^2 PLC is constructed from the point set within MeshLab via Poisson Surface Reconstruction [144]. The result surface is cleaned from manifold edges and triangles, which potentially occur during the surface reconstruction from noisy artefacts. In addition, the surface model is checked and cleaned from triangle self-intersection. After final checks within MeshLab, jmesh[21] [12] or Computational Geometry Algorithms Library (CGAL) [22] [32, 115, 182] guarantee a closed, non-self-intersection surface, the tetrahedral volume reconstruction via Tetgen [270] is applied. This results in a fine-grading, tetrahedral FEA volume mesh applicable for subsequent physical simulation and analysis. In order to be applied for

further geological case studies, the 3D model needs to be interpreted with respect to its constituting geological facies. Approaches that potentially allow this volumetric incorporation of geological knowledge based on DOMs was recently presented by Caumon et al. [47]. The resulting mapping leads to the formation of interfaces from geological features along which the mesh is segmented [46]. Alternatively, the 3D geometry can be assembled from a set of shared interface vertices $\mathcal{V}_{Int}$ into multi-material meshes [26, 148, 202], potentially facilitating subsequent geophysical simulations.

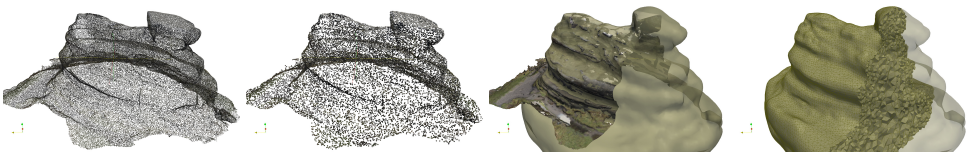

(a) (b) (c) (d)

Figure 2.6: Workflow of volume reconstruction of geological outcrop models: starting with an initial point set (a), the point set is cleaned and subsampled (b). The clean point set is the basis for the C^2 surface reconstruction (c). After establishing the geometric guarantees expected for C^2 surface, a tetrahedral volume meshing algorithm creates a FEA-ready 3D geometric model of tetrahedral elements (d). Further processes within petroleum geology demand at this stage an interpretation of the model to proceed.

2.6 Conclusion and Discussion

This work presented a new formulation and notation for the surface geometries and their relation to photo textures of digital outcrops in a mathematically consistent framework. The relation of definitions on the subject, the dimensionality, topological shape and projectivity with respect to their geometric description have been highlighted for geometries commonly used within the geosciences. More specific to the surface geometries of outcrops, the distinction between continuous, consistent piecewise linear complex representations and less rigorous polygonal soups has been highlighted, as these are the currently existing forms of representation in use. The relation of the surface description and its photo texture for both forms of representation has been analysed via local parameterisation.

One of the prominent drawbacks of polygonal soups is their inability to be used for volumetric approximations. As we have shown on the example of Brimham Rocks, a continuous representation of PLCs resolved the issue and allows a direct volume reconstruction via tetrahedralisation. Although presented on the scale of a full outcrop, the presented mathematical concepts are scale-independent by design and thus hold also true for the volume reconstruction of hand samples (i.e. digital rock samples [10]) and the volume extrusion of partial surfaces of the outcrop.

[19] MeshLab - `http://www.meshlab.net/`

[20] CloudCompare - `www.danielgm.net/cc/`

[21] The jmesh library - `http://jmeshlib.sourceforge.net/`

[22] Computational Geometry Algorithms Library - `http://www.cgal.org/`

One limitation of the presented work is that the notations and concepts hereby presented are only complete for geometries up to the second dimension (i.e. points, lines and surfaces). The complete description of axioms for 3D geometry is more involved in terms of sampling criteria and further topological constraints. As a consequence of that, the actual volume reconstruction process is not explained in mathematical detail. Unconstrained, generally applicable reconstruction procedures of volumes from arbitrary point samples of their shape is still an active research domain in applied mathematics. The currently most consistent way described in this work is to validate and modify a given point sample for its surface reconstruction so that it fulfils volume reconstruction criteria (e.g. ε-sampling [8, 24, 201, 269]). Iff the given sampling conditions are met, the statement is true that every closed C^2 surface can be unambiguously tetrahedralised without the addition of artificial surface samples (i.e. Steiner points), as proven by George et al. [107]. This process of tetrahedral volume mesh generation is currently dependent on the knowledge and complete comprehension of reconstruction algorithms for closed C^2 surfaces by the modeller.

With respect to the presented work, we also point out that the applied *nD* generalisation is only meant for the generalisation of the notation and formulation. The reconstruction of surface geometry in higher-dimensional spaces demands more than just the limited set of axioms and terms presented in this work's notation. The reconstruction of *nD* geometry itself is a major research domain in theoretical mathematics, and this work claims not to be applicable to any *nD* reconstruction for $n > 3$.

Also, the work did not discuss the dimensionality of attribute data of related geometries, which is a separate subject unrelated to the representation of object geometry. This discussion is out of the scope of this work.

Considering the application side of the given notation, a re-occurring topic within digital outcrop geology is the three-dimensional extrusion of surface-mapped facies geobody boundaries through outcrops. Practically, this technique only works reasonably reliably if there are studied digital outcrops with enough dimensional variability (referred to as "degree of three-dimensionality“ in popular terminology) so that geobodies intersect the terrain surface multiple times. Technically, the clean extrusion of the geobody surfaces along arbitrary orientations resulting in convex-concave 3D geometry is not possible with the polygonal soup DOMs. If the interpretation's surface and its vertices are member of separate polygonal sets, their surface orientations is potentially inconsistent. Inconsistent surface descriptions prohibit the semi-automatic extrusion of reference cross-section surfaces towards their three-dimensional envelope or its volumetric geometry in ways previously demonstrated in CG [266]. In fact, the statement can be generalised as the majority of geometric algorithms, which are necessary to achieve some of the desired 3D analytical capabilities for DOMs, do not process polygonal soups due to the known inconsistencies. Some dedicated geometry software packages (e.g. CGAL) allow the conversion of polygonal soups to C^1 or C^2 geometry to solve the issue for specific cases.

With respect to the original paper of Jones et al. [140], we propose an adapted categorisation of the dimensionality of given datasets in table 2.1. The *structure of subsurface* scenario is left out intentionally because its distinction with deep seismic surveys is irrelevant to this specific discussion. In addition to the original categories, digital rock models [10], sealed geological models [48], CT stacked image analysis [184] and geobody extrusion from outcrops are added. Changes to the original classification are

highlighted in grey. Furthermore, the column of "positional data" is replaced by the space dimensionality of the encompassing space of the vertex information that is commonly used for the respective data. While the sampling technology has an influence on the vertex information dimensionality and it is vital for the geoscientist to know about each technology so much in order to make educated conclusions of what a technology can and cannot deliver, there are too many technologies that are applicable to each study purpose so to justify listing them all. Thus, the technology column of Jones et al. is omitted for brevity and clarity reasons and a technological note is appended to the vertex space dimensionality where distinction is necessary.

Table 2.1: Descriptions of Dimensionality, following the principles of discrete geometry and topology

Purpose of the study	(Vertex) space dimensionality	(Geometric) data dimensionality
Fracture spacing analysis	3D	1D
Mineral concentration in soil	2D	0D = 2D point set
Water contaminant concentration	3D	0D = 3D point set
Geological mapping	2D (pen-and-paper)	2D
Geological mapping	3D (GPS)	2D
Detailed geological surveying	2D (plane table)	2D
Detailed geological surveying	3D (GPS)	2D
Fold curvature analysis	3D	2D
Fault plane roughness	3D	2D
Contour map	3D	2D
DEM	2D	2D
DEM	3D	2D
DTM	3D	2D
DOM	3D	2D
Shallow subsurface (GPR)	3D	3D
Deep subsurface (seismic)	3D	3D
CT analysis	3D	3D
Sealed geological modelling	3D	3D
Digital rock models	3D	3D
Outcrop geobody extrusion	3D	2D–3D

III

Chapter 3

Interpreting Digital Outcrops

3.1 Geological Interpretations

The development of digital interpretation techniques for outcrop geology demands initially a clear distinction between *observation* and *interpretation*. In short, observation refers to the objective documentation of visual properties of the outcrop and is directly connected to the measurement and logging of geological quantities. The interpretation subsequently refers to the subjective synthesis of the collected information, putting them into a specific context of an underlying geological concept and concluding on potential geological links of structures and processes that formed the observed outcrop.

More specifically, the aim of geological observations is the documentation of the rock structure and its content across different scales. The major scales for geological reservoir modelling are illustrated by Issautier et al. [134], which is subsequently also taken as the basis for the different scales in geological observation. The major documentation tools for the observations are geological sketches (general), sedimentary logs (sedimentology), tilt meters (angular measurements) and stereonets (statistical plots of angular measurements). On larger scales (i.e. along the full outcrop face), the observations concern major structural- and stratigraphic features, such as strata boundaries (i.e. *horizons*), and structural fault- and fold events (e.g. fault geometry and sediment offset). On intermediate scale regarding spatially limited sections of an outcrop, boundaries of sedimentary objects become visible. Furthermore, within larger sedimentary objects (e.g. meandering channels) depositional details (e.g. accretion lines) become apparent. A major visual indicator for observations at this scale is the rock texture. On even smaller scale, sedimentary logging is used to document grain properties and biocontent for distinct sections of an outcrop. Section 1.3 already discussed the following list of visually observable attributes for the geological interpretation at this scale:

- rock hue (colour) and saturation
- texture- and surface irregularities, such as cleavage and fossils
- ridges and scratches

Micro-scale observations, documented in the lab using microscopes, are out of the scope of this study.

The interpretation stages gathers the observed information in order to reconstruct the originally deposited structures and the geological processes that built and deformed

them during their burial history. Therefore, the reconstruction of depositional processes is of key concern. Furthermore, the interpretation also attempts to extend and extrude the observed two-dimensional information through the rock in three dimensions. As discussed by Issautier et al. [134], the target scale is also of importance for the interpretation. At outcrop-scale, a structural reconstruction of the outcrop in terms of faulting events can be conducted. The reconstruction and correlation of major litho- and chronostratigraphic zones is performed on outcrop scale. In addition, the volumetric reconstruction of geobodies is done at this scale as it involves the correlation of possibly sparsely distributed cross-sections of the geobody objects on the outcrop surface. This step involves including soft knowledge on the local geomorphology. Igneous intrusions such as dykes and sills (if existing in within the formation) can be interpreted at this scale [265]. At smaller sections, the available stratigraphic logs are to be correlated to one another (see Lallier et al. [167] for details). Facies mapping can be performed as a result of the sedimentological analysis and the sedimentary log correlation. The interpretation of erosional surfaces is performed for each individual sedimentary object. Point bar aggradation, paleocurrent directions and other sedimentary details are resolved at smaller scales.

A prime application for digital surface models of outcrops is the interpretation of the previously described sedimentary features. Amongst the various concepts concerning the interpretation, we are interested in the delineation of stratigraphic boundaries and sedimentary objects (i.e. geobodies), and the mapping of sediment facies that describe depositional elements visible in an outcrop. The mapping of structural features (e.g. fractures, faults) only receives auxiliary considerations in this work.

3.2 Digital Interpretation Mapping - A Classification of Existing Representations

As previously discussed, it is possible to distinguish several geobody objects and especially their enveloping boundary from available detailed, centimetre- to decimetre-scale information. The individual, delineated surface objects of a DOM allow the extrusion or extrapolation into consistent 3D geobodies for volumetric analysis, if multiple surface intersections of one and the same geobody are visible on the outcrop. These objects, on the other hand, can be clustered into a predefined facies classification scheme. The semantic grouping of similar regions of the outcrop facilitates statements on the depositional history. The facies description also allows for a probabilistic distribution of continuous, physical attributes based on the semantically delineated regions, which is performed in later stages of the reservoir modelling process (e.g. porosity and permeability distribution). Lastly, the indicator-attributed objects can be intersected with rectangular cells of a gridded geomodel to derive geocellular facies attributes. In this way, the categorisation represents a bridge between the high-resolution, accurate outcrop interpretations and the coarse resolution of common geocellular models, for example MPS TIs. Facies-attributed DOMs can hence be used directly within reservoir modelling for the property population of 3D geocellular grids. Alternatively, the individual objects, on which the facies mapping is based on, can be used to derive statistical geobody shape attributes (e.g. width, height, orientation) to guide the TI construction

indirectly via object-based modelling. The (computational) connection between objects and facies is the indicator value attributed to each object to express its related facies. For objects composed of multiple facies (*at smaller scales*), multiple facies attributes may be possible.

Several approaches are currently available to perform digital facies mapping and object delineation. Traditionally, digital facies mapping is performed on point set surface DOMs by marking all points within an area and directly attach the indicator attribute to each vertex in the point set. In triangulated surface representations of DOMs, the mapping can be integrated as vertex attributes or alternatively derive new surfaces for each object from the underlying DOM. Line digitisations that delineate the geobody object envelopes based on geological interpretations are also common. For completeness, it is also possible to express the facies indicator function in a separate texture overlay. This form of facies representations only recently found its implementation in existing interpretation software and has to date not been applied in a specific case study. Reasons for the slow adoption of this digital facies mapping technique are issues related to derive a geometric facies description from the texture and the lack of texture support in commonplace reservoir modelling software packages (e.g. Irap RMS (Roxar)[15], Petrel E&P (Schlumberger)[16]). As an overview, the digital facies mapping techniques are listed as follows:

- Point-based facies mapping
- Facies mapping on surface geometries
- Line digitisations
- Facies attribute texture mapping

Point-based facies mapping is performed directly on the point set surface that is acquired from the range of optical scanning instruments (e.g. lidar, photogrammetry; see section 1.1) as a first step in the geological interpretation workflow. It is followed by structural modelling of faults and the attribution of sedimentary objects with paleocurrent directions, which are not within the focus of this research. The attribution process marks all points within a polyhedral boundary description with a selected facies indicator. Therefore, there is a *hard link* between the DOM itself and the facies description. The interpretation accuracy is limited to the acquired point density of the DOM, which complicates a facies delineation and makes the extraction of fine details impossible. Examples of a point-based facies mapping are shown in fig. 3.1(a) [244] on a case study of the Nukhul half-graben formation (Suez Rift, Egypt), and fig. 3.1(b) [246] of a case study of the carbonate Gresse-en-Vercors formation (France).

Line digitisations rely on the *picking* [308] operation, in which a ray from virtual viewpoint of the user is cast towards the triangulated DOM surface. The first intersection between the ray and a triangle of the surface model is taken as vertex of a polyline that encloses the delineated sedimentary object. The resulting corner vertices

[15]Roxar Integrated Irap RMS Solution Platform - `http://www2.emersonprocess.com/en-US/brands/roxar/reservoirmanagement/Pages/ReservoirManagementSoftware.aspx`

[16]Schlumberger Petrel E&P Software Platform - `https://www.software.slb.com/products/petrel`

[17]Paradigm GoCAD - `http://www.pdgm.com/products/gocad/`

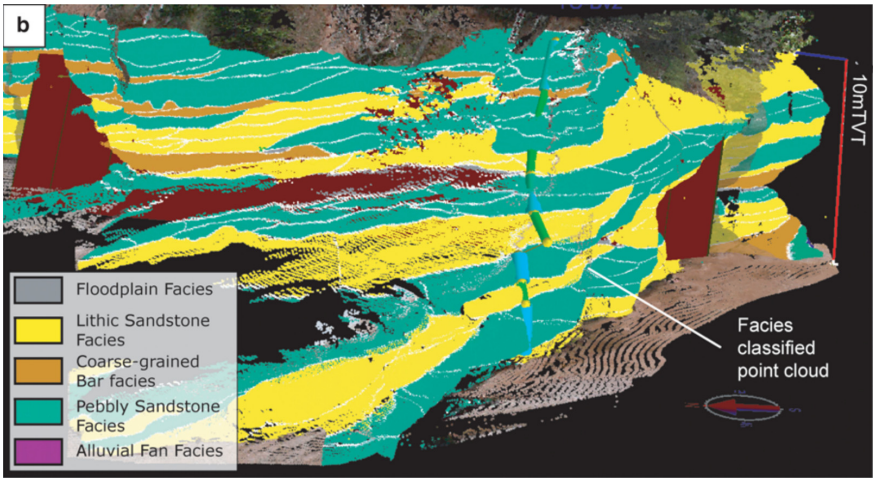

(a) Nukhul half-graben, from Rarity et al. 2014 [244]

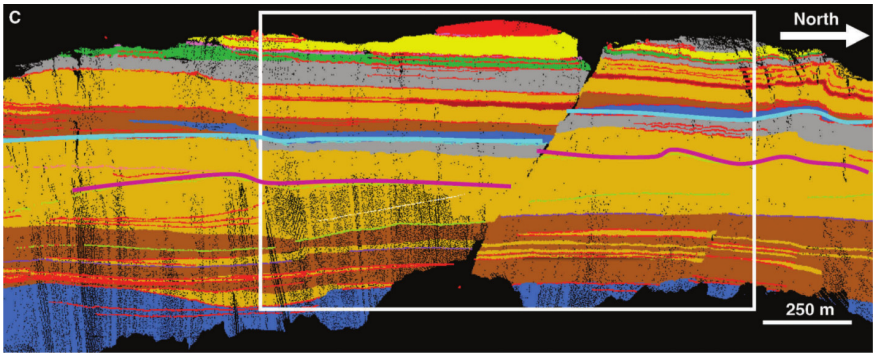

(b) Gresse-en-Vercors, from Richet et al. 2011 [246]

Figure 3.1: Point-based facies mapping techniques

are separate from the underlying DOM, which results in a *soft link* between the facies description and the scanned surface. The resulting (often topologically open) line segments are subsequently used to derive object width and height attributes for a statistical evaluation in the subsequent object-based geomodelling. The work of Eide et al. [84] and Rittersbacher et al. [252] on outcrops of the Book Cliffs and the Wasatch Plateau (Utah, USA), shown in fig. 3.2(a) and 3.2(b), are typical examples for line digitisations.

Facies mapping on surface geometries also relies on the picking operation, but it can be realised twofold:

1. analogous to the line digitisation, but instead of modelling polylines, the interpretation guarantees the creation of closed polygonal surfaces. These can be subsequently triangulated using available geometric algorithms, such as ear clipping [225] or polygonal-constrained Delaunay triangulation [54, 269]. The result is, as with line digitisations, a *soft link* between the DOM and the sedimentary objects. It is alternatively also possible to delineate the of target facies areas.

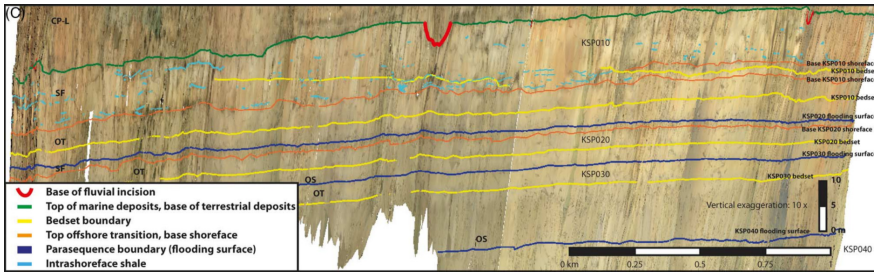

(a) Eide et al. 2014 [84]: Book Cliffs and Wasatch Plateau

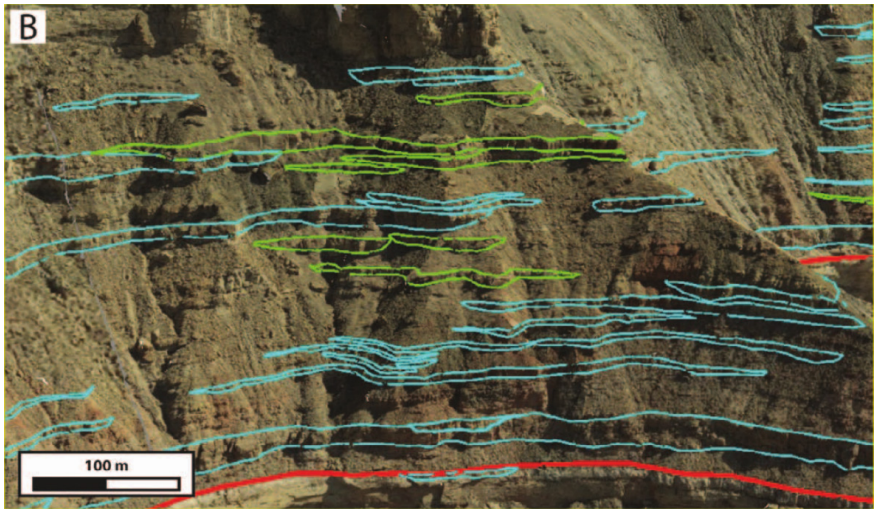

(b) Rittersbacher et al. 2011 [252]: Wasatch Plateau

Figure 3.2: Digital facies mapping via line digitisation

2. compute picking intersection but not utilize the picked vertex directly. Instead, determine the closest triangle vertex within the underlying TIN. The interpretation then spans the area of the DOM enclosed by the interpretation and a facies indicator attribute is derived as triangle or vertex attribute for the constituting DOM elements. The facies mapping is in that case a *hard link*. For preserving the accuracy of the conducted interpretation vertices rigorously, the picked intersection points can be incorporated as geometric elements of the underlying surface (i.e. injecting the picked vertex into the DOM and splitting the related intersection triangle in three distinct elements).

While examples for hard-linked surface-based facies mapping are rarely found in the literature, Olariu presented an example for soft link surface interpretation in a study on the Big Rock Quarry (USA) [224], shown in fig. 3.3.

As formerly explained, facies attribute texture mapping has only recently found its prototypical implementation and integration in Lidar Interpretation Mapping Environment (LIME), shown in fig. 3.4 [39]. The difficulties of the texture mapping approach

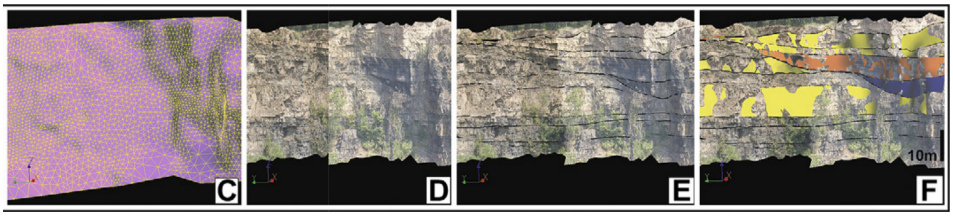

Figure 3.3: Soft link surface-based facies mapping, performed by Olariu [224] on the Big Rock Quarry

are potentially because of the issues arising from transferring the texture-based facies indicators into existing reservoir modelling software. These facies maps are considered *hard links* between the interpretation and the DOM as the facies indicator can be directly determined from the DOM at each scanned vertex position, but they are not directly a geometric attribute as such. A technique that is technically similar to the facies attribute texture mapping is the mapping of synthetic seismic images of an outcrop, illustrated by Lecomte et al. [169].

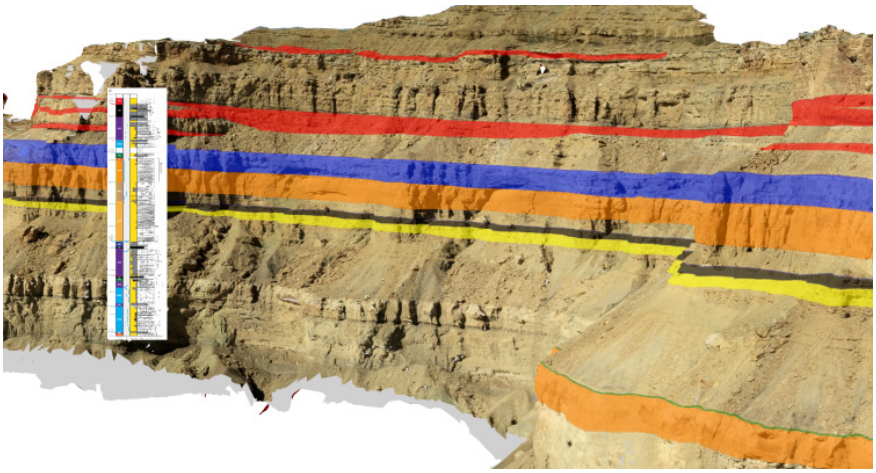

Figure 3.4: Exemplary demonstration of facies attribute texture mapping in LIME at `http://virtualoutcrop.com/lime` [39]

3.3 Classification of published literature

In table 3.2, we deduce an overview of the published research on digital outcrop modelling and digital interpretations (i.e. object delineation and facies mapping) in several case studies that utilise different techniques, and the range of possible interpretation information that can be expressed by each method. As can be seen in the table, the applied digital interpretation method in a study strictly depends on the utilised software packages. Within the current literature, stratigraphic zonation and closed-boundary geobody facies mapping is tied to point-based facies mapping. Line digitisations more directly concentrate on the zone- and boundary transitions, and the modelling of boundary envelopes. The extracted stratigraphic line segments are to be directly imported in reservoir modelling software for surface interpolation, whereas the delineated sediment objects are measured and their shape properties documented for statistical shape replication in object-based modelling. Facies mapping on surface geometries, as presented to date, allows for geometrically precise and consistent geobody facies characterisation and their extrusion to deterministic volume objects [224].

Table 3.1: Overview of existing digital facies mapping approaches in office environments

study	Pringle et al. 2004 [238]	Trinks et al. 2005 [293]	McCaffrey et al. 2005 [199]	Labourdette et al. 2007 [165]	Enge et al. 2007/10, Rittersbacher et al. 2014 [88, 89, 252]	Jones et al. 2009/10 [137, 139]	Wilson et al. 2009, Rarity et al. 2014 [244, 312]	Olariu 2011 [224]	Richet et al. 2011 [246]	Hodgetts et al. 2013 [125]	Eide et al. 2014/16 [84, 86]
Stratigraphy boundaries:											
lines		X	(GIS)(X)	X	X	X	X	X	X	X	X
straight planes			X								
curved planes	X	X			X		X	X		X	
facies & areas:											
Zones				X		X	X	X	X		(X)
point attributes				(facies)X		X	(facies)X		(facies)X		
suppl. information:											
glyphs				(well)X		(well)X	X		(well)X	X	
system(s)	VRGS	VRGS	Hive, ArcGIS	?	LIME, RMS	ArcGIS, Petrel	VRGS, Petrel	Cyb.Map., GoCAD	GoCAD	VRGS	LIME

Table 3.2: Overview of existing digital facies mapping approaches in office environments

study	Pringle et al. 2004 [238]	Trinks et al. 2005 [293]	McCaffrey et al. 2005 [199]	Labourdette et al. 2007 [165]	Enge et al. 2007/10, Rittersbacher et al. 2014 [88, 89, 252]	Jones et al. 2009/10 [137, 139]	Wilson et al. 2009, Rarity et al. 2014 [244, 312]	Olariu 2011 [224]	Richet et al. 2011 [246]	Hodgetts et al. 2013 [125]	Eide et al. 2014/16 [84, 86]
Dep. elem. object boundaries:											
Lines	X			X	(chan.)X			X			X
facies & areas:											
polygonal sets	?						X	X			
textured elem.											
geobody repr.:											
volume geometry	?										
system(s)	VRGS	VRGS	Hive, ArcGIS	?	LIME, RMS	ArcGIS, Petrel	VRGS, Petrel	Cyb.Map., GoCAD	GoCAD	VRGS	LIME

3.4 Facies interpretation capabilities of existing software

The presented application cases relate back to the different forms of surface modelling and representation: The point set representation on which Virtual Reality Geological Studio (VRGS) operates allows for flexibility in the facies mapping, but suffers from the geometric drawbacks of point sets (such as the comparably large size of the model and the lack of connectivity between the vertices). This prohibits the extrusion of the facies and sedimentary objects into 3D volumes. LIME, which is based on textured polygonal soup-surfaces as DOMs, allows a very precise delineation of objects, supported by high-quality photo textures that ease the interpretation. Due to its limitation of polygonal line modelling though, the described envelopes can not be extruded into 3D geobodies and external tools are necessary to model surfaces (such as stratigraphic bedding). GoCAD works on the basis of PLC surfaces derived from geometrically-consistent point-sampled surface triangulation, but optionally also operates on the underlying point set representation of the DOM. This allows for flexibility in the facies mapping and, crucially, the extrusion of facies and objects into 3D [224].

3.5 Conclusions for the development of mobile interpretation software

With respect to the development and extension of the available techniques for digital facies mapping and interpretation on mobile devices in the field, there are several points to consider from this overview.

First, the digital interpretation of facies and stratigraphic units can be done directly on the underlying point set that results from the DOM acquisition process. This way of interpretation, on the other hand, is tightly connected to an interpretation procedure of point sets in 3D space. Whilst possible to realize, dedicated ways of interaction then need to be developed for mobile devices so to facilitate an easy and intuitive interpretation interface. Free–form 3D space navigation within physically-challenging outdoor environments on small-screen displays of mobile devices is specific to outcrop studies for field geology and demands fine-tuned interaction approaches.

Second, a facies mapping method that a larger geological community is accustomed with is line digitisation, which can be simply integrated in mobile devices applications. Such line digitisation can also be done on 2D images, where the delineating lines are subsequently projected on the underlying 3D surface of the DOM [50]. The challenge remaining in this approach is to find a precise and robust method for registering the images and their 2D interpretations to a 3D surface model. This challenge is covered in detail in this dissertation.

Third, surface-based interpretations in their soft-link form can also be incorporated in the illustrated mobile devices approach. Surface-based interpretations in their hard-link form require again a more involved 3D interaction and a constant interplay with the 3D surface DOM.

A final point of consideration for the development of visual techniques for field geology is to provide a fluent and simple data transfer of the interpreted structures from the mobile device to available desktop tools. The interpretations that are made in the field are potentially coarse and subject to refinement in an intermediate stage between fieldwork and reservoir modelling. It is therefore advantageous to provide a simple export- and import interface of interpretations to existing digital outcrop modelling packages, such as VRGS, LIME or GoCAD.

IV

Chapter 4

Direct Image-to-Geometry Registration Using Mobile Sensor Data

Kehl, Christian; Buckley, Simon J.; Gawthorpe, Robert L.; Viola, Ivan; Howell, John A.

ISPRS Annals of the Photogrammetry, Remote Sensing and Spatial Information Sciences, **III**, 2 (2016)

ISPRS Annals of the Photogrammetry, Remote Sensing and Spatial Information Sciences, Volume III-2, 2016
XXIII ISPRS Congress, 12–19 July 2016, Prague, Czech Republic

DIRECT IMAGE-TO-GEOMETRY REGISTRATION USING MOBILE SENSOR DATA

C. Kehl[a,b,*], S. J. Buckley[a], R. L. Gawthorpe[b], I. Viola[d], J. A. Howell[c]

[a] Uni Research AS - Centre for Integrated Petroleum Research (CIPR), Allégaten 41, 5007 Bergen, Norway - (christian.kehl, simon.buckley)@uni.no
[b] Department of Earth Science, University of Bergen, Allégaten 41, 5007 Bergen, Norway - (christian.kehl, rob.gawthorpe)@geo.uib.no
[c] Department of Geology & Petroleum Geology, University of Aberdeen, AB24 3UE Aberdeen, UK - john.howell@abdn.ac.uk
[d] Inst. of Computer Graphics and Algorithms, Technical University of Vienna, 1040 Vienna, Austria - viola@cv.tuwien.ac.at

Commission II, WG II/6

KEY WORDS: Image-to-Geometry, Automatic Pose Estimation, Mobile Devices, Registration Interfaces, Virtual Outcrop Geology

ABSTRACT:

Adding supplementary texture and 2D image-based annotations to 3D surface models is a useful next step for domain specialists to make use of photorealistic products of laser scanning and photogrammetry. This requires a registration between the new camera imagery and the model geometry to be solved, which can be a time-consuming task without appropriate automation. The increasing availability of photorealistic models, coupled with the proliferation of mobile devices, gives users the possibility to complement their models in real time. Modern mobile devices deliver digital photographs of increasing quality, as well as on-board sensor data, which can be used as input for practical and automatic camera registration procedures. Their familiar user interface also improves manual registration procedures. This paper introduces a fully automatic pose estimation method using the on-board sensor data for initial exterior orientation, and feature matching between an acquired photograph and a synthesised rendering of the orientated 3D scene as input for fine alignment. The paper also introduces a user-friendly manual camera registration- and pose estimation interface for mobile devices, based on existing surface geometry and numerical optimisation methods. The article further assesses the automatic algorithm's accuracy compared to traditional methods, and the impact of computational- and environmental parameters. Experiments using urban and geological case studies show a significant sensitivity of the automatic procedure to the quality of the initial mobile sensor values. Changing natural lighting conditions remain a challenge for automatic pose estimation techniques, although progress is presented here. Finally, the automatically-registered mobile images are used as the basis for adding user annotations to the input textured model.

1. INTRODUCTION

Textured surface models are used in a widening range of application domains, such a urban planning (Semmo and Döllner, 2015), cultural heritage (Potenziani et al., 2015), archaeology (Van Damme, 2015) and geological outcrop modelling (Howell et al., 2014, Rarity et al., 2014). After a model has been captured, often by means of terrestrial laser scanning (TLS) or photogrammetry, it may be desirable for domain experts to supplement the model with novel images to make initially-hidden features visible, or to add annotations. In the geosciences, researchers are often interested in annotating and interpreting available models for communicating insights, highlighting data anomalies and regions of interest, or for further processing in application-specific workflows. With recent advances in mobile devices (e.g. tablets, smartphones), the possibility for users to capture new images and create annotations using this new colour information is becoming increasingly important. Retexturing models, introducing supplementary textures, or annotating (i.e. interpreting, mapping) 3D structures in novel 2D images is based on retrieving accurate exterior orientations using Image-to-Geometry registration. Available tools to obtain the pose of a captured image commonly rely on complex, time-consuming, perceptually challenging and error-prone manual 2D-3D registration methods. This leads to a bottleneck in geoscientific workflows.

The goal of this study is to improve Image-to-Geometry registration for application workflows, by obtaining exterior orientations through reliable automatic- or less error-prone manual procedures. Automatic pose estimation is a traditional photogrammetric research topic, where recent approaches provide applicable poses if initialised with coarse approximations for position and orientation. This paper presents an extension to automatic Image-to-Geometry procedures using the in-built sensor data from mobile devices, as well as a novel approach for manual registration, taking the perceptual challenges into account, as a robust automation backup. This manual approach makes use of standard mobile device user interfaces (smartphones and tablets), which are centered around touch-based, visual, and immediate feedback interaction using fingers or a stylus. The applicability of the proposed techniques is evaluated in detail on urban- and geological case studies, focussing on the achievable accuracy, sensitivity to user-defined parameters, and success in challenging imaging conditions. The impact of the proposed approaches to the tasks of model retexturing and 2D–3D annotation is discussed in the final section of the article.

2. RELATED WORK

A vast body of literature is available on Image-to-Geometry registration. This is commonly a multi-stage process, consisting of coarse estimation followed by fine alignment. A generic setup starts with an image or a collection of images, capturing a scene from varying, unknown angles and positions (possibly without overlap) relative to geometric data. The algorithmic goal is to recover each camera's exterior orientation parameters (i.e. pose). Camera parameters such as focal length and CCD chip dimensions are directly obtained during the photo capturing (e.g. using EXIF tags), or pre-calculated for static lens configurations (e.g.

*Corresponding author

ISPRS Annals of the Photogrammetry, Remote Sensing and Spatial Information Sciences, Volume III-2, 2016
XXIII ISPRS Congress, 12–19 July 2016, Prague, Czech Republic

during camera calibration).

Several registration approaches, emerging from recent advances in computer vision, are further discussed. We refer to the review of augmented reality (AR) pose estimation (Nöll et al., 2011) for further details. Our study objective differs from AR requirements, as marker-based pose estimation is often not viable in a geoscientific setting, due to general difficulties of placing targets in remote and inaccessible natural environments.

2.1 Manual, Correspondence-Based Methods

Manual approaches rely on user-defined image–geometry point correspondences. Spatial resection (Moffitt and Mikhail, 1980) and Direct Linear Transform (DLT) are classic, correspondence-based photogrammetric techniques for pose estimation. Tsai presented a camera calibration technique that incorporates extraction of position and orientation in its solution, giving a lower point bound for a robust pose estimation (Tsai, 1987). Non-linear global optimisations, such as Levenberg-Marquardt (LM), generate numerical approximations of the exterior orientation parameters. Recent analytical solutions (Lepetit et al., 2009) to the Point-n-Perspective (PnP) estimation (Quan and Lan, 1999) give robust, real-time estimates. Existing challenges for correspondence methods are the provision of accurate, well-distributed 3D markers for each camera view, and user-friendly methods for defining correspondences. Current registration software (Chen et al., 2008) and commercial tools demand correspondence definition in 3D, which is perceptually problematic to novice users (Brunnett et al., 2003), and therefore time-consuming, error-prone and inefficient. Correspondence-based methods are incorporated in complex algorithms (Pintus et al., 2011, Sottile et al., 2010), or serve as a comparison baseline.

2.2 Statistical Correlation-Based Methods

Statistical correlation-based methods register unorientated images with a synthesised rendering of a surface geometry. This requires a coarse pre-registration to obtain approximate pose parameters for viewport definition and rendering. The photographs and synthetic images are then statistically evaluated (e.g. using information value and entropy) and their Mutual Information (MI) is iteratively maximised to obtain a pose (Viola and Wells, 1997, Maes et al., 1997). MI has computational advantages over comparable methods due to rapid image generation using computer graphics (CG) (Pluim et al., 2003), and is also used for the fine alignment in complex image registration frameworks (Corsini et al., 2013).

Hybrid methods combine the simplicity and accuracy of correspondence based approaches with the speed and robustness of statistical approaches. Mutual Correspondences is such a hybrid method (Sottile et al., 2010). The initially proposed algorithm minimizes the reprojection error between keypoints of the synthetic scene and a photograph, and maximizes their mutual information. A comparable algorithm minimizes the keypoints' reprojection between the synthetic and real image with strict spatial correspondences, eliminating the need for MI maximisation (Bodensteiner et al., 2012). Both approaches depend on a priori coarse registration as initialisation, which is currently achieved via manual 2D–3D correspondence selection.

3. CONTRIBUTIONS

In this paper, we propose an extension to hybrid registration methods by using mobile sensor data as the coarse initialization for Image-to-Geometry fine alignment. The extension results in a computationally lightweight, ad-hoc, fully-automatic registration procedure that can be used during fieldwork. In addition, we propose a simplified, user-friendly manual registration approach on mobile devices by mapping the 2D–3D correspondence selection to a 2D-2D task, and by exploiting increasingly-familiar mobile device interfaces. The paper further includes an in-depth study of feature matching parameters and illumination influence on the automatic registration accuracy. A novel combination of keypoint detection algorithm and pose optimization parameters is introduced and tested, which improves image registrations with moderate illumination differences. The method's applicability is demonstrated using case studies from urban- and geological field environments.

4. ASSISTED MANUAL REGISTRATION

Manual Image-to-Geometry methods are based on 2D–3D point correspondences, where the selection of occlusion-free and well-defined points in 3D can be problematic in natural scenes, particularly for novice users. In the presented workflow, 3D control points are defined as part of the surface model processing stage, prior to the model's distribution to practitioners. Points are defined at multiple, expert-selectable scales (i.e. varying distances to the object under study), depicting visually prominent, easily-recognisable object segments with respect to the chosen view. These 3D control points are stored along with the surface geometry, essentially as part of the object's metadata. Then, the textured geometry and control points are rendered from numerous viewpoints. While the viewpoints are currently selected manually, this process can benefit from automatic viewpoint selection algorithms (e.g. using MI (Feixas et al., 2009)) in the future. In this process, the control points are projected into the synthetic images as spherical glyphs, giving the basis for defining 2D–3D correspondences on the mobile device.

The rendered images and their point correspondences are loaded onto the mobile device for use by practitioners in their fieldwork. When capturing a new photograph from the in-built camera, the user selects one or more appropriate shared viewpoints. They are then prompted to define a 2D control point within the photograph using the mobile device interface shown in fig. 1. The interface then switches to the shared synthetic image, and the user selects the corresponding 3D control points as superimposed 2D marker on the rendered image. Because of selection inaccuracies on small screens, a distance-ranked marker list is created. The closest non-occluded marker to the user-selected point is chosen as correspondence. The user repeats the correspondence selection until enough links have been defined for exterior orientation estimates (minimum of seven (Tsai, 1987)). Finally, the pose estimation proceeds according to a LM or Efficient PnP (EPnP) scheme using the defined correspondences.

Registering the image via point markers demands easily identifiable, relatively accurate and well-distributed control points. Inaccuracies in the point marking propagate to the final pose estimation. Though it is possible to use fingers on the touch screen for marking, a stylus-enabled device is advantageous for defining the correspondence.

5. AUTOMATIC REGISTRATION AND MATCHING

The proposed automatic approach extends former pose estimation research, based on a Random Sampling Consensus (RANSAC) scheme of LM pose estimation using Scale-Invariant Feature Transform (SIFT) points. In our method, features are matched between the captured camera photograph and a rendering of the existing textured model, which delivers the 3D reference points. We use

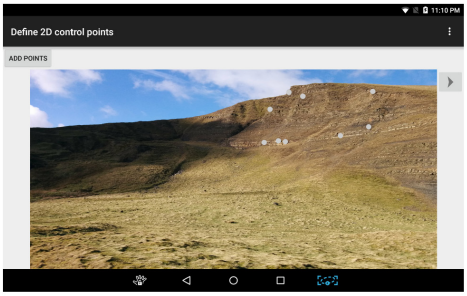

Figure 1: The manual registration interface, defining 2D correspondence points (grey circles) within the photograph, captured via smartphone.

the on-board sensor data from the mobile device to automatically determine the initial exterior orientation for the object rendering. This is in contrast to the user intervention required in comparable previous approaches and the manual interface presented in section 4 The full algorithm is outlined in fig. 2 and described below.

5.1 Mobile Sensor Orientation Estimate

Prior to image capture, the mobile device's magnetometer and accelerometer should be calibrated per field locality, using applications such as GPS Status [1]. Following this, new images can be acquired, and the global position and orientation are recorded at the time of capture. The global orientation using the *rotation vector* is referenced to magnetic north and earth's gravitational centre. In order to fuse the sensor data, the orientation, given as a quaternion, is corrected with the magnetic declination and the device orientation (e.g. portrait, landscape). A locally consistent pose is derived using the UTM coordinates of the recorded textured model. The varying coordinate systems are illustrated in fig. 3.

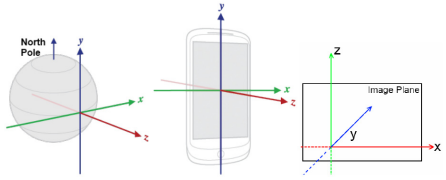

(a) ©Android manual, 2015, Google (b) ©Android manual, 2015, Google (c)

Figure 3: Schematic of coordinate systems defined in the Google Android operating system (a and b)[2] , and the system used later in this article (c).

Because of the low quality sensors commonly built into mobile devices, initial pose errors originate from both GPS and orientation measurements. A detailed overview of mobile device sensors and their calibration, error sources and error margins is available in the literature (Blum et al., 2013).

[1]GPS Status & Toolbox for Android - `http://play.google.com/store/apps/details?id=com.eclipsim.gpsstatus2`

[2]Sensor Event - Android Dev. `http://developer.android.com/reference/android/hardware/SensorEvent.html`

5.2 Image Synthesis

Using the given textured surface model and the initial pose, a synthetic image is generated on the Graphics Processing Unit (GPU) of the device using off-screen rendering. Camera interior orientation is used as input for the viewport definition. Furthermore, the utilization of the GPU allows adapting certain image parameters (e.g. contrast, brightness, gamma function) in real-time using post-processing shaders, which is potentially beneficial to the feature detection and mapping process reported later.

5.3 RANSAC-Based Pose Refinement

After obtaining the photo and the corresponding synthetic image, a feature detector (e.g. SIFT (Lowe, 2004), Speeded-Up Robust Features (SURF) (Bay et al., 2006), Maximally Stable Colour Regions (MSCR) (Forssén, 2007)) extracts 2D keypoints and descriptors. These descriptors are matched using symmetry- and homography constraints. Using raycasting, 3D points are obtained for matched keypoints in the photo. A PnP RANSAC scheme uses the 2D–3D correspondences to compute a pose. The pose with the biggest support is iteratively refined using LM. An example comparison between the captured photograph, the initial mobile sensor pose and the refined position and orientation is shown in fig. 4.

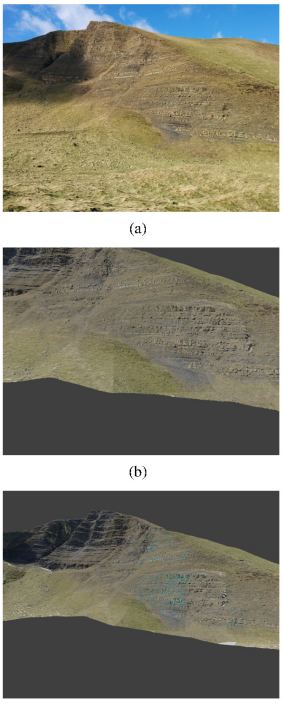

(a) (b) (c)

Figure 4: Comparative image series between a captured photo (a) and its corresponding synthetic images using the initial pose (b) and the final pose (c) after optimisation.

ISPRS Annals of the Photogrammetry, Remote Sensing and Spatial Information Sciences, Volume III-2, 2016
XXIII ISPRS Congress, 12–19 July 2016, Prague, Czech Republic

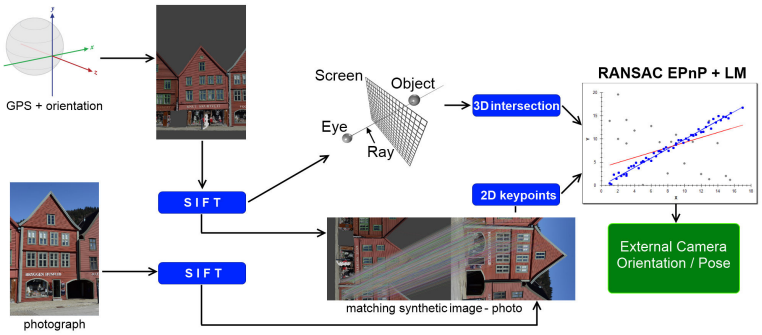

Figure 2: Outline of the proposed automatic registration algorithm, from capturing a new photograph using the device's on-board camera and sensor data (left) to the solved exterior orientation parameters (right).

6. EXPERIMENTS

The focus of the experiments is to assess the advantages and disadvantages of the automatic registration relative to manual Image-to-Geometry registration methods that are currently in use. Our interest is i) on the usability and sensitivity of mobile sensor pose input to the final registration, ii) the impact of tunable parameters during the image matching and pose estimation, and iii) the impact of changing lighting conditions on the final external orientation parameter accuracy.

The assessment uses two different datasets, both derived from time-of-flight TLS using the Riegl VZ-1000. The "Bryggen" dataset represents an urban use case, comprising the UNESCO World Heritage Site [3] late-medieval wharf of the former Hanseatic League in Bergen, Norway. The objects of interest within the Bryggen dataset were captured in high detail and consist of well-defined, easily-recognisable shapes. A challenge of the dataset is that image information contain reoccurring patterns (e.g. shop insignia, wood-panel facades), which can lead to mismatches of local image feature descriptors. Fig. 5 shows a captured dataset as coloured point set and textured surface model.

The second dataset, "Mam Tor", is a geological outcrop in the Peak District, Derbyshire, UK, with relevance for geological mapping. The area consists of a hillside with exposed sedimentary strata. The section of interest covers 280 metres (lateral) by 140 metres (vertical). Compared to the Bryggen dataset, less detail is available over comparable areas. In addition, the less well-defined object shape creates major challenges for the registration, as does vegetation within the scene and differing lighting conditions between textured model and mobile device image captures. Figure 6 shows the captured textured surface model and a selection of mobile device images to be registered.

The image texture is captured in both cases using a scanner-mounted, calibrated Nikon D800E camera. The laser-generated point set is processed according to established workflows (Buckley et al., 2008, Buckley et al., 2010), resulting in a textured triangulated irregular network (TIN). The image dataset for benchmarking the accuracy assessment is taken from the mounted Nikon camera with calibrated Nikkor 85mm prime lens (resolution: 7360x4920 pixels), while the mobile images are captured with a Google Nexus 5 smartphone (resolution 3262x2448 pixels).

[3] Bryggen World Heritage Center - `http://whc.unesco.org/en/list/59`

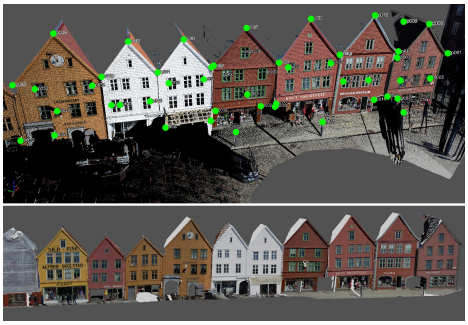

Figure 5: Rendering of the Bryggen dataset as coloured point set (top) and textured surface model (bottom), stretching along 40 m laterally. The green markers (top) highlight 3D control points for manual registration procedures.

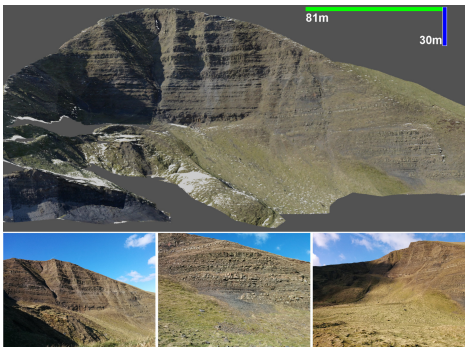

Figure 6: Overview rendering of the Mam Tor dataset as textured surface model (top, scale included) and a selection of supplementary photos to be incorporated (bottom).

This contribution has been peer-reviewed. The double-blind peer-review was conducted on the basis of the full paper.
doi:10.5194/isprsannals-III-2-121-2016

ISPRS Annals of the Photogrammetry, Remote Sensing and Spatial Information Sciences, Volume III-2, 2016
XXIII ISPRS Congress, 12–19 July 2016, Prague, Czech Republic

In the presented experiments, manual control points are evenly distributed in the image plane, ignoring extremely close- and far range areas in the image's depth plane (see fig. 5 top for Bryggen and fig. 7(a) for Mam Tor). Automatic control points are reasonably well-distributed, though mainly cover the exposed rock areas rather than vegetated slopes. Foreground objects receive the majority of control points due to their more distinct feature separation (as in fig. 7(b)). The orientation optimisation process does not demand strictly even distributions, although the control points need to represent variation within all three dimensions. Also, the point distribution should not be collinear.

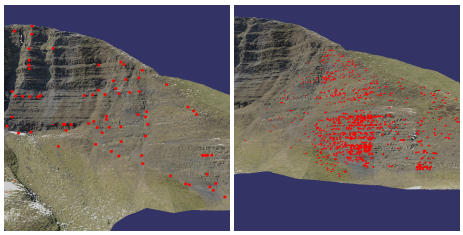

(a) manual (b) automatic

Figure 7: Comparison of manual (a) and automatic (b) control point distributions.

6.1 Accuracy Assessment

Images and pose parameters from the calibrated, scanner-mounted, globally-referenced camera serve as baseline for comparing other registration algorithms. The Bryggen dataset is used for the assessment due to its simplicity and accessibility. The mounting registration is compared to poses obtained via spatial resection, the proposed manual method using the projected markers in fig. 5, and the automatic registration with optimised parameters. The comparison metrics include the image reprojection error $\Delta_{pxl}[px]$ of pre-defined markers (see fig. 5), the rotational deviation of the orientation quaternion ΔQ, and the translational deviation of the position $\Delta\vec{t}[m]$. The deviation quaternion ΔQ is split into view direction vector $\Delta\vec{q}$ and view roll $\Delta\varphi(\vec{q})$, which is similar to the mobile device screen orientation. The clamped roll $\Delta\varphi(\vec{q}), \{-\pi, \pi\}$ is measured in rad, the direction vector $\Delta\vec{q}$ is unitless. The experiment results are given in tab. 1. The measured reprojection error for the baseline, camera-mounted configuration is due to the 2D–3D correspondences being human-selected within the photograph and the original lidar pointset, which means their selection accuracy is subject to human perception limitations. The automatic registration uses the default SIFT parameters by Lowe (2004) for feature matching in this experiment.

method	$\Delta_{pxl}[px]$	$\Delta\vec{q}$	$\Delta\varphi(\vec{q})$	$\Delta\vec{t}[m]$
mounting	35.21	0	0	0
spat. resection	32.42	0.00091	0.000738	0.053
manual reg.	43.35	0.01419	0.008197	0.080
automatic reg.	28.75	0.00021	0.000028	0.034

Table 1: Comparative accuracy of camera mounting, manual- and automatic registration with respect to Δ_{pxl}, rotational errors $\Delta\vec{q}$ and $\Delta\varphi(\vec{q})$, and $\Delta\vec{t}$.

6.2 Parameterization Sensitivity

The objective of the parametrization study, carried out on the Bryggen dataset, is to assess the impact of parameter variations in the keypoint matching and pose estimation procedure. The applied algorithm for feature detection and description is SIFT. The impact of SIFT internal parameters for keypoint matching has been assessed by Sima and Buckley, whose results are also applicable to the overall pose estimation (Sima and Buckley, 2013).

First, SIFT features are extracted in the photo and the rendered image using the method's default settings. In a second step, the two closest features are matched for each keypoint of one image within the respective other image. In step three, a ratio test is applied comparing the descriptor distances of both closest features. Iff the ratio between both distances is less than ratio parameter r_d, the matching is preserved. In step four, we assure a symmetric match between both image keypoints, reducing the closest two matches to one unique mapping. In the final step, the homography transformation is extracted from the matched keypoint pairs (introducing a confidence ratio parameter c_f), and only keypoints within a distance to the epipolar line $d(P, \vec{e}) \leq d_H$ are kept (with $\vec{e}$ being the epipolar line, P being a keypoint of the image in question, and d_H being the user parameter to study).

The RANSAC-based pose estimation procedure is controlled by the minimum point reprojection error E_p, which defines the optimisation target, the target ratio of inlier points after reprojection r_p, and the maximum number of iterations. The pose optimisation ends when the target ratio of 3D control points is within the given minimum reprojection error, or the maximum number of iterations is reached. In our experiments, the maximum number of iterations is fixed to 500. Table 2 shows the assessed value range for each parameter.

parameter	value range	std. value
c_f	$[0.85 : 0.01 : 0.99]$	0.92
d_H	$[0 : 0.5 : 15]$	7.5
r_d	$[0.55 : 0.01 : 0.84]$	0.7
E_p	$[0.5 : 0.5 : 3.0]$	2.0
r_p	$[0.6 : 0.02 : 0.8]$	0.7

Table 2: Overview of studied parameters, value ranges (given in the format of $[v_0 : \Delta v : v_N]$), and empirical standard values. Byggen

The influence of each parameter on the final pose quality is studied by observing the average pixel reprojection error, the average number of detected points, and the average percentage of correct correspondences. Based on the experiments (assessing each independent parameter combination for five Nexus 5 images of Bryggen), the following behaviour can be observed:

- the confidence ratio c_f is a stable parameter with moderate influence, while generally higher ratios result in better correspondences;
- the homography distance d_H is an unstable parameter with minor influence (weak correlation);
- the feature ratio r_d is a stable parameter with significant influence (strong correlation, see fig. 8(a)), where larger values yield better estimations;
- the allowed point reprojection error E_p (within the studied boundary) is an unstable parameter with significant influence;

This contribution has been peer-reviewed. The double-blind peer-review was conducted on the basis of the full paper.
doi:10.5194/isprsannals-III-2-121-2016

ISPRS Annals of the Photogrammetry, Remote Sensing and Spatial Information Sciences, Volume III-2, 2016
XXIII ISPRS Congress, 12–19 July 2016, Prague, Czech Republic

- the target point inlier ratio r_p is a stable parameter with minor influence (weak correlation, see fig. 8(b)), where the studied value range always resulted in a applicable pose estimates. The trend of retrieved number of points and inlier percentage depicted in fig. 8 is representative for comparable radiometric setups of registering natural scene images.

- a parameter optimization, as given in this study, can yield registration accuracy improvements on a per-dataset basis

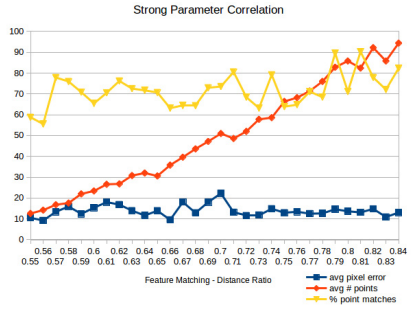

(a) parameter r_d

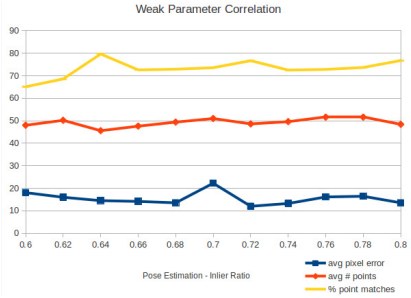

(b) parameter r_p

Figure 8: Graphs showing the difference between strongly-correlated parameters (such as r_d in (a)) and weakly-correlated parameters (such as r_p in (b)) by observing average pixel errors, number of detected features and ratio of correct correspondences.

6.3 Lighting Sensitivity

Using the Mam Tor dataset, we can assess the impact of lighting conditions on the automatic registration, as two image sets, captured in different field campaigns (March and September 2015), are available. Lighting conditions have a major impact on the registration due to the feature descriptor extraction and matching. In the first assessment, we use the March dataset, which was captured simultaneously with the textured model in identical lighting conditions. The measured metrics are equal to Section 6.1, but the comparison baseline is the manual mobile registration. The results are presented in tab. 3.

The automatic procedure is able to retrieve acceptable poses for all ten images, acquired via mobile devices, at equal lighting conditions. The September dataset consists of 20 images captured

method	$\Delta_{pxl}[px]$	$\Delta\vec{q}$	$\Delta\varphi(\vec{q})$	$\Delta\vec{t}[m]$
manual reg.	31.78	0	0	0
mobile sensors	<100	0.203	0.0916	45.33
automatic reg.	9.92	0.018	0.0086	8.76

Table 3: Comparative accuracy of initial sensor data, manual- and automatic registration with respect to Δ_{pxl}, rotational errors $\Delta\vec{q}$ and $\Delta\varphi(\vec{q})$, and $\Delta\vec{t}$. Mam Tor, March 2015

when lighting conditions were significantly different to the textured model input images. Moreover, due to rainfall in preceding days, the mudstone beds in the outcrop are significantly darker in colour. Keypoint matching and pose retrieval failed with the optimised parameter set of sec. 6.2, as shown in fig. 9(a). We apply a gamma adaptation as a post-processing shader to the synthetic image because of the stronger reflectance of the rock. This improves the keypoint matching, though pose extraction still fails (see fig. 9(b)). Only by applying the post-processing and changing the keypoint extraction to MSCR - a feature extraction algorithm considering colour information instead of just greyscale values - the automatic procedure is able to retrieve an acceptable pose for 4 out of 20 images, as shown in fig. 9(c).

7. DISCUSSION

As can be seen from the measurements in sec. 6.1 and 6.3, all methods are able to retrieve accurate external camera parameters with a reprojection error of less than 1% of the diagonal image resolution, a positional error between 8 cm (for calibrated, mounted, high-resolution camera images) and 9 m (for uncalibrated, noisy, handheld mobile device images), and accurate rotational parameters. Using the raw mobile device sensor data for image registration is insufficient, as this leads to positional errors in the retrieved pose of up to 45 m within the presented experiments. In urban environments, reoccurring texture patterns within the scene lead to some incorrect point correspondences being found. However, the automatic Image-to-Geometry registration is able to retrieve a pose closest to the fixed camera mounting, yielding the smallest reprojection error of all methods.

In the geological setting, mobile device images are easily registered using the novel manual registration approach. Particularly, with a growing number of images to register, the novel workflow promises significantly less processing time due to the simple 2D-2D matching. We observed that a trained operator takes close to 20 minutes for selecting the minimum number of correspondences per image (for PnP pose estimation), where the mobile device approach demands between 5 and 7 minutes per image. The automatic registration is able to consistently estimate acceptable pose parameters for mobile devices images when the lighting conditions of the textured surface model and the acquired additional images are similar. The major issues for the automatic registration are twofold: First, the acquired GPS position data are often inaccurate using the built-in sensor. Using the GPS data demanded visual checks and minor manual corrections before running the automatic registration. Apart from insufficient GPS reception and noise, a major error source (and thus source of correction) is the lack of a built-in geoid model for referencing altitude measurements relative to the orthometric textured model. In the future, this can be bypassed by including a geoid model or snapping the height value to a local elevation model. Secondly, changing lighting conditions are largely problematic to feature-based pose estimation, where the use of colour feature descriptors and appropriate post-processing shaders improve the process to a certain degree. Still, more significant improvements

This contribution has been peer-reviewed. The double-blind peer-review was conducted on the basis of the full paper.
doi:10.5194/isprsannals-III-2-121-2016

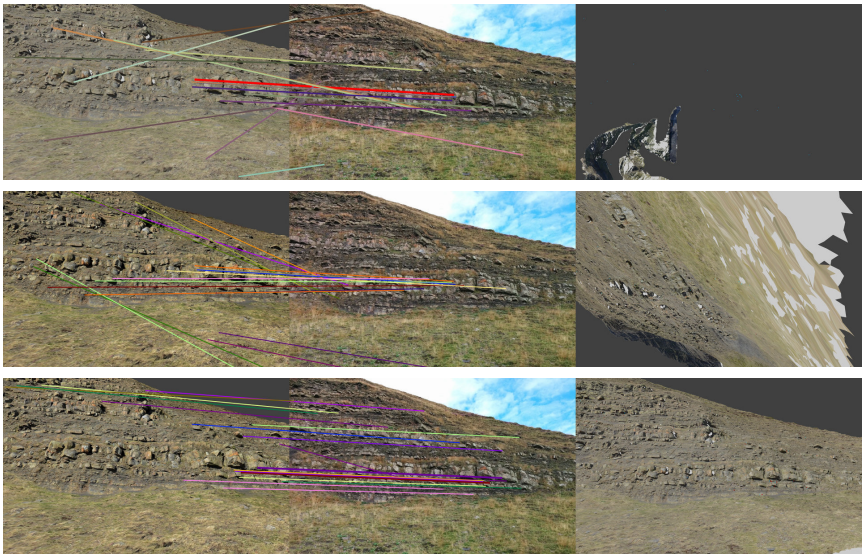

Figure 9: Results of pose estimation for changing lighting conditions for SIFT with default parameters (top), SIFT-optimised (middle) and MSCR-optimised (bottom) keypoint matching. Each example shows the mobile sensor-based rendering (left), the captured mobile image (middle), and their 2D correspondences, and a rendering from the calculated pose (right). With successful pose estimation, the viewport of the right-hand image should match the input photograph (middle).

are potentially to be gained by using the available geometry information for combined statistical pose estimation (Sottile et al., 2010).

The resulting exterior orientation parameters of the presented methods can be used in the projective mapping of areas of interest, such as sediment bedding and faults in geological applications (see fig. 10), as well as for adding new images to the existing textured models (fig. 11). This can be useful where initial texture quality is poor (lighting conditions, obliquity or low resolution) or 2D features have changed since the initial 3D model acquisition (new coat of paint for the urban environment). For the latter, the registration procedure is flexible enough to also register handheld, consumer-grade or SLR camera images to a given textured model (on desktop computers), thus replacing the need for a lengthy manual registration of additional photographs: a user can manually define a small number of coarse overview poses and link them to the freely-captured images. With these coarse initial pose estimates, the proposed automatic Image-to-Geometry procedure is able to automatically register the images, leading to a significant reduction in manual input for texturing workflows (Sima, 2013).

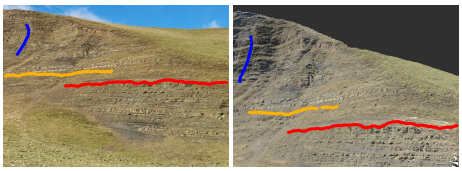

(a) 2D annotation, Nexus 5 image (b) 3D annotation, projected on model

Figure 10: Geological annotation mapping of a virtual outcrop model from mobile device imagery.

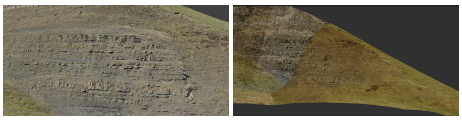

(a) initial texture (b) mobile device image texture

Figure 11: Re-texturing a textured model with mobile device (Nexus 5) image collection.

ACKNOWLEDGEMENTS

This research is part of the VOM2MPS project (proj. number 234111/E30), funded by the Research Council of Norway (RCN) and FORCE consortium through Petromaks 2. Mam Tor data are provided and used by the SAFARI project [4]. The Bryggen dataset is collected for VGC 2016 [5]. The authors thank Sophie Viseur for insightful research discussions on the topic of pose estimation,

ISPRS Annals of the Photogrammetry, Remote Sensing and Spatial Information Sciences, Volume III-2, 2016
XXIII ISPRS Congress, 12–19 July 2016, Prague, Czech Republic

and Riegl LMS GmbH is thanked for continued software support.

REFERENCES

Bay, H., Tuytelaars, T. and Van Gool, L., 2006. SURF: Speeded Up Robust Features. In: *Computer vision–ECCV 2006*, Springer, pp. 404–417.

Blum, J. R., Greencorn, D. G. and Cooperstock, J. R., 2013. Smartphone sensor reliability for augmented reality applications. In: *Mobile and Ubiquitous Systems: Computing, Networking, and Services*, Springer, pp. 127–138.

Bodensteiner, C., Hebel, M. and Arens, M., 2012. Accurate single image multi-modal camera pose estimation. In: K. Kutulakos (ed.), *Trends and Topics in Computer Vision*, Lecture Notes in Computer Science, Vol. 6554, Springer Berlin Heidelberg, pp. 296–309.

Brunnett, G., Hamann, B., Müller, H. and Linsen, L., 2003. *Geometric Modeling for Scientific Visualization*. Mathematics and Visualization, Springer Berlin Heidelberg.

Buckley, S. J., Howell, J. A., Enge, H. D. and Kurz, T. H., 2008. Terrestrial laser scanning in geology: data acquisition, processing and accuracy considerations. *Journal of the Geological Society* 165(3), pp. 625–638.

Buckley, S. J., Schwarz, E., Terlaky, V., Howell, J. A. and Arnott, R., 2010. Combining Aerial Photogrammetry and Terrestrial Lidar for Reservoir Analog Modeling. *Photogrammetric Engineering & Remote Sensing* 76(8), pp. 953–963.

Chen, B., Ramos, G., Ofek, E., Cohen, M., Drucker, S. and Nistér, D., 2008. Interactive techniques for registering images to digital terrain and building models. Technical report, Technical report, Microsoft Research.

Corsini, M., Dellepiane, M., Ganovelli, F., Gherardi, R., Fusiello, A. and Scopigno, R., 2013. Fully Automatic Registration of Image Sets on Approximate Geometry. *International journal of computer vision* 102(1-3), pp. 91–111.

Feixas, M., Sbert, M. and González, F., 2009. A unified information-theoretic framework for viewpoint selection and mesh saliency. *ACM Transactions on Applied Perception (TAP)* 6(1), pp. 1.

Forssén, P.-E., 2007. Maximally Stable Colour Regions for Recognition and Matching. In: *Computer Vision and Pattern Recognition, 2007. CVPR'07. IEEE Conference on*, IEEE, pp. 1–8.

Howell, J. A., Martinius, A. W. and Good, T. R., 2014. The application of outcrop analogues in geological modelling: a review, present status and future outlook. *Geological Society, London, Special Publications* 387, pp. SP387–12.

Lepetit, V., Moreno-Noguer, F. and Fua, P., 2009. EPnP: An Accurate O(n) Solution to the PnP Problem. *International Journal of Computer Vision* 81(2), pp. 155–166.

Lowe, D. G., 2004. Distinctive image features from scale-invariant keypoints. *International Journal of Computer Vision* 60(2), pp. 91–110.

Maes, F., Collignon, A., Vandermeulen, D., Marchal, G. and Suetens, P., 1997. Multimodality image registration by maximization of mutual information. *Medical Imaging, IEEE Transactions on* 16(2), pp. 187–198.

[4]Sedimentary Architecture of Field Analogues for Reservoir Information (SAFARI) - `www.safaridb.com`

[5]Virtual Geoscience Conference - `www.virtualoutcrop.com/vgc2016`

Moffitt, F. and Mikhail, E., 1980. *Solutions Manual to Accompany Photogrammetry*. Harper & Row.

Nöll, T., Pagani, A. and Stricker, D., 2011. Markerless camera pose estimation-an overview. In: *OASIcs-OpenAccess Series in Informatics*, Vol. 19, Schloss Dagstuhl-Leibniz-Zentrum fuer Informatik.

Pintus, R., Gobbetti, E. and Combet, R., 2011. Fast and robust semi-automatic registration of photographs to 3d geometry. In: *Proceedings of the 12th International conference on Virtual Reality, Archaeology and Cultural Heritage*, Eurographics Association, pp. 9–16.

Pluim, J. P., Maintz, J. A. and Viergever, M. A., 2003. Mutual-information-based registration of medical images: a survey. *Medical Imaging, IEEE Transactions on* 22(8), pp. 986–1004.

Potenziani, M., Callieri, M., Dellepiane, M., Corsini, M., Ponchio, F. and Scopigno, R., 2015. 3dhop: 3d heritage online presenter. *Computer & Graphics* 52, pp. 129–141.

Quan, L. and Lan, Z., 1999. Linear n-point camera pose determination. *Pattern Analysis and Machine Intelligence, IEEE Transactions on* 21(8), pp. 774–780.

Rarity, F., Van Lanen, X., Hodgetts, D., Gawthorpe, R., Wilson, P., Fabuel-Perez, I. and Redfern, J., 2014. Lidar-based digital outcrops for sedimentological analysis: workflows and techniques. *Geological Society, London, Special Publications* 387(1), pp. 153–183.

Semmo, A. and Döllner, J., 2015. Interactive Image Filtering for Level-of-Abstraction Texturing of Virtual 3D Scenes. *Computers & Graphics* 52, pp. 181–198.

Sima, A. A., 2013. An Improved Workflow for Image- and Laser-based Virtual Geological Outcrop Modelling. Phd thesis, University of Bergen. 180p.

Sima, A. A. and Buckley, S. J., 2013. Optimizing sift for matching of short wave infrared and visible wavelength images. *Remote Sensing* 5(5), pp. 2037–2056.

Sottile, M., Dellepiane, M., Cignoni, P. and Scopigno, R., 2010. Mutual correspondences: An hybrid method for image-to-geometry registration. In: *Eurographics Italian Chapter Conference*, pp. 81–88.

Tsai, R. Y., 1987. A versatile camera calibration technique for high-accuracy 3d machine vision metrology using off-the-shelf tv cameras and lenses. *Robotics and Automation, IEEE Journal of* 3(4), pp. 323–344.

Van Damme, T., 2015. Computer vision photogrammetry for underwater archaeological site recording in a low-visibility environment. *ISPRS-International Archives of the Photogrammetry, Remote Sensing and Spatial Information Sciences* 1, pp. 231–238.

Viola, P. and Wells, W. M., 1997. Alignment by maximization of mutual information. *International journal of computer vision* 24(2), pp. 137–154.

VIII

Chapter 8

Discussion

The discussion concludes this dissertation by returning to the initial research question and challenges stated in section 1.5. Subsequently, some technical challenges are explained that persist beyond the presented research period. Although these challenges need to be addressed, approaches to deal with them are already known. Therefore, it is not a lack of knowledge but the issue of implementing the known approaches that prevents further research along related directions. These technical challenges are largely solvable by engineering efforts. After the technical challenges, a larger passage is discussing the applicability of the visual techniques, presented and developed within this work, to petroleum geology as well as other geoscience disciplines. A final section discusses future research directions based on the knowledge and prospective future developments that have their foundations within the introduced visual, statistical or geometric methods of this thesis.

8.1 Research Conclusion

The introduction to the thesis states in section 1.5 a list of expected challenges that are to be addressed within this research. One of the challenges was to optimise the available 3D surface geometry for its presentation and interpretation on mobile devices. As section 1.6 states, limits for the robust and fluent presentation of DOM data on mobile devices have been determined. Mobile device limitations are discussed in detail in section 8.2 of this chapter. Furthermore, the conference paper in appendix A covers the performance and memory size limitations for DOMs in detail, with focus on its use for the interpretation mapping.

The next challenge is the capturing and co-registration of arbitrarily-positioned outcrop photos with an available DOM on mobile devices using the on-board sensor data. The image-to-geometry registration, particularly within realistic outdoor illumination settings, is the main subject within the scientific articles in chapter 4, 5, 6, and appendix A and B. Because of the limited computational capabilities available, a feature-based registration approach has been adopted within this research. Illumination conditions represented the one most-significant challenge during the registration, for which novel feature detection algorithms and a framework of visual influences proved advantageous for successively improving the image-to-geometry registration in real-world cases.

One final challenge estimated at the project start is the provision of intuitive, humanly-abstracted user interfaces that support interpretation purposes. A considerable amount of time was invested into the human-computer interface design of the Geological Registration and Interpretation Toolset (GRIT) application (see appendix G), but apart from the supportive interface for photo registration in chapter 6, the scientific output of GUI design is minor in com-

parison to the invested time. The application lacks visual appeal, which can be remedied by graphical designers and illustrators in the future. The visual appeal of the standard graphical user interface (GUI) itself does not address a scientific challenge or provides novel computer- or geoscientific insight. Therefore, the time spent on GUI development is of limit value as publication material. Extended, smart interaction paradigms (in 2D as well as 3D) on mobile devices are human-computer interaction (HCI) research topics that still provide challenges for future ideas. The challenge of surface-constrained 3D navigation on mobile devices is further discussed in section 8.5.1.

Taking the research output of chapter 1 to 7 and the appendices as a basis, the main research question can now be addressed:

How can visual techniques, made available on mobile devices, support and improve geological fieldwork ?

First of all, the mobile device apps that are made available outside the development within this thesis already contribute several visual techniques for geological field work. Apps such as FieldMove for geological measurements, Adobe Sketchbook for geological sketching and map creation, geological mapping services such as iGeology, and Strataledge as sedimentary logging application – documented in detail in section 1.4.2 – address specific tasks within geological fieldwork appropriately and in a visual manner.

The dominant use of mobile devices, for a larger part of the geological community, is the measurement of values such as strike and dip or the paleocurrent flow direction using FieldMove. Even though these applications catch the interest of domain experts with their simplicity and user friendliness, the calibration of the mobile device sensors is all too often neglected. An initial check and measurement synchronisation between the digital app and the physical compass at the start of the fieldwork activities is advised to verify the correctness of the measurement instrument. Another issue with field measurements is the integration of these small measurement tools into the larger geological workflow. The measurement's best export option are Google Maps or Google Earth-projectable tabular information. The acquisition of the field measurements is technically very simple and yet so fundamental to subsequent geomodelling steps that it should be possible to export the data into wide array of open formats consumable by various desktop applications.

Sedimentary logging applications have shown potential for their more rapid adoption by geologists due to their obvious digital advantages to paper-based logging (i.e. multi-page fieldbook drawings and the inflexibility for corrections and modifications). Recent developments in LIME allow the quick import of the logs as images and their mapping on the digital outcrop face, as shown by J.R. Mullins in the paper of chapter 7 on the Whitby case study. A brief comparison between Strataledge and SedMob resulted in Strataledge being the geologists tool-of-choice because of its advanced, highly organised layout that shared many similarities with the quasi-standard of fieldbook sedimentary logs. An issue that currently prevents the wider spread of sedimentary logging apps is their limited data export capability, as already mentioned for sensor logging. A smaller set of geologists adopted sketching and drawing applications in their normal field workflow, which is still preferably done on pen-and-paper by a majority.

The pivot challenges covered by this thesis is the (semi-)automatic mapping of 2D interpretation sketches onto DOM surfaces. The successful methods presented in the main part of the thesis allow for a quick transition from field observation to digitally-documented interpretation. Their integration by import- and export functions to LIME allows to enhance previous DOM workflows [84,88,252] for converting outcrop data into reservoir modelling supplements

for object-based modelling. Object-based modelling is currently still the dominant method to generate MPS TIs from outcrop interpretations.

One of the largest obstacles for a wide-spread adoption of mobile devices by field geologists is the lack of mutual data format support and interoperability. Data that is being measured, logged, drawn and defined on mobile devices in the diverse collections of apps is shared via online storage services. It demands furthermore commitment, especially by expert software development companies for field-geology tools such as Midland Valley and Endeeper, to open data exchange formats and standards. Examples of open data formats for specific categories of collected information is given in the following list.

- Extensible Markup Language (XML) for workspace information and generic data that have no further correspondence
- Scalable Vector Graphics (SVG) for 2D vector data
- Geography Markup Language (GML) or Keyhole Markup Language (KML) for 3D vector data, such as: DOMs, line & polygonal interpretations
- Stanford polygonal file format (PLY) for surface data in 3D
- JPG or PNG for low-/mid-resolution 2D raster images
- TIFF for high-resolution 2D raster images

The outlined issue of exchange formats is addressed on various smaller scales within this research and the development of GRIT. The paper of appendix D describes in detail how to store large surface geometries within the GML format. It shows the rendering of the GML-stored information within several geospatial information systems, such as ArcGIS. The potential of the use of open data formats for surface models is evident from the cadastral case study. The paper also illustrates how to store split geometry within GML in multiple levels of detail, addressing some limitations further explained in section 8.3. A drawback of GML is its inadequate support of surface texturing from related imagery, but such extensions to the format can be officially proposed at the Open Geospatial Consortium (OGC).

The rendering capability for DOMs within GRIT, demonstrated in the articles of the main section, is also achievable on smartphones (as shown in appendix A and fig.8.1), but 3D data processing drains smartphone batteries much quicker than for tablets. Furthermore, the NVIDIA shield tablet (being developed by a GPU manufacturer) demonstrates the cutting-edge in 3D mobile graphics processing performance, which is necessary for displaying the large 3D surface models in geology.

In conclusion, the support for various file formats and the guarantee of interoperability between mobile device and desktop software is of key importance for geologists in the adoption of new technology. Extending mobile device applications (e.g. GRIT, Sketchbook, Dabbler, Strataledge and FieldMove) towards this interoperability goal is not a scientific inquiry but an opportunity for engineers in the future, in particularly with respect to the commercialisation of research prototypes.

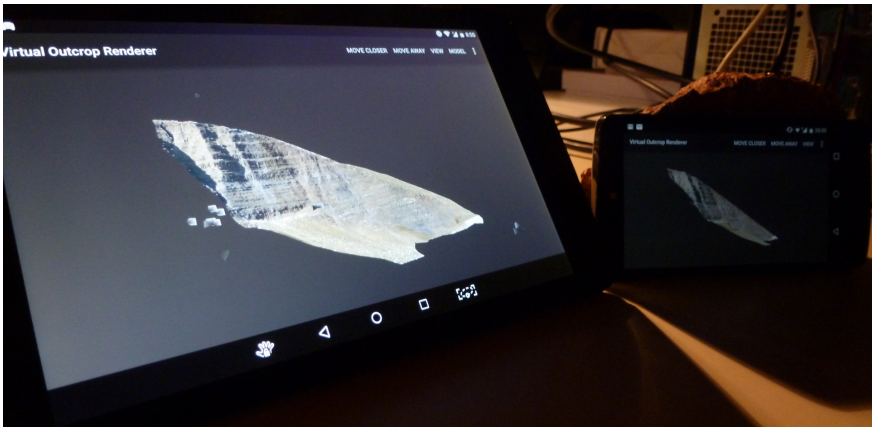

Figure 8.1: Proof of concept, showing the rendering of digital outcrops on tablets and smartphones directly on the device.

8.2 Limitations of Mobile Device Technology

8.2.1 Graphics

The current graphical capabilities that can be realised on mobile devices is highly dependent on the hardware aspect of the technology (e.g. component layout of the device, chip technology, manufacturer). Existing DOMs within databases such as SAFARI can be used, in some cases, directly and without modification on very few devices, such as the NVIDIA Shield tablet used in this research. Most application domain experts potentially have a wide range of devices with varying technical capabilities.

A first issue commonly encountered when developing graphics applications for different devices is the support for image textures. Texturing relies on a large instruction set for GPUs, related to texture compression, multiple texture projection setting, and blending options between image texture and vertex attributes for colouring (i.e. scalar- and colour attributes, material properties). The instruction set on mobile devices is drastically limited for reasons of miniaturisation (i.e. shrinking the GPU integrated circuit to fit into the mobile device and to reduce heat radiation). Thus, discrete cosine transform (DCT)-compressed textures, commonly used on traditional desktop computers, are often not supported on smartphones and tablets. Other texture-related techniques such as environment mapping projection are also not part of the standard GPU instruction set on mobile devices.

Another problem is the limited internal memory size and main memory of mobile devices. The internal memory size is often given as technical detail for each device and currently ranging between 16GB and 128GB. The main memory is originally unrelated to the internal memory size. As an analogy for desktop computers, the main memory in both devices describes the same chip, which is a dynamic RAM (DRAM) connected to the main processor. The internal memory of mobile devices maps to the harddrive built into the computer. External memory of mobile devices maps to external harddisks. In practice, there is a connection between internal memory and main memory due to the *swap memory* or *pagefile*, which is an extended space of the main memory in the internal memory. The technical details are important as 3D graphics performance (i.e. render speed; refresh rate) relies on main memory,

where the geometric data reside. Therefore, devices with larger internal memory are beneficial to graphics. As an example, the GRIT application has been tested for the Google Nexus smartphone described in section 1.2.3 and a recent Samsung Galaxy device with both equal internal memory deliver comparable graphics performance, whereas the NVIDIA Shield tablet is an order of magnitude faster in graphics performance having only double the available internal memory. In terms of DOMs, the NVIDIA tablet can display up to three million triangles interactively, while the Google smartphone and the Samsung tablet reach their limit of interactive DOM display at around 150,000 triangles (5% of the NVIDIA performance). Therefore, determining an optimal size of a DOM for a large audience is logistically and technically problematic.

Moreover, the memory issue is probably not going to disappear by future advances in the manufacturing technology of mobile devices without compromises in battery consumption and application operation times. The amount of internal random access memory (RAM) is closely connected to the problem of power consumption. The rapid static memory (SRAM), which is integrated into the mobile device CPU, needs to be periodically charged to update the memory state (electronic principles of computer architectures and memory technology, see [22]). Therefore, CPU-integrated, fast SRAM actively consumes energy at any time the device is physically switched on, which in return results in a trade-off limit between internal RAMs capacity and minimum operation time within the battery capacities of a given device. As an overall conclusion, waiting for future-generation mobile devices is probably not completely removing memory capacity limitations and 3D graphics rendering speed, although the problem will be reduced. The data size of 3D surface models will arguably persist as a limiting factor.

8.2.2 Sensors

The presented approaches for photo-registered interpretation rely strongly on mobile device sensor data, such as the magnetometer and the GNSS receiver. The academic paper contributions presented in chapters 4, 5 and 6 as well as appendices A and B highlight the application challenges of the provided, inaccurate mobile sensor data. Smartphones and tablets allow to determine the position and orientation of device around the globe without WiFi reception, but the quality and accuracy of the received information varies considerably. Blum et al. [21] provide an in-depth overview of mobile device sensor precision and limitation in urban environments. Sensor accuracies are also further discussed by Clegg et al. [56] in an extended review of geological field application software. Recently, the accuracy of mobile device sensors have been assessed case studies on structural geology for feature orientation measurements [51, 218], highlighting reliability and variability issues. One reason for the lack of accuracy is the use of consumer electronics in mobile devices and their condensed layout within mobile devices, the latter of which leads to electromagnetic interference between the device's components. Another problem specific to geo-localisation during fieldwork is the generic frame within which the data are obtained and valid.

In the experiments conducted within this research, we rely on the internal, standard global positioning system (GPS) signal. GPS signals are known to be insufficiently accurate. The Android computing platform provides an accuracy approximation measure on signal reception. This accuracy value is reasonable for the lateral geo-position, though still deviates by up to two metres itself. The phenomenon has been observed during the research period by experimentally comparing reference points on the lidar-derived surface with GPS sensor data from the field, which are internally fixed to a maximum reception deviation of three metres. Within these experiments, the sensor data varied up to eight metres (absolute value). Vertic-

ally, the provided accuracy measure is wrong, as the internal GPS raw data from the satellite (i.e. the altitude) has a measured standard deviation of tens of metres up to a hundred metres, as shown in chapter 6. In all measured cases, the accuracy approximation of Android was assured to be three metres or less. A commercial solution to the accuracy problem is the usage of differential GPS (dGPS) in field geology [127], which provides centimetre accuracy [187]. This solution has not been considered within the thesis, as the costs of dGPS devices prohibit a wide-spread use during normal fieldwork. Additionally, the field equipment of dGPS (e.g. antenna and receiver pack) would remove the advantages of mobility and flexibility in the field gained by using mobile devices. Instead, DEMs have shown to be a vital source of supplemental information to correct for GNSS inaccuracies, as discussed in chapter 6.

An intuitive, simple solution to improve sensor accuracies is to internally track the raw data of GNSS and magnetometer over time to provide smooth, average-filtered positional values. Although intuitive, the solution comes with a significant drawback: physical sensors, such as GNSS and magnetometer, are the most battery-consuming hardware components of mobile devices. The case study of Brimham Rocks (as shown in section 1.6) quantifies the battery consumption problem. During the fieldwork at Brimham Rocks, the objective was to obtain a maximum number of supportive outcrop images for their subsequent interpretation and mapping. In order to stretch the battery runtime, a strict battery management was applied, the screen illumination has been reduced to a minimum, 3D surface data access modules have been switched off, and the mobile sensors were set to be activated only upon request (i.e. upon picture acquisition). The batteries of the NVIDIA Shield tablet and the Google Nexus 5 smartphone were emptied multiple times, each individual time between full- and empty charge lasting 0:50 to 1:20 hours. For common fieldwork activities, this is already a significant restriction. If less care is taken to minimize memory consumption and if possibly tracking the sensors continuously, the battery of each device could be emptied within approximately 25 to 35 minutes, which is not acceptable for field geology instruments.

Apart from electronic hardware improvements by mobile devices manufacturers, the use of coarse DEMs has shown to be a practical solution to reduce altitude errors in the positioning. Furthermore, improved signal processing and sensor fusion (e.g. real-time kinematic (RTK) libraries[26]) lead to more accurate sensor data – at the expense of higher battery power consumption.

8.2.3 Software

Despite the discussed hardware problems and limitations, mobile device hardware is very powerful considering the small form factor (i.e. physical size of the device) and also comparing it to previous, portable computing equipment (e.g. laptops, notebooks, field computers). From a hardware point-of-view, even complicated software and algorithms that demand massive calculations (e.g. SfM, 3D modelling and VR) are possible to be developed on mobile devices in a prototypical manner, as presented in section 1.4.1. Therefore, there is no reason with respect to the integrated circuit architecture of mobile devices that prohibits the implementation of physical simulations, facies-based reservoir modelling or 3D volume analysis in prototypical manners and on small scale examples in the future. Data size, as a result of scale, is a considerable limiting factor, as previously discussed in section 8.2.1.

Basic computer vision and 3D rendering libraries (e.g. OpenCV[27] [142] and OpenSceneGraph[28] [306]) have been implemented and extended by this thesis' author for mobile devices during development cycles of the three-year research period. During this development, the lack of

[26] RTKLIB - `www.rtklib.com`

basic calculation software largely prohibited further scientific advances on mobile platform applications. Most established scientific- and engineering software packages on desktop computers (e.g. Petrel and RMS, MatLab, ANSYS[29]) rely on a complex system of software libraries, algorithms and technical contributions that developed over the past decades. Discrete algebra and analysis libraries, such as the linear algebra package (LAPACK) and basic linear algebra subprograms (BLAS), facilitate the execution of complex mathematical operations used in scientific applications. These de-facto standard libraries are not available or accessible on mobile devices. In order to see more sophisticated applications appearing for mobile devices, trusted and applied to real-world challenges by both the scientific community and the commercial sector, these standard libraries need to be made available and accessible to developers in the future. It is particularly important for geoscience applications that rely statistical calculations (e.g. MPS) on a large scale.

8.3 Remaining Technical Challenges

Several operational and technical limitations became apparent from the work during the research period, the tests of geological mobile device software and the re-formulation of available 3D surface DOMs. These are subsequently discussed. As the encountered issues are of technical or operational concern, various papers in existing literature discuss partial solutions that can be adapted to the given problems. The implementation of the available, proposed methods and algorithms within the literature is not trivial, but solving the technical details is to be covered by future engineering development.

8.3.1 Geometrically-consistent Modelling and Parameterization of DOMs

All datasets encountered during the research period are stored as textured surfaces of polygonal soups, as explained in section 1.3 and chapter 2. The boundaries of each polygonal soup correspond to a boundary of surface-parallel photo imaging plane and rarely to actual geometric boundaries, e.g. boundaries delimiting non-manifold surface regions. This way of geometry representation is advantageous for two scenarios: (1) the texturing of surface areas from a vast collection of corresponding photographs with a minimal requirement on texture units in a simple manner, and (2) a simple yet rapid extraction of 3D positions from 3D surface data, using ray casting and ray intersection. While the implementation and data structures for the data are kept simple and allow easy processing of their texture-mapped images in particular, there are several problems and drawbacks with this representation (see chapter 2).

The presented polygonal soup representation allows for the existence of holes within the geometry. During the experiments conducted in chapter 6 and chapter 7, it was recognised that missing geometry in the surface intersection of image salient points leads to issues for the image registration. More specifically, it leads to an unbalanced salient point sample distribution that results in translational offsets after the pose estimation of the images (consult section 4.4 of chapter 7 for details). This resulted, in the Whitby case study, in a vertical offset of up to 2 metres of the re-mapped geological interpretations, which is not within common tolerance limits for geological applications. As a comparison for the demanded mapping precision required within digital outcrop geology, see Buckley et al. [38]. Additionally, chapter 2 dis-

[27] Open Computer Vision - `http://opencv.org/`

[28] Open Scene Graph - `www.openscenegraph.org`

[29] ANSYS Simulation-driven product development - `http://www.ansys.com/`

cusses in-depth the disadvantages of polygonal soups for volume geobody extrusion based on interpretation. A final drawback to be mentioned is that the splitting of geometry also leads to a split of the parameterization (i.e. the texture space). Several extensions to existing techniques based on image analysis have been internally proposed to elevate the geological capabilities of GRIT. They cannot be realised because the evaluation of local neighbourhoods (i.e. regions) around vertices is inconsistent due to the split (see fig. 2.5). It is, for example, rather simple to compute local edges along the outcrop so to highlight geobody boundaries. Because of the split geometry, the boundaries between the polygon sets themselves also appear as edges within texture space. This leads to confusion for the geologist observing the DOM, because some pronounced features within the outcrop do not correlate with any geological feature, as illustrated in fig. 8.2.

(a) original, textured DOM

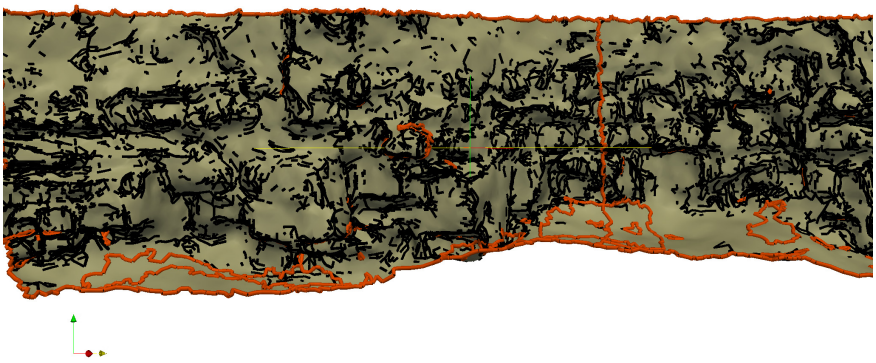

(b) illustration of ”feature“ edges

Figure 8.2: Illustration of feature edge appearance problem (in 3D space). Based on the original DOM (a), feature edges are extracted on the basis on dihedral angles (which correspond to edges in local parameter space). As seen on the filtered illustration (b), some edges correspond to geological features based on the outcrop's geometry (black lines), while others are just due to geometric consistency errors shown in chapter 2 (red lines). As it is non-trivial to distinguish between both cases, a simple and direct application of visual analysis techniques inevitably leads to a confusing behaviour of the software for the domain expert.

The geometric inconsistencies and the discontinuity within the parametrization have implications for the target geological application and advanced interpretations techniques. The short-comings and inconsistencies can be neglected in simple workflows and case studies, but they have an impact on complex cases and future extensions (e.g. surface extrusion, facies mapping, numerical simulation).

For some technical illustrations and proofs-of-concept in chapter 1, the related DOM was completely reprocesses by means of accurate mathematics with the proposed workflow in chapter 2. The proposed workflow extends the current capabilities and does not replace or remove them, meaning that applications such as hyperspectral texture mapping (as in [38, 163, 271]) will continue to be possible within the novel approach.

8.3.2 Dynamic DOM Rendering for Large Models on Mobile Devices

During the experiments with GRIT on DOM rendering and the image-to-geometry registration, performance issues with respect to the rendering speed and the 3D reprojection have been experienced. The lack of performance in these cases is due to the memory limitations (section 8.2.1). The performance of the registration procedure alone can be simply improved by providing separate files for textured- and untextured surfaces. Bare 3D coordinate information can also be obtained from the untextured surface, saving a large amount of memory and possibly leading to improved performance. Another way to avoid the performance limit is a web-based rendering approach, which was out of the scope of this research due to fieldwork restrictions (see section1.4.1).

A solution that was formerly introduced for memory-limitation problems of 3D graphics data on desktop computers can be adapted to solve the issue on mobile devices in the same way. The term *dynamic data loading*, which offers a solution to the rendering problem, refers to a variety of techniques to dynamically retrieve and suspend data relative to the current vantage point of the user within the virtual scene. Borgeat et al. proposed a Level-of-Detail (LoD) rendering technique for terrain models that is directly applicable to the rendering of DOMs [29]. Several further studies of LoD data structures appeared within the past decade [65,186] and the technique found its application across all sciences that require the presentation of 3D data [20,135]. Bettio et al. introduced compressed rendering to significantly reduce the memory requirements of 3D geometry [19]. Advanced compression techniques are typical initial engineering solutions to approach rising data memory requirements. Out of core rendering [298] is an extension to the LoD idea by (a) only loading the segments that are within the view of the spectator into the virtual scene, and (b) load different parts of the scene as different detail levels, so closer objects appear more detailed than objects further away [249, 288]. This principle was investigated by the candidate during the research period, specifically addressing how the technique can be embedded and realised in publicly available 3D geospatial rendering software with open data formats, such as GML. The results are presented as a summary in appendix D and in detail in the related article. A final interactive, quasi-limitless rendering approach is ”rendering-on-budget“, which measures the available rendering performance while displaying the data and, in subsequent render operations, optimizes the presented data fidelity to the available performance of the specific device [147, 254]. An out-of-core rendering technique is already available to the adjunct research group to realise full-scale display of DOMs via web interfaces. During the research, an out-of-core rendering approach by Kehl et al. [147] has been prototypically tested on artificial 3D surfaces (e.g. cubes and spheres) and is approved to work on mobile devices (see fig. 8.3). The realisation of the technique, on the other hand, demands the re-processing of available DOM data from the SAFARI database,

which has been avoided due to time constraints.

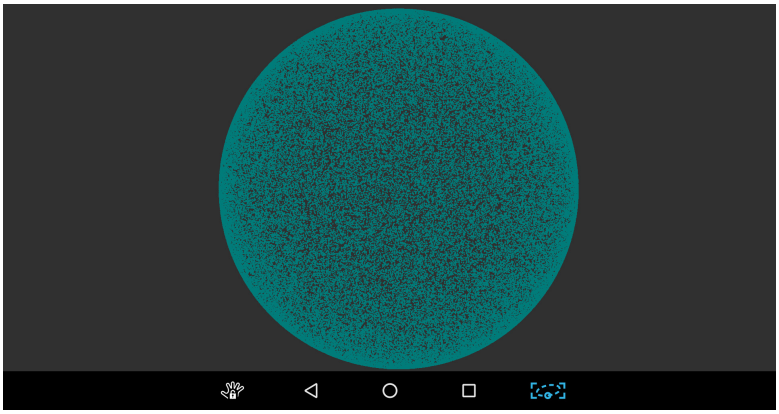

Figure 8.3: Proof of concept for out-of-core rendering running natively on mobile devices: Example of a synthetically-created sphere with a large, high-density point sample.

The workflow for using DOMs on mobile devices potentially benefits in multiple ways from the introduction of dynamic data loading. First, it leads to a significant rendering speed increase when displaying digital outcrops. Apart from the 3D surface geometry, the technique is equally applicable to the photographic surface texture to allow fine-grained quality control over the presented data. The increased responsiveness of the data display leads to a fluent 3D navigation, which may in return also allow to do the data interpretation in 3D within a more sophisticated approach. In the end, the smart data organisation reduces memory consumption and thus potentially reduces the power consumption of DOM mobile apps. The implementation of available techniques for DOMs on mobile devices is within reach of short-term extensions to GRIT.

8.4 Applicability to Geosciences

After having discussed the research results as well as the emerging scientific- and technical limitations in a critical manner, this sections aims at the implications, extensions and applications of the presented research in petroleum geology, geology in general, and other branches of the geosciences.

8.4.1 Field-based Outcrop Interpretations

The research insights of this thesis are integrated in the GRIT application that allows geological interpretations in the field. A limited number of generic interpretation tools are offered to the geologists, due to the limited time frame of the project and the wide scope of the conducted research. The software offers the possibility to create facies interpretations in form of lines, polygons and brushes, as shown in fig. 8.4, which are widely applicable and flexible in their use. As pointed out by Lidal et al. [179], the development of geological sketching tools demands a trade-off between flexible but generic techniques that impose minimal constraints to the geologist, and a small subset of dedicated, highly specific, constrained modelling

techniques that address details within the geological domain terminology. This statement is equally true for the development of interpretation tools. In future development efforts, the geologically-specific techniques can be deduced as a subset of the available, generic interpretations (i.e. lines, polygons, brushes) for extracting channels, point bars, or crevasse splay zones according to a given facies standard (e.g. SAFARI). The translation of the generic geometry descriptions into dedicated tools for each of the currently 441 depositional elements of the SAFARI standard is out of scope of this dissertation.

Figure 8.4: Overview of the interpretation tools provided by GRIT: brush (top-left), line segments (top-right) and polygons (bottom).

Another intuitive split of the generic interpretation tools into geologically more meaningful description can be done by targeting specific geological elements. The line segments and polygons can be classified into geobody boundaries within sedimentology, lithostratigraphic limits, or fracture clusters and fault lines within structural geology. Intuitively, line orientation constraints could be used to differentiate between the different line segment classes, but the arbitrary orientation of the underlying outcrop photo and the geological feature (e.g. caused by folding) prohibit such simple heuristics. An additional class can be used to describe higher-level annotations (e.g. strike-dip direction, paleocurrent direction, cross bedding) that afterwards are not mapped to actual facies geometry but are instead kept within the image as supplement information for the statistical modelling stage. The brushing tool can theoretically be extended for closed-geometry facies mapping by reprojecting the centre of each brush stroke on the surface geometry to obtain a 3D anchor. Subsequently, the vertices and triangles that are spherically enclosed by the brush are then tagged with the related facies indicator. A practical issue currently prohibiting this extension is the estimation of the related spherical radius from the pixel-scale size of the brush. Furthermore, the brushing tools allows a more artistically-styled interpretation, as shown in apps such as Sketchbook and Dabbler (see section 1.4.1).

Apart from the future extension possibilities, a significant advantage of GRIT is its versatility: the developed application can be used even in remote field environments and for various types of outcrops and outcrop study cases. It facilitates an easy and rapid creation of outcrop

interpretations. The 3D component, if interpretation registration in 3D is successful, provides an on-spot overview of a running outcrop study. It means that the field geologist can quickly respond to data- and interpretation gaps in the field, which prevents the need for unnecessary fieldwork repetitions. As former studies on carbonate outcrops have shown, the completeness of a study is of high importance as some outcrops (e.g. degrading cliff sections, active quarries) may deteriorate over time, which makes fieldwork repetitions impossible. In other cases, for example roadcut-outcrops, the rock exposure may be covered over time, which also prevents further studies. An extended visual overview of the data coverage with outcrop images potentially further improves such overview assessments. Tunnel outcrop studies are not facilitated by GRIT due to its reliance on GPS reception.

8.4.2 VOM2MPS - Building MPS Training Images

Chapter 7 shows in detail how the mobile device interpretations can be included in a standard, outcrop interpretation-based MPS modelling workflow. A major drawback of the current methodology is the in-between step of data export to LIME that itself is then only used for data export to Petrel. The devised methodology would hence largely benefit from an engineering extension to directly support data export to reservoir modelling software, such as Petrel or GoCAD. The integration of LIME in the workflow has been chosen for the simplicity and extendibility of its workspace format. The workflow is illustrated in fig. 8.5.

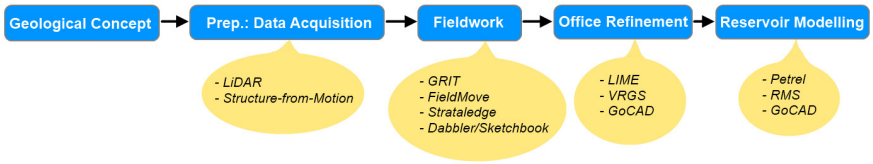

Figure 8.5: The reservoir modelling workflow, from mobile device outcrop interpretations to MPS TIs, developed in shared collaboration with James R. Mullins (Uni. Aberdeen).

Another issue within the reservoir modelling software export step is the limited support for (textured) surfaces in Petrel and RMS. While it is possible to import surface vertices in these software packages, the surface construction needs to be repeated with the (possibly suboptimal) internal interpolation methods. On the other hand, the mentioned modelling applications support point set surfaces comparatively easily. It may hence be advisable to create a dense vertex sample from each interpretation surface (e.g. geobody cross-section on the outcrop), attached with a facies indicator attribute, and export surfaces structures in this representation format. The dense surfaces sampling can be easily facilitated by Poisson disk sampling [61, 166]. It provides sufficiently dense information so that any interpolation algorithm correctly recreates the underlying interpretations of the geologist and proceed further within the modelling workflow.

The previously described interpretations initially reside on the mobile devices. After the actual fieldwork, they can be sent directly to desktop-based digital outcrop software on laptop computers in a base camp (if available) or later be imported into such software in the office. There, the interpretations can be refined and transferred to reservoir modelling software. It is possible to derive a coarse, small-scale approximation of the related, artificial reservoir on modern laptop computing equipment.

Appendix C shows a simple application, technically possible to implement on mobile devices, that facilitates volumetric analysis with smart, statistically-derived facies filter operations. An example of this is shown in fig. 8.6. Volume visualisation tools such as that can be used in the field after the coarse, small-scale reservoir computation to compare and related the statistical output to the observations in the field.

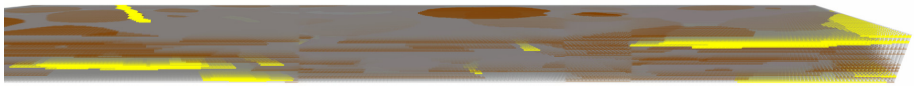

Figure 8.6: Semi-transparent volume visualisation of a regular-gridded geocellular reservoir model of the Saltwick formation, based on the Whitby cliff outcrop. Brown areas depict crevasse splay, yellow areas depict channel body facies and the grey surrounding represents the overburden.

8.4.3 Interpreting Structural Features for Fault Facies Geomodelling

The dissertation and the VOM2MPS project specifically target the interpretation of sedimentary facies within outcrops. Despite this focus, the generically-designed interpretation tools also extend to applications within structural geology. As such, it is possible to use GRIT for structural fieldwork to interpret fault features by facies [295] on outcrops, as shown in fig. 8.7 on a case study in Utah (USA). The figure illustrates the method using facies indicators to delineate a lens fault core, its smear membrane and some adjacent fractured zones with the polygonal envelope tool of GRIT. The picture was provided by J. Tveranger. A fault facies conceptual geomodel, visualised in the volume visualisation software presented in appendix C, is presented for comparison next to it.

The vast majority of currently available DOMs pose a challenge for a further, thorough assessment of the fault facies modelling: as explained in chapter 3, digital outcrop data are commonly subject to geometric pruning at sections covered in scree and vegetation. Scree and vegetation often occur close to fault features within outcrops as fault zones are subject to extensive weathering and erosion [260]. A thorough assessment therefore demands completeness of DOMs without excessive geometric pruning close to fault-related features.

The acquired 3D surface interpretations can be imported into the fault facies modelling workflow via their boundary vertex sets. These can be imported in a reservoir modelling software to generate the related surface shapes using a local b-spline interpolation. The related fault core then needs to be extruded manually. A more volumetric description of the fault facies, as illustrated in general for sediments in the case study of Brimham Rocks (see chapter 2), is an objective of future research. Once the facies interpretations are integrated within the gridded geocellular volume, established workflows [91,240,241] can be used to study the fluid flow behaviour of analogue structural formations using the outcrop interpretation. Ideally, the resulting, volumetric fault models are fused with MPS-generated reservoir models of sedimentary facies for a more complete representation of related geology, as previously envisaged [295]. The fusion can be done by placing the volumetric fault core along previously-defined planar fault positions.

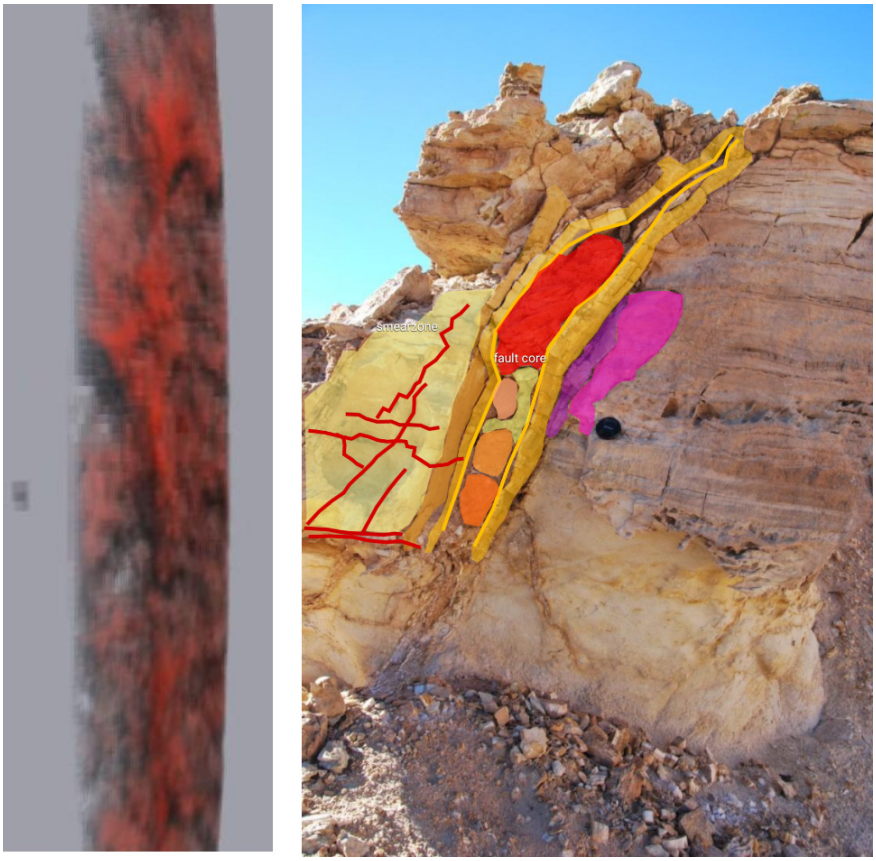

Figure 8.7: Outcrop-based fault facies interpretation example created on a tablet using the GRIT application.

8.4.4 Applications to Other Domains in the Geosciences

Because the field-based interpretation tools are kept within a generic frame (as explained in section 8.4.1), the developed techniques, algorithms and tools are also applicable to other disciplines within geology and stretch even to other branches of the geosciences.

First of all, we assess the applicability of the chosen, visual approach to fieldwork for novel applications within geology. Two increasingly important topics within petroleum geology are CO_2 storage and geothermal energy, as already mentioned in the introduction (chapter 1). The insights and tools originally conceived for hydrocarbon reservoir modelling are commonly applied as-is to the outcrop-based assessment of CO_2 storage sites, as shown by Senger et al. [265] and subsequent studies [222]. These studies use a DOM of the Botneheia outcrop to get an understanding of the formations relevant to the sealing assessment of a prospect CO_2 storage at Longyearbyen, Svalbard, Norway [33]. A considerable amount of field data has been collected in the course of the study, such as sedimentary logs and field measurements of the formation's strike and dip direction at various structural measurement- and observation stations. Such a study can benefit from digital field tools when already considering its spatial extent: the related fieldwork took place over several days to document geological details as well as making a connection between the different datasets of the study. This is simplified if the digital data can be directly taken into the field, focussing the actual fieldwork on filling the conceptual gaps of the study, refining the geological concept digitally during fieldwork and re-assess field plans based on the refined concept. Furthermore, the desktop-based assessment of the Botneheia outcrop can be problematic as some essential stratigraphic boundaries are covered by scree from loose sediments. By taking the DOM to the field, the geologists can carefully remove the scree at selected locations, take a picture of the revealed geological boundary and integrate the mobile device photo interpretation into the DOM. This comes at the cost of slight positional inaccuracies: as the scree layer is removed, so do the 3D positions of the interpretations not accurately correspond to the formation. This is considered minorly relevant when comparing the scale of the position error (approx. few metres) to the length of the outcrop (several kilometres). A problem for the extension of the visual approach with the current mobile equipment to these large-scale CO_2 studies is power consumption and battery capacity of mobile devices, as discussed in section 8.2.2. A large study area needs to be covered in the course of the geological investigation, so the mobile device should be used at carefully selected positions to save battery power. Mobile device external batteries should be taken to the field to extent the mobile device use. At the specific location of Svalbard, the lack of accessible electrical plugs for recharging the equipment is an additional problem that limits the extension of the proposed, visual approach for mobile devices to this specific case of Longyearbyen CO_2, but it is generally an increasingly rare problem during fieldwork.

The mobile device, 3D-space, DOM-derived interpretations also potentially help to reduce the uncertainty within the geological modelling. Currently, outcrop interpretations are performed on statically-acquired outcrop models, where the 3D surface information stays fixed after an initial scan. In reality, dynamic processes such as erosion, weathering and landslides deform a once-scanned terrain surface, which, as a result, uncover previously hidden geological information. While these dynamic processes are currently more often seen as hazards to the scanning, the newly-uncovered information can be used beneficially by carrying out monitoring surveys over time for digital outcrops (previously analysed within photogrammetry [207] for coastal regions). The temporally re-acquired and co-registered 3D information can be simultaneously interpreted with the help of mobile device DOM applications, such as GRIT. The temporally-related interpretations of multiple outcrop surveys can subsequently be integrated in a consistent project coordinate reference system. This leads to multiple geobody cross-

section surfaces that can be interconnected within the consistent reference system to support the actual 3D geobody extrusion and reduce the uncertainty of the extrusion process. Although the process requires multiple 3D data acquisition surveys, modern photogrammetry, UAVs and the SfM reconstruction via mobile devices (as outlined in section 1.4.2) simplify the acquisition process in the near future. The mobile device photo acquisition for Brimham Rocks (section 1.6) has already been carried out simultaneously to the lidar survey, illustrating the conceptual applicability of such a monitoring workflow.

An prospect application case outside geology (i.e. petroleum geology) is glacial monitoring. Lannutti et al. [168] recently presented a case study on the Viedma glacier in the southern Patagonia ice field that measures the glacial motion in an optical monitoring setup and utilising image-based optical flow. With the help of the presented mobile device application, it is possible to link the optical flow motion estimation of the glacier with the image-to-geometry registration (see chapter 4 and 5) to obtain 3D metric measurements in a technically simplified manner. The resulting increase in quantitative data of glacial motion supports subsequent application studies and decision making on issues such as sea-level change or ocean salinity. The measurement of glacial motion by mobile device-captured, co-registered imagery, on the other hand, requires the availability of at least one initial 3D surface model at the start of the monitoring. Additionally, the article's authors point out that changing lighting conditions complicate the optical flow estimation, respectively due to the inter-image registration [168]. This problem can, to a certain extent, be accounted for with the improved feature-based registration methods presented in chapter 5. There are other domains within the geosciences that essentially depend on fieldwork observations, and their embedding in a coherent 3D spatial frame, that potentially benefit from the ubiquitously-available, cheap, visual mobile device technology. Despite this wide range of potential applications, the presented technology has limitations in optically challenging environment. The photos on which field interpretations are based need to be registered with the related (textured) 3D surface model, which presents a problem if the objects of interest are highly refractive (e.g. glaciers) or commonly exceed the quantization range of mobile device camera exposures (e.g. lava observations in volcanology). Accounting for these optical disturbances exceeds the capabilities of comparably simple, feature-based image registration techniques, as presented in this thesis. Another issue with the optically-challenging application cases is the acquistion of reference 3D data themselves: outcrop formations have very beneficial reflection properties for optical measurement instruments, such as lidar, structured light and image-based reconstruction (i.e. SfM), which makes their precise digital acquisition easy. Light refraction patterns from glaciers or the SfM acquisition in volcanology pose 3D scanning challenges for the future, which in return opens up new possibilities for mobile device visual techniques to conduct fieldwork within the related geoscience domains.

A geoscience application that is well within the technical capabilities of the presented visual mobile device approach is hydrology, more specifically the analysis of free-surface flow and water protection and management. Currently, geoscientists and decision makers in the Netherlands use lidar data on a massive scale to plan water protection measures on a local and national level [173]. Coloured lidar point sets are used in virtual environments [147, 149] to inform decision makers, communicate water planning to the general public and visually assess artificial protection measure construction. In the spirit of this already graphical, 3D lidar development, mobile device applications such as GRIT can be integrated in the water protection workflow to assess and document the state of existing protection measures, such as barriers and levees, and highlight flaws, damage and potential future points of protection failure in the data. These annotations, technically treated in equal manners to line segments for geological features (see section 8.4.1), can be created on lidar subsection of datasets such

as AHN-2 or AHN-3[30] and then be re-integrated in larger, visual decision making platforms as presented by Leskens et al. [173]. This provides detailed information collected in the field as a supplement to large-scale visualisation and simulation data of typically coarser resolution.

[30] Actueel Hoogtebestand Nederland - `http://www.ahn.nl/index.html`

8.5 Research Outlook

Next to the technical extendibility and the various geoscientific applications that the presented research already allows to address, there are a large number of novel scientific research directions that unfold from the content and the visual approach given in this dissertation. Five interesting future research directions are further detailed and discussed, out of the large selection of future topics.

8.5.1 Guided Segmentation and Interpretation of Geobodies on DOMs

The interpretation within the presented approach exclusively relies on the interpretation of acquired photos and their projection from the two-dimensional image space to the three-dimensional outcrop space. Although the techniques are working as presented, drawbacks with respect to image registration remain as obstacles, and issues of occlusion and inter-image consistency have not been addressed during the research period. Section 1.4.1 already introduced an alternative, based on the interpretation of the outcrop directly in 3D space, comparable to the approach of Viseur et al. [302]. The major research challenges posed within the direct 3D interpretation approach is the convenient navigation for DOMs in 3D space on mobile devices and intuitive, accessible means of interpretations for the field geologists. These challenges are currently investigated.

This ongoing research is split into two parts. The first part deals with the interaction design in 3D on mobile devices. 3D navigation in mobile- and web-based virtual environments is a topic of recent investigations within the computer graphics community [192, 234, 317]. The current interaction scheme within GRIT, as illustrated in chapter 7, is designed around a simple, single-hand interaction that can be used intuitively outdoors. This design allows the geologist in the field to have interactive discussions and physically point out interpretation features while navigating within the 3D view. This feature is supported by using on-board mobile device motion sensors (i.e. gyro and accelerometer) for scene navigation without direct, haptic interaction. An issue with the currently available navigation schemes is the large amount of freedom in the navigation motion. Emerging from interviews with geologists, it becomes apparent that a surface-constrained motion is more applicable to digital outcrops. Additionally, there are two different interaction modes applicable to DOM navigation. Panoramic overviews in virtual scenes of outcrops lend themselves to a first-person view interaction (fig. 8.8), whereas close-up views to the outcrop are more applicable to orbital interaction (fig. 8.9). The difference between the two modes is illustrated by the changing motion element (i.e. the view centre or the view position) in table 8.1. New ideas for the translational movement of both cases of navigation are required. Further potential interaction schemes could be inspired by pivot vantage point–view centre pairs, where the view transition is smoothly realised in a Google StreetView-like manner.

Interaction Element	first-person		orbital	
	rotation	translation	rotation	translation
view centre	move	move (view-ortho.)	fixed	move (surface-ortho.)
view position	fixed	move (view-ortho.)	move	move (surface-ortho.)

Table 8.1: Comparison of surface-constrained navigation (motion) with first-person and orbital interaction with respect to view centre and view position changes.

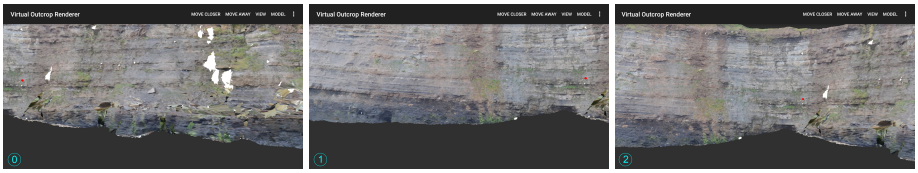

(a) (b) (c)

Figure 8.8: Illustration of a first-person rotational view motion, where the view centre moves while the view position stays fixed.

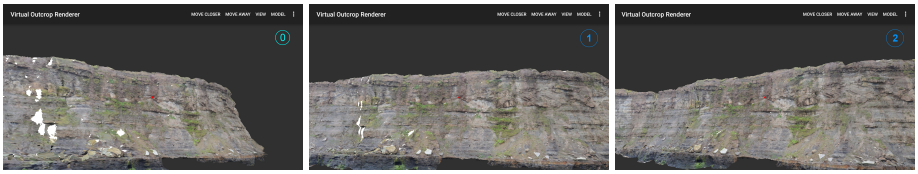

(a) (b) (c)

Figure 8.9: Illustration of an orbital rotational view motion, where the view position moves while the view centre stays fixed.

The surface-constrained motion, in the end, couples well with the second research trajectory of guiding user interpretations and simplifying the geobody interpretation in 3D. Currently, a combinatorial (i.e. morphological) approach is taken, based on computational geometry principles for PLCs, as explained in chapter 2. First of all, the interpretation of line-segment geological features (e.g. strata boundaries and fractures, see section 8.4.1) can be supported by snapping the line-describing touch-based interaction to close-by valley feature line segments in a weighted distance scheme. The basic technique was introduced by Kudelski et al. [13, 160, 161] and is shown on a DOM segment in fig. 8.10. Secondly, the extraction of actual geobodies can be simplified and enhanced by computing the geometric envelope of rugged surface structures occurring along a given touch-based interaction path, as illustrated by fig. 8.11. The technique can potentially be enhanced by including radiometric DOM properties to solve geometric ambiguities.

Although the research is still in an early phase, it becomes apparent how the evaluation of digital outcrops in a geometric manner potentially supports development of smart and intuitive navigation and interpretation interaction tools. The available, geometric information can also be used by non-photorealistic rendering (NPR) techniques to highlight DOM features in a subtle manner, for example by highlighting sharp edges and casting artificial light and shadow on a DOM that visually elevates objects of interest. The use of the proposed techniques in an enhanced visual approach for digital fieldwork, in return, can lead to a wider acceptance of the presented, novel technologies in the geoscientific community.

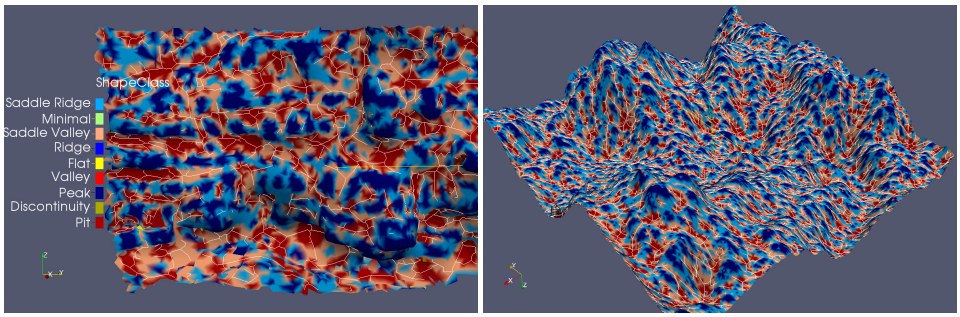

(a) (b)

Figure 8.10: Illustration of the valley feature line extraction on DOM subsection at Cloughton Wyke, North Yorkshire, UK (a), and large-scale mountain range example (b). The colours indicate the curvature class based geometric mean- and gaussian surface derivatives explained in Kudelski et al. [161]. The feature lines describe the centre of valleys of a DOM surface, as seen in the stratigraphic bedding and faults of outcrops.

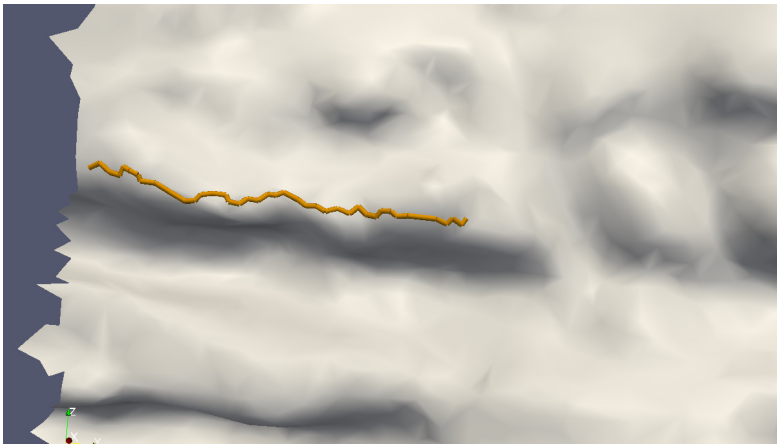

(a) initial interpretation line placement

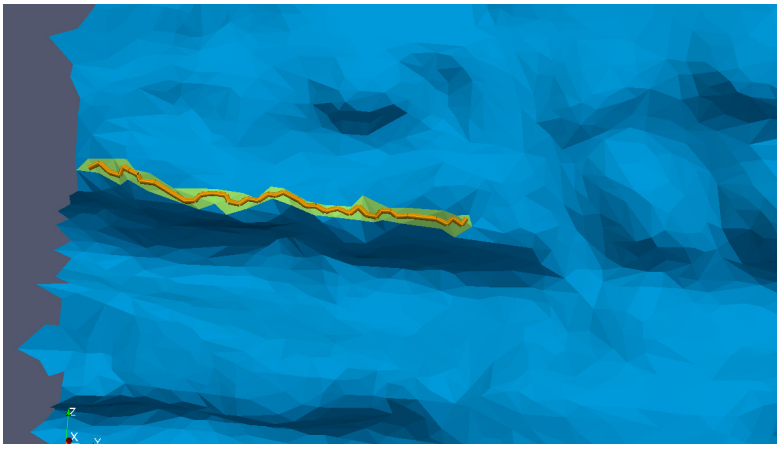

(b) initial boundary envelope of the interpretation line

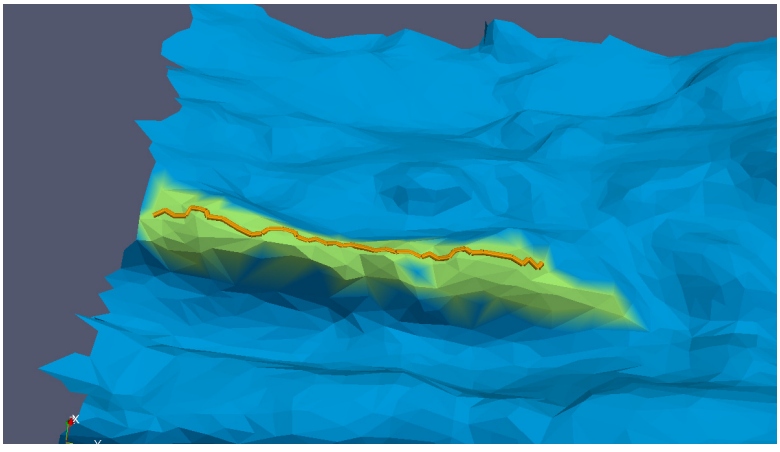

(c) resulting boundary envelope of the outcropping channel sandbody

Figure 8.11: Illustration of the extraction of geobody envelopes on DOMs (c) from an initial line segment located on the outcrop surface (a).

8.5.2 Mobile Device Digital Outcrop Geology Across Scales

The presented techniques in this thesis only show the integration of projective interpretations and field photographs to outcrop-scale lidar models. Although this is a good starting point, section 1.4.2 already presented a variety of additional mobile device tools for geological purposes that are used for geological characterisation of outcrops. Section 8.1 already discusses the potential added value from integrating these information into the digital outcrop. In this section, it is further discussed how to link the visualisation of the data across scales.

The integration of sedimentary logs into the digital outcrop introduces a new scale to the analytical capabilities of the mobile device field application. Sedimentary logs allow detailed information to be included in the field study that is not visible is the DOM or disappeared as compression- and data reduction artefacts (see section 1.6 for an explanation on the data reduction techniques). Applications such as Strataledge currently allow the export of logs as raster image information, although future extensions promise to support LAS as export format. Irrespective of the data format, the mobile device outcrop application can provide anchor points for the stratigraphic interpretations in the form of straight line segments sketched on outcrop photos or directly on the DOM in 3D, as illustrated in fig. 8.12. The straight line segment then provides a reference for the projection of sedimentary log information (e.g. facies indicators) onto the DOM.

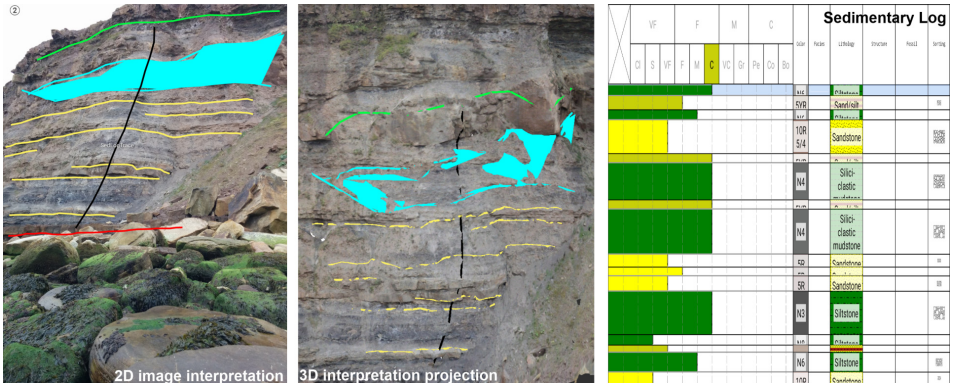

Figure 8.12: Illustration defining anchor points (in 2D) and image plane centerlines (in 3D) for the projection of sedimentary logs on DOMs on mobile devices.

Another image information source already discussed in section 1.4.1 are photo-based geological maps, created by geologists in the field using apps such as NVIDIA Dabbler or Adobe Sketchbook. Because the geological maps are based on previously-acquired images, a possible software extension can allow to attach supplement raster images to the outcrop photo that is currently registered with the DOM. In this manner, additional texture overlays (e.g. geological maps, edge maps for structural highlights) can be coherently mapped with the outcrop photo. This provides additional information to assess a cluster of geological interpretations within the 3D viewer for their coherence. Hyperspectral information (where available) can also be blended with the existing DOM in the field in the same manner as the geological map. In order for this to be possible, the mineral classification mapping product of a previously-conducted hyperspectral scanning assessment is necessarily prepared before fieldwork, so to deal with the immense size of hyperspectral information. Even more sore, the classification map needs to

be stored coherently next to the DSLR photo textures [38]. The spectral information provide rapidly-accessible mineralogy information to field geologists that are otherwise hard to extract and require geochemical analysis of the rocks in the lab [162]. Thus hyperspectral scans gives access to information at significantly smaller scales than otherwise covered with ordinary DOMs in the field.

In this decreasing scale, rock samples are typically collected in the field for subsequent laboratory analysis. Apart from the expensive and logistically-involved transportation process of large rock sample collections, some countries also prohibit the export of rocks by legislation for cultural heritage reasons. SfM, potentially executable on mobile devices as discussed in section 1.4.1 and 8.2.3, provides a cheap and tangible solution to acquire high-resolution, high-detail information of hand samples via mobile devices, as shown on a lab example in fig. 8.13(a). The digital hand sample can be co-registered within the DOM to its place of origin, for example by marking the location on a related outcrop photograph and intersecting the marker location with the surface model. The rock sample's reconstruction as closed C^2 surface geometry (see chapter 2) is easier to realise than the accurate C^1 reconstruction of a whole DOM. Fig. 8.13(b) shows an example of such a valid C^2 reconstruction of the hand sample, which was achieved by Poisson surface reconstruction [144]. A volumetric model can then be constructed from the scanned surface (see fig. 8.13(c)), which can later be used for physical simulations (e.g. small-scale fluid flow [216] or THMC physical simulation [229]) to complete the "geological picture" of a case study. Inspiration to such physical rock samples and their applications in the field can be taken from recent developments in digital rock physics [10, 11]. Moreover, the resulting digital rock sample and its physical simulation properties can be re-imported to the field application within subsequent fieldwork to provide detailed, small-scale context information. The delineated, volumetric mineral structure could possibly be used as template for procedurally generating rock samples of other locations with similar lithology. The representativeness of the digitised hand samples is guided by the geological knowledge of the field expert, as it is also the case for less digitised field studies.

Overall, the multi-scale visualisation capabilities, ranging from wide-scale outcrop surface data and geological maps, over hyperspectral image textures and sedimentary logs, down to small-scale digital rock samples, potentially improve the geological analysis in the field with digital, mobile device technology. Each individual technological contribution is well within the state-of-the-art capabilities of available techniques in computer graphics, visualisation, photogrammetry and computational geometry. It is the synthesis of all the available techniques and their interplay that is the contribution to computational geosciences and that provides the added value in the field.

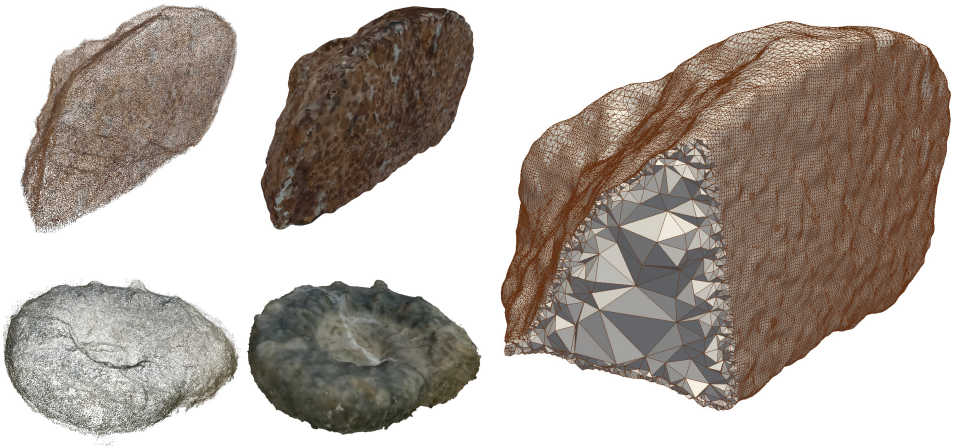

(a) (b) (c)

Figure 8.13: Illustration of the scanning and reconstruction of hand-sized rock samples from points (a) to closed surface (b) and physical volume (c) for their multi-scale integration to DOM field software.

8.5.3 Stylised, Illustrative Visualisation of Facies

Chapter 3 mentions that currently prevalent digital outcrop software tends to represent facies information by mapping the facies indicator values to the visual hue channel, often via jet- or divergent colour schemes. Although this kind of visualisation gives a brief, visually easy-to-understand representation of the facies categories, it inadequately presents the variety of available information associated with a facies mapping. In particular, this visual representation often only conveys the lithological category of a specific outcrop section. This is even more problematic as the lithostratigraphic categorisation is represented in the same visual channel as, for example, sedimentary geobodies and fault facies, leading to visual ambiguities of what the coloured segments actually represent. This ambiguity makes it problematic for outsiders, as well as external experts not intimately familiar with a specific study, to understand the categorisation scheme. On large outcrop studies that assess a multitude of geological features on the same case, the ambiguity may even become an issue for the geological modellers that are familiar with the study. Additionally available information that are crucial for understanding the geological context, such as fossil occurrences and root content from a geobiological perspective, or sediment deposition information, such as grain sizes, matrix order and cross-bedding orientations, are completely neglected in this visualisation approach. The contextural information further provide an understanding of the classification basis itself, which can otherwise only be recovered by manually scanning through the fieldbook information that are available to the facies mapping.

In spite of what current visualisations provide, the information are traditionally covered by field observations. Sedimentary logs traditionally include annotation columns for each sediment section that reflect information about cross-bedding, biological content and matrix order. Grain sizes are meticulously documented in sedimentary logs using a specific classification- and depiction scheme. This becomes evident from an example sedimentary log shown in fig. 8.14(a), created via Strataledge and highlighting the respective columns. The inclusion of the visual supplementary information is even visible in actual geological fieldbook sketches. Fig. 8.14(b) shows such a fieldbook sketch by Jon Noad, presented as a representative guideline for geological interpretation [217].

This assessment shows that next to the plain facies indicator, a collection of additional information is available that can be included into a more informative visualisation, which is currently not been realised. It is suggested to, in accordance with graphical perception principles [213], include these information directly into the digital outcrop visualisation using further visual channels. The grain size can, just as its natural depiction by geologists, be included as grainy texture with modulating circle sizes or adapted dithering of spot noise. Cross bedding can be visualised using a randomly-spaced curved line segment texture, which orientation is adapted to the cross-bedding orientation of the channel fill. Glyph visualisation lends itself ideally for the depiction of geobiological content. Geobiology is also a good indicator for the geological time scale of the sediment deposition [23], as some fossil species only occurred in a specific geological age. The glyph depiction's hue channel can hence also be modulated with the colour code of the geological time scale [223], as mentioned for stratigraphy hue mapping in section 1.3 and chapter 3.

The integration of texture-based visualisation techniques is currently problematic because of the ways DOMs are represented. A point-based surface representations does not lend itself well for texture mapping - particularly for stylistic textures. The problem becomes evident when imagining a point-dithered grain size texture being mapped on a point set surface representation: it becomes ambiguous if the visibility of a point is due to its existence or its favourable texture mapping modulation. TIN-based outcrop surfaces generally allow for this

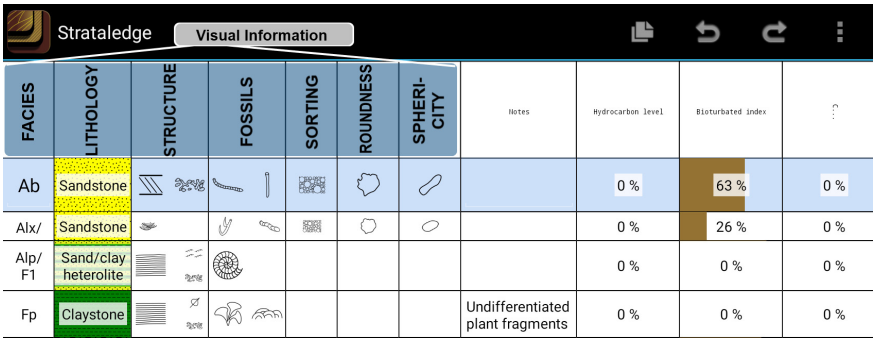

FACIES	LITHOLOGY	STRUCTURE	FOSSILS	SORTING	ROUNDNESS	SPHERICITY	Notes	Hydrocarbon level	Bioturbated index	⋮
Ab	Sandstone							0 %	63 %	0 %
Alx/	Sandstone							0 %	26 %	0 %
Alp/ F1	Sand/clay heterolite							0 %	0 %	0 %
Fp	Claystone						Undifferentiated plant fragments	0 %	0 %	0 %

(a) Sedimentary log information

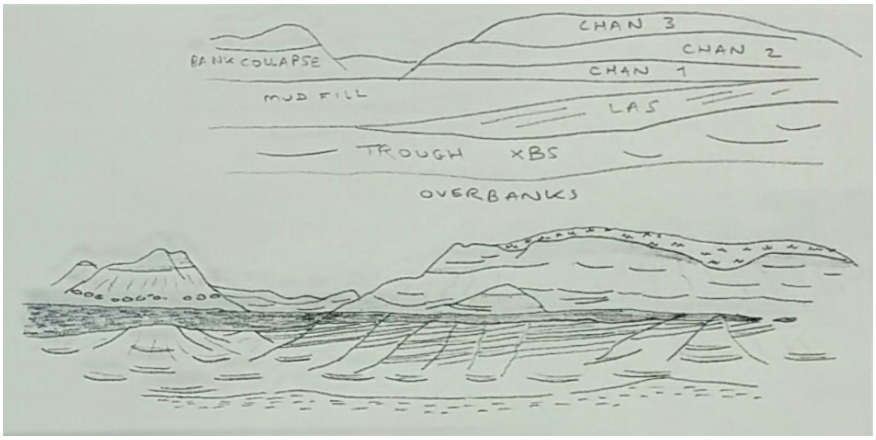

(b) Information from fieldbook sketches, by Jon Noad [217].

Figure 8.14: Visual context information in field geology, as apparent from sedimentary logs (a) and field sketches (b): biological content, grain size, matrix oder, cross-bedding.

texture mapping approach, but their segmentation into different facies, geobodies and stratigraphic regions is currently just soft-linked to the DOM (see the differentiation of soft-linked and hard-linked facies mapping on surfaces in chapter 3). A hard-link facies mapping on TIN-geometric DOMs would allow for the implementation of the proposed, new geological surface visualisation strategies, as proposed in section 8.5.1.

Alternatively, to convey the supplement geological information, it is also possible to design a complex geological glyph, of which a prototype is shown in fig. 8.15. This design is derived in the spirit of complex glyphing for flow analysis [67] and shall adhere to known glyph-based design principles [30]. Alternative glyph designs could depict the surface texture in an abstract mode, or be deduced from local geostatistical properties and their depiction in glyphs via information visualisation. The application case for the complex glyph is rather targeted toward interactive probing operations than full-scale surface data visualisation.

The design of such extended visualisation features is ideally done in constant feedback-and-adaptation collaboration between visualisation experts and field sedimentologists. A prospect outcome of the visualisation research may resemble the emergence of stylistic, domain-specific mapping concepts analogous to Cartography-Oriented Design and Visualisa-

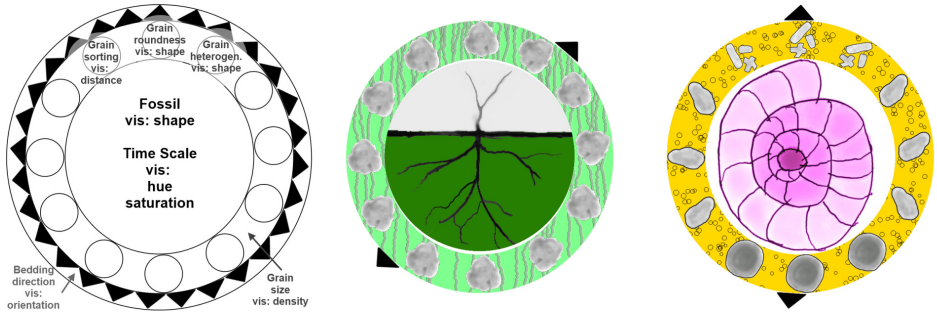

Figure 8.15: Prototypical design of a complex geological glyph for DOM investigation. A key visual component within sedimentary logs is the existence of biological content, which is thus designed as central element. Around the central element (possibly empty) a ring of spherical shapes, representing mineral content, is organised, for which surface sinuosity, elongation and their size is adapted. Modulating each ring element separately allows to express a degree of heterogeneity within a selected segment. The background colour and texture allows to convey further lithological information.

tion, formerly introduced to the digital representation of cartographic elements in thematic 3D terrain visualisation [264]. Cartography-oriented design is illustrated in fig. 8.16, taken from Semmo et al. for water (a, [262]) and city visualisation (b, [263]), and Samsonov for terrain visualisation (b, [259]) .

The added value, besides the higher visual information density and the extended analytical capabilities of digital outcrops, is the possibility to visually analyse and compare multiple (compatible or opposing) geological interpretations in a rapid manner. Each geologists can create, with the given tools, the digital representation of his fieldbook sketches in a coherent framework with the maximum amount of collected information visually available. In a comparative study, multiple interpretations and stylistic visualisations can be toggled in sequence or blended together to highlight commonalities and difference. In this visual manner, it may be easier to qualify and quantify the uncertainty that is inherent to the different geological points-of-view and perceptions [27] of the outcrop in question.

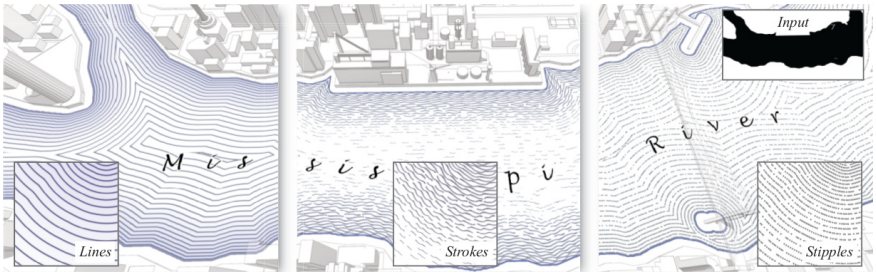

(a) Water visualisation; from Semmo et al. [263]

(b) Stylistic city visualisation; from Semmo et al. [262]

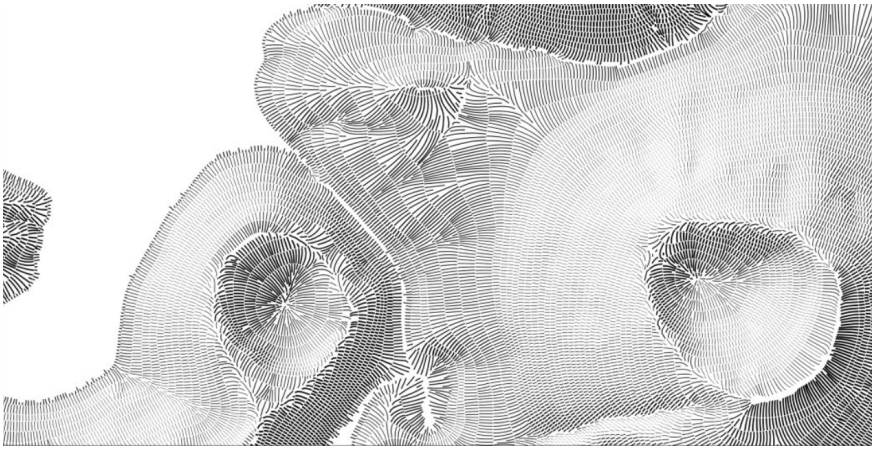

(c) Hachures-based terrain visualisation; from Samsonov [259]

Figure 8.16: Examples for stylistic 3D visualisation of geographic information via Cartography-Oriented Design. Inspiration about the use of visual channels to convey context information can be drawn from this cartographic paradigm.

8.5.4 Stereoscopic 3D, VR and AR in Geological Visualisation

Stereoscopic rendering and VR technology currently gain increasing interest across scientific disciplines, which also holds true for geology and the stereoscopic presentation of DOMs and reservoir models. The interest in stereo-rendering and VR within petroleum geology is actually experiencing a revival, as former VR systems have been in use by petroleum companies such as Statoil and Chevron for exploring subsurface hydrocarbon reservoir models. A cave automatic virtual environment (CAVE) system has been formerly used in interactive steering applications for hydrocarbon production well placement within facies-based geomodels. This application lends itself well to VR technology because of the dense-grid 3D environment and the sparsely distributed drill wells as objects of interest.

The advent of cheaper 3D stereo-display equipment is currently driven by the consumer electronics and entertainment industry in an attempt to firmly establish the technology within society and make it accessible and affordable to the wider public. This has been problematic in the past, especially with the high manufacturing costs of VR equipment. Current VR solutions range from simple shutter glass-technology by NVIDIA (3D Vision), over standalone 3D displays with varying display quality and resolution, up to recent trends in immersive VR using the Occulus RIFT[31], HTC VIVE[32], PlayStation VR[33] and custom-built, fully immersive VR treadmills in the short-term future, as displayed in fig. 8.17 (KAT VR treadmill[34]). The large variety of available technical solutions in different price categories makes the 3D stereoscopic technology interesting again for a variety of applications. Google Cardboard, as mentioned in section 1.4.1, is of particular interest for 3D VR in outdoor environments on mobile devices, for example field geology, which this dissertation addresses. Fig. 8.18 shows the Google cardboard VR technology. It is a comparably simple solution of external lens systems to focus the view on each half-screen of the mobile device. The respective render view is a split-screen setup to display the virtual scene for each eye separately according to the configured view parallax. For more information on the technical details of VR devices, the interested reader is referred to Hainich and Bimber [117].

In order to realise the vision of 3D stereoscopic display and VR on a wider scale and to make it applicable within field geology, a number of technical and conceptual challenges need to be addressed. The technical issue are discussed first. An obvious issue already addressed in section 8.2.1 is the memory requirement of outcrop-scale DOMs. This becomes an increasing issue for VR rendering: without the use of out-of-core rendering concepts the rasterisation is already limited and the load of another view (rendering each eye separately) further decreases the rendering speed. In out-of-core rendering setups, as the whole scene graphs needs to traversed twice (i.e. once per eye) as the visible objects and their level of detail can very per eye. This results also in a memory-bound setup for the digital outcrop presentation, as different objects per view need to be managed in the memory. The problem can be reduced or mitigated for prototypical proofs-of-concept by surface- and photo texture simplification, as explained in section 1.6. Another technical problem is presented by the outdoor usage of the VR system on mobile devices, more specifically the interconnected real world–virtual world navigation. Users of the VR system need to be localised and tracked within their physical surrounding as the VR systems deprives them from their real-world vision and perception (by design). The accurate localisation of the users with integrated mobile device sensors poses a challenge with respect to current technical limitations of the positioning sensors, as explained in section 8.2.2.

[31] Occulus RIFT - `https://www.oculus.com/rift/`

[32] HTC VIVE - `https://www.vive.com/`

[33] PlayStation VR - `https://www.playstation.com/en-gb/explore/playstation-vr/`

[34] KAT - WALK INO VR - `http://www.katvr.com/English.html`

Figure 8.17: Custom-built design of a VR treadmill by KAT VR. Important to notice is the lack of a waist-bound ring that was common to previous VR treadmills, which considerably limit the motion freedom of the VR user. The user experiences the 3D world via VR goggles, which are connected to the flexible, top-mount backpack, which is in the end connected to a computing platform. The motion of the user is measured through the parabolically-shaped surface through frictionless shoes, specifically designed for the VR instrument.

Figure 8.18: Image of the Google Cardboard VR conversion of a mobile device in a VR-goggle like box, with focus on the lens focus system (left). The CGI process is adapted by configuring a split-screen setup according to a pre-defined parallax and rendering the virtual scene accordingly per eye.

This problem necessarily needs to be addressed by smart sensor systems, reliably providing at least decimetre-scale accuracy in all three spatial dimensions, before any field trials can be conducted. Alternative, in a financially less-constrained setup, dGPS can provide the required localisation sensor accuracy.

The conceptual challenges for VR systems are considered to be of even higher importance than the actual technical limitations. After observing the progress and usage of previous VR systems, the computational geoscience- and the visualisation community shall potentially investigate the reasons of why previous, elaborate VR systems are nowadays rarely used in routine workflows within the petroleum industry. In contrast to the entertainment industry, where the major obstacle for establishing VR is the cost for the target audience, the petroleum industry was able to afford and mitigate the costs of professional VR equipment to be used within industrial workflows. Despite the availability of the technology, VR has still not emerged as a practical tool for routine tasks, even in desktop-based geomodelling environments. One reason for the slow adoption of the technology can potentially be found by the elevated expectation of automation for VR systems: in conclusion of informal discussions, it appears that geology experts expect the system to work "as-is", meaning that the connection of the hardware device to the related rendering system readily provides a smooth stereoscopic visual experience. The professional user base possibly neglects at times that an artificial vision system from stereo-rendering needs to be adapted to each individual's complex, physical visual system. As an example, the optical parallax of the eyes is not a fixed value but differs amongst the human population. Visual deficiencies, commonly corrected by glasses and contact lenses, are physical proof of the variances of the human visual system amongst the population. In order to account for these variances, VR needs to be calibrated to each individual user to provide a smooth visual experiences that is comfortably endurable over stretched work periods. Analogous to initial (i.e. first-time) use of physical visual system corrections (e.g. glasses), an extended, undisturbed training period for VR- and stereo-rendering systems needs to be planned so that the target user can accommodate to the changed visual perception and, as a final result, accepts the new visual perception as "natural". The outlined perceptual challenges are potentially difficult to address within a fieldwork environment. Further information on stereoscopic perception and VR design are given by Parisi [227] and Fuchs [99].

Another point of more fundamental nature that needs to be addressed is the purpose of stereoscopic- and VR visualisation for petroleum- and outcrop geology workflows. Plain geomodel- and DOM data presentation and virtual 3D navigation within the volumetric data has possibly limited added value compared to established workflows with traditional computing equipment. The interactive steering of well placement and drilling coordination within a subsurface volume is a very suitable application case for VR, but currently remains a niche case within petroleum geology. Future development within geology that incorporates modern visual techniques and equipment potentially benefits from a task-driven requirement analysis and development cycle for visualisation systems (as laid out in the nested model for visualisation design by Munzner et al. [212]). The adoption of this design methodology allows to incorporate VR technologies at the stages and tasks it is best suited to address. Novel application scenarios within geology that can make use of VR are manifold: large-scale CO_2 storage reservoirs are typically designed based on a variety of heterogeneous and sparse data across dimensionality scales (e.g. 1D-4D data). The task to statistically correlate features of interest on density-heterogeneous data (e.g. DOM interpretations, high-resolution seismics, well log) on such large scales is possibly well addressed by VR visualisation, as there is arguably no combined projective space that allows a clutter- and occlusion-free data assessment.

Outside the known application boundaries of VR for petroleum- and geomodelling and its

future prospect application in the field, the technology may open geological studies in other domains and towards other audiences. VR technology can be used to bring geological studies to audiences with disabilities, which commonly prevents them to conduct actual fieldwork. The immersive nature of the technology potentially allows to partially share the physical field experience on outcrops with an audience that is usually prohibited from fieldwork. Moreover, expanded VR technology has a place in teaching and collaborative, remote-connection meetings. An initial study by Kehl [145] has shown the use and some novel approaches for collaborative interaction in virtual environments on case studies within hydrology (i.e. flood management and mitigation). The initial ideas can be expanded to provide a larger user group with a consistent 3D world that can not only be explored collectively but also modified by each participant individually, targeted to digital outcrop geology and the analysis of DOMs. The case study naturally extends towards and shares concepts with *virtual fieldtrips*, as discussed in section 1.4.1. A final geological application case that utilises DOM data are extra-terrestrial- and planetary geological studies. Here, the benefits of VR systems are manifold: planetary studies principally suffer from physical inaccessibility. Therefore, as in the case of outcrop VR studies aimed for people with disabilities, the technology allows to create the illusion and partial experience of an actual fieldtrip under conditions where physical access is impossible. In addition to addressing the physical access issue, planetary studies commonly require participants with various expertise to create adequate geological interpretations. A shared virtual environment and extended VR interaction possibilities address this special case of virtual fieldtrip scenarios, as recently discussed by Traxler et al. [292].

Augmented reality has possibly an even larger, wider impact on geoscientific fieldwork in the future. As explained in section 1.3, AR aims at supplementing the natural perception (i.e. physical observation) of the world with visual, digital data. This is currently achieved by visual overlays. AR allows to circumvent technical issues of VR systems as it is often localised imagery that needs to be correlated to 3D background information. A high-accuracy 3D localisation can be circumvented as it is only the observed image (e.g. via Google glasses) that needs to be correlated, and the user still has its natural means of orientation and vision for navigating in his environment. Because of this fact, it is also possible to apply AR technology in geological environments where localisation is proven difficult, such as in tunnels or caves (example by Ortner et al, [226]). Application domains for extended AR use hence include infrastructure construction, underground- and cave mineral studies (for mining operations of rare minerals as well as environmental protection from hazardous minerals such as asbestos), urban construction and planning and outcrop field studies. AR technology can also be interpreted in a wider sense, meaning that it is not only the visual perception (e.g. through glasses with digital overlay) that is augmented. The use of so-called "wearables", which includes digital smart-watches and electronically-supplemented clothing, present another dimension of AR. Even these technologies have potential applications to the geosciences outside acting as bare physical sensors: Digital watches can act as ubiquitous compass- and navigation devices that help to rapidly locate, visit and survey and array over pre-planned locations for outcrop studies or hydrological protection structure assessment. In the same way, smart clothing that is digitally- and remotely connected to a base station can forward remotely-sensed physical data, such as micro-scale ground motion or humanly imperceivable environmental heat changes, during volcanic studies to the expert on the ground. The physical perception of the remotely-sensed, measured property is then enhanced by stretching the fabric or changing the isolation properties.

In conclusion and with respect to the geosciences, stereoscopic rendering, VR and AR technology present opportunities for improved data exploration. The technology is increas-

ingly accessible and affordable, and allows to address multiple issues with respect to digital outcrop studies. Technical and conceptual challenges in the usage of VR, in particular in field-work environments, need to be adequately addressed. Even more so, lessons from past case study experiences of VR within petroleum geology should possibly be considered in order to refine workflows and design tasks that draw maximal value from the new technology. The connection between 3D view and appropriate interaction components to provide simple user interfaces is also very important. Insights, principles and development methodologies from the domains of visualisation and perception can support the the investigation of appropriate tasks and visual approaches within geological frontier applications, such as CO_2 storage, geothermal energy and planetary geology.

8.5.5 Applications of Artificial Neural Networks in Digital Outcrop Geology

Another technology that recently attracted significant academic, industrial and public attention is the use of artificial neural networks (ANNs) within artificial intelligence (AI), also better known under the term *Deep Learning*. ANNs are applied within a large range of scientific branches, from astronomy [77, 95][35] over medicine [231, 319] to geospatial localisation [311][36], to make fully-automatic predictions and complex decisions based on a large amount of training data. ANNs have shown to be particularly good at fuzzy classification problems, which relates to certain tasks within geology and reservoir modelling such as facies mapping classification and stochastic reservoir modelling. They have even been applied for geological applications such history matching [42], facies indicator mapping on seismics [44] and, with early designs of ANNs, facies mapping on outcrop data [43]. The development of neural networks (NNs) experienced a drastic boost in recent years after a milestone publication by Krizhevsky et al. in 2012 [158], which means that ANN results before and after that study are rarely comparable and, to the least, technically only loosely related. A large number of current applications use an extended version of the visual- and human perception-related *convolutional neural network (CNN)*.

Subsequently, a short introduction to the working principle of ANNs and the relation rationale to human learning are presented. The summary is based on the original key literature by LeCun et al. [170] and Krizhevsky et al. [158], and the published extended abstract presented in this dissertation as appendix E, which assesses the possibility of human feedback and adaptation on neural networks on a media archive case study. The insights and conclusions drawn in appendix E are equally applicable to geological, image-based case studies, which is explained afterwards.

Neural networks is a technique emerging from the domain of pattern recognition that shares similarities with the neural principles of human recognition and learning. An *artificial* neural network – highlighting the computational component in broader discussions – is a collection of computational entities that each represent a single, simple mathematical equation, such as the weighted transfer ($y_j = \sum x_i \omega_{i,j}$) or the sigmoid activation function ($\sigma(t) = \frac{1}{1+e^{-\beta t}}$). Each entity is called a *perceptron* and is the computational equivalent of a human, neural synapse. Perceptrons, as well as their physical counterparts, are highly interconnected with a multitude of input and output connections. Fig. 8.19 illustrated the similarity.

[35] Winning the Galaxy Challenge with convnets - `http://blog.kaggle.com/2014/04/18/winning-the-galaxy-challenge-with-convnets/`

[36] Google Unveils Neural Network with "Superhuman" Ability to Determine the Location of Almost Any Image - `https://www.technologyreview.com/s/600889/google-unveils-neural-network-with-superhuman-ability-to-determine-the-location-of-almost/`

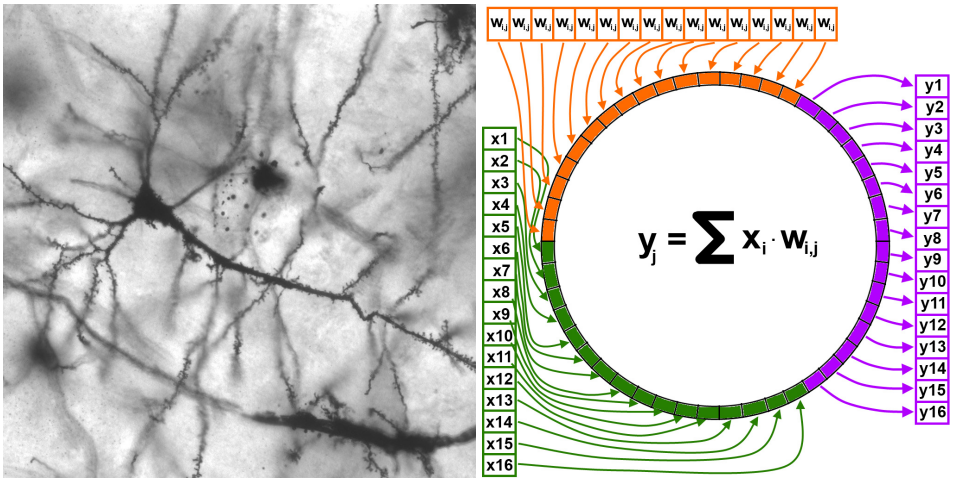

(a) Illustration of a connected synapse; from Wikipedia by MethoxyRoxy (license CC-AS 2.5)

(b) Illustration of a connected perceptron

Figure 8.19: (Interconnectivity) similarity between (physical) neural and (artificial) perceptron.

All perceptrons that operate on the same input data, and commonly computing the same class of function, are summarised into a *layer*. A full ANN is a sequence of layers with mixed evaluation function. ANNs for classification and value prediction contain one final layer with an activation function. The layout of layers and their interconnections is referred to as the *NN architecture*. The architecture, the amount of input data and the actual learning algorithm, which adapts the perceptrons' weights in an iterative process, define the resulting prediction capacity of ANNs [170]. The training set input data are typically structured in such a way that each data entry is composed of a pair with *observation data* and *reference data*, where the reference data describe the expected pattern that is to be predicted from the observation by the NN. The learning algorithm, for example stochastic gradient descent (SGD) [171], iteratively adapts the weights of each perceptron so that the difference between the network's prediction (output) and the data reference (input) becomes minimal.

ANNs "learn from the data", which means that the algorithm learns the functional expression of how to best approximate the input data reference. Depending on the application scenario and the prediction target, a potentially massive amount of input references is necessary to train a NN. It is necessary so that the NN can abstract the prediction goal and give reasonable predictions on fuzzy, real-world tasks. It needs an abstract functional descriptions. This process has an analogy to human perception in form of *abstract thinking*: children can learn the abstraction of objects using a large amount of different, actual examples. Using a large amount of examples, the human brain is able to abstract specific, fuzzy features of real objects and classify them. Because of the high demand for training data, modern NNs and AI are often coupled with advances in "Big Data".

After the completion of the network learning, which is a time-consuming process that commonly required state-of-the-art high-performance computing facilities, the trained weights of the perceptrons are fixed. After a verification stage, the NN can be provided with new input

data without reference values. Their classification or behaviour is predicted by the NN, based on the learned data patterns represented in the perceptrons' weights.

At the state-of-the-art in computational geosciences, NN approaches by Caers et al. have only been realised on well-constrained problems using traditional, fully-interconnected layer architectures. The recent developments in CNNs and Deep Learning demand a re-assessment of the technique for less-constrained geological problems. In a reservoir modelling target application, one can extend the existing idea by Caers [41] to use NNs directly for reservoir facies distribution prediction with the insights from Krizhevsky et al. [158] on CNNs. The currently most complex approach in sparsely-conditioned, exploration scenario-reservoir cases is MPS modelling, which is the target modelling approach of the VOM2MPS project. Although MPS is a powerful geostatistical tool, it contains certain limits and problems: highly unconstrained case study for which the TI is based on a few or, commonly, even only one object-based modelling scenario, the algorithm will replicate the input TI as an average of large numbers of realisations. In response to this drawback, the modeller can change the conditioning, the parameterization or the TI itself. In the end, a collection of geocellular models are determined that approximate the target geology well, but the knowledge obtained in the modelling process is lost for subsequent studies. MPS itself does not "learn" the appropriate patterns – it just replicates them. Here, particularly 3D CNNs show their advantage: the results accepted by geologists and reservoir engineers is attached to the learned perceptron weights (i.e. the patterns), which can be re-used and refined in subsequent reservoir cases of similar sedimentary depositional environments. More ideas towards this neural network extension is going to be provided in the future.

Another application case for NN-based AI is the generation of geological interpretations and TIs themselves. Nyberg recently presented sedimentological studies on modern analogues to be used as TIs for reservoir modelling [221]. A vast amount of modern analogues of diverse sedimentary depositional systems are available in nature that can be taken as TIs. In a NN point-of-view, satellite imagery is an applicable source of observation data for which reference facies mapping can be obtained by via GIS approaches [220] or by geometric shape modelling and fitting [256]. Although the amount of available analogues themselves is not enough to prevent overfitting [158], each analogue covers large areas which can be subdivided into a large collection of smaller entities. Geometrically affine transformations and radiometric satellite image modulation (similar to the L-U modulation [158]) of the images can ultimately result in an applicable training dataset size for NN training. The trained patterns then conceptually allow a prediction of facies distributions of analogous modern sediment systems as well as ancient systems in the rock record.

Similar to the computational facies modelling for modern analogues, the NN approach can be extended to DOMs assessed in this dissertation. The idea was already initially presented with traditional NNs [43]. An obvious problem of the approach is the generation of training data from outcrops, as the number of outcrops of a specific depositional system is limited. On the other hand, similar to modern analogues, DOMs cover large areas which can be subdivided in smaller entities. In this manner, it is possible to extract a large number of training data with observation and reference values from a single, fully facies-mapped DOM. Visual techniques and tools for the facies mapping and interpretation of DOMs can be taken directly from this thesis' research results. In order to generate training data in image formats, desktop DOM software such as LIME, VRGS and GoCAD could allow in the future to define animation paths at pre-defined surface distances along the digital outcrop surface. The animation paths can be traversed in a deterministically or stochastically sampled spacing distance. At each control point of an animation path, synthetic images of the 3D textured surface models are

obtained (as in approaches presented in chapter 4 to 7) with their corresponding interpretation layer, which in sum represents the training dataset on which the NN can be trained. The outcome of such a machine learning approach and the related NN is a system that automatically provides probability-weighted facies mapping interpretations. With respect to this application scenario, it is also possible to envisage submitting fieldtrip photos to such a trained NN for online evaluation. This scenario is more directly connected to mobile case studies in this thesis. The NN subsequently evaluates the submitted field photo with the patterns previously trained in the proposed framework. The evaluated photo is subsequently sent back to the mobile device to give a first-order approximation of the geological interpretation, which can be refined in the field.

It is to be noted that the involvement of geologists in this computational approach for facies mapping and interpretation, both for digital outcrops and modern analogues, is crucial: sedimentologists and geologists (in general) need to provide accurate and applicable facies mapping interpretations for the remotely-sensed data to derive the NN training datasets. Furthermore, as explained in appendix E, domain experts need to be involved in the selection of features on which the actual training image sets are selected to avoid an over-representation of particular features in the learned patterns. In order to assess and refine the NN patterns, geologists need to judge the results of the NN verification stage for specific cases and adapt the training dataset sample in response to their evaluation. The potential advantages of the approach are obvious: automatic, smart AI systems that learn geology by example – roughly analogous to the manner humans learn about geology, its processes and concepts – from accurate training data that are provided by geological experts allows for faithful digital interpretation of geological data on massive scales.

IX

Bibliography

[1] ADAMS, A., JACOBS, D. E., DOLSON, J., TICO, M., PULLI, K., TALVALA, E.-V., AJDIN, B., VAQUERO, D., LENSCH, H. P. A., HOROWITZ, M., PARK, S. H., GELFAND, N., BAEK, J., MATUSIK, W., AND LEVOY, M. The frankencamera: An experimental platform for computational photography. Commun. ACM 55, 11 (Nov. 2012), 90–98, doi: 10.1145/2366316.2366339. 1.2.3

[2] AGUS, M., GOBBETTI, E., MARTON, F., PINTORE, G., AND VÁZQUEZ, P.-P. Mobile Graphics. In EuroGraphics 2017 - Tutorials (2017), A. Bousseau and D. Gutierrez, Eds., The Eurographics Association. 1.4.1

[3] AIKEN, C., XU, X., THURMOND, J., ABDELSALAM, M., OLARIU, M., OLARIU, C., AND THURMOND, A. 3-d laser scanning and virtual photorealistic outcrops: Acquisition, visualization and analysis. AAPG Short Course (2004). 2.1

[4] AKENINE-MÖLLER, T., HAINES, E., AND HOFFMAN, N. Real-Time Rendering, Third Edition. CRC Press, 2016. 1.3.3, 1.3.5, 2, 2.1

[5] ALEXA, M., BEHR, J., COHEN-OR, D., FLEISHMAN, S., LEVIN, D., AND SILVA, C. T. Point set surfaces. In Proceedings of the conference on Visualization '01 (Washington, DC, USA, 2001), VIS '01, IEEE Computer Society, pp. 21–28. 1.3.2, 2.1

[6] ALLARD, D., FROIDEVAUX, R., AND BIVER, P. Conditional simulation of multi-type non stationary markov object models respecting specified proportions. Mathematical geology 38, 8 (2006), 959–986. 1.2.1

[7] AMENTA, N., AND BERN, M. Surface reconstruction by voronoi filtering. In Proceedings of the fourteenth annual symposium on Computational geometry (New York, NY, USA, 1998), SCG '98, ACM, pp. 39–48. 2.1, 2.3, 1

[8] AMENTA, N., BERN, M., AND EPPSTEIN, D. The crust and the β-skeleton: combinatorial curve reconstruction. Graph. Models Image Process. 60 (March 1998), 125–135, doi: http://dx.doi.org/10.1006/gmip.1998.0465. 1.3.2, 2.6

[9] AMENTA, N., CHOI, S., AND KOLLURI, R. K. The power crust. In Proceedings of the sixth ACM symposium on Solid modeling and applications (New York, NY, USA, 2001), SMA '01, ACM, pp. 249–266. 1.3.2

[10] ANDRÄ, H., COMBARET, N., DVORKIN, J., GLATT, E., HAN, J., KABEL, M., KEEHM, Y., KRZIKALLA, F., LEE, M., MADONNA, C., MARSH, M., MUKERJI, T., SAENGER, E. H., SAIN, R., SAXENA, N., RICKER, S., WIEGMANN, A., AND ZHAN, X. Digital rock physics benchmarks – part ii: Computing effective properties. Computers & Geosciences 50 (2013), 33 – 43, doi:

http://dx.doi.org/10.1016/j.cageo.2012.09.008. Benchmark problems, datasets and methodologies for the computational geosciences. 2.6, 8.5.2

[11] ANDRÄ, H., COMBARET, N., DVORKIN, J., GLATT, E., HAN, J., KABEL, M., KEEHM, Y., KRZIKALLA, F., LEE, M., MADONNA, C., MARSH, M., MUKERJI, T., SAENGER, E. H., SAIN, R., SAXENA, N., RICKER, S., WIEGMANN, A., AND ZHAN, X. Digital rock physics benchmarks – part i: Imaging and segmentation. Computers & Geosciences 50 (2013), 25 – 32, doi: http://dx.doi.org/10.1016/j.cageo.2012.09.005. Benchmark problems, datasets and methodologies for the computational geosciences. 8.5.2

[12] ATTENE, M., CAMPEN, M., AND KOBBELT, L. Polygon mesh repairing: An application perspective. ACM Computing Surveys (CSUR) 45, 2 (2013), 15. 2.5

[13] BAC, A., MARI, J.-L., KUDELSKI, D., TRAN, N.-V., VISEUR, S., AND DANIEL, M. Application of discrete curvatures to surface mesh simplification and feature line extraction. Courbure discrète: théorie et applications (2013), 31. 8.5.1

[14] BAYER, P., COMUNIAN, A., HÖYNG, D., AND MARIETHOZ, G. High resolution multi-facies realizations of sedimentary reservoir and aquifer analogs. Scientific data 2 (2015). 1.2.1

[15] BELLIAN, J. A., JENNETTE, D. C., KERANS, C., GIBEAUT, J., ANDREWS, J., YSSLDYK, B., AND LARUE, D. 3-dimensional digital outcrop data collection and analysis using eye-safe laser (lidar) technology. American Association of Petroleum Geologists Search and Discovery Article 40056 (2002). 1.2.2, 1.2.3

[16] BELLIAN, J. A., KERANS, C., AND JENNETTE, D. C. Digital outcrop models: applications of terrestrial scanning lidar technology in stratigraphic modeling. Journal of sedimentary research 75, 2 (2005), 166–176. 1.2.3

[17] BERG, M. D., CHEONG, O., KREVELD, M. V., AND OVERMARS, M. Computational Geometry: Algorithms and Applications, 3rd ed. ed. Springer-Verlag TELOS, Santa Clara, CA, USA, 2008. 1.3.2, 1.3.5, 2.1, 2.2

[18] BERNARDINI, F., MITTLEMAN, J., RUSHMEIER, H., SILVA, C., TAUBIN, G., AND MEMBER, S. The ball-pivoting algorithm for surface reconstruction. IEEE Transactions on Visualization and Computer Graphics 5 (1999), 349–359. 1.3.2

[19] BETTIO, F., GOBBETTI, E., MARTON, F., AND PINTORE, G. High-quality networked terrain rendering from compressed bitstreams. In Proceedings of the twelfth international conference on 3D web technology (New York, NY, USA, 2007), Web3D '07, ACM, pp. 37–44. 1.3.3, 8.3.2

[20] BILJECKI, F., LEDOUX, H., STOTER, J., AND ZHAO, J. Formalisation of the level of detail in 3d city modelling. Computers, Environment and Urban Systems 48 (2014), 1–15. 8.3.2

[21] BLUM, J. R., GREENCORN, D. G., AND COOPERSTOCK, J. R. Smartphone sensor reliability for augmented reality applications. In Mobile and Ubiquitous Systems: Computing, Networking, and Services. Springer, 2013, pp. 127–138. 8.2.2

[22] BLUNDELL, B. Computer Hardware. FastTrack (Series). Thomson, 2008. 8.2.1

[23] BOGGS, S. Principles of Sedimentology and Stratigraphy. Pearson Prentice Hall, 2012. 1.3.1, 8.5.3

[24] BOISSONNAT, J., AND OUDOT, S. Provably good sampling and meshing of surfaces. Graphical Models 67, 5 (Sept. 2005), 405–451, doi: 10.1016/j.gmod.2005.01.004. 2, 2.1, 2.3, 1, 2.6

[25] BOISSONNAT, J., AND YVINEC, M. Algorithmic Geometry. Cambridge University Press, 1998. 1.3.5

[26] BOLTCHEVA, D., YVINEC, M., AND BOISSONNAT, J.-D. Feature preserving delaunay mesh generation from 3d multi-material images. Computer Graphics Forum 28, 5 (2009). 2.5

[27] BOND, C., GIBBS, A., SHIPTON, Z., AND JONES, S. What do you think this is? "conceptual uncertainty" in geoscience interpretation. GSA today 17, 11 (2007), 4. 8.5.3

[28] BORDEN, M. J., HUGHES, T. J., LANDIS, C. M., AND VERHOOSEL, C. V. A higher-order phase-field model for brittle fracture: Formulation and analysis within the isogeometric analysis framework. Computer Methods in Applied Mechanics and Engineering 273 (2014), 100 – 118, doi: http://dx.doi.org/10.1016/j.cma.2014.01.016. 2.1

[29] BORGEAT, L., GODIN, G., BLAIS, F., MASSICOTTE, P., AND LAHANIER, C. Gold: Interactive display of huge colored and textured models. ACM Trans. Graph. 24, 3 (July 2005), 869–877, doi: 10.1145/1073204.1073276. 8.3.2

[30] BORGO, R., KEHRER, J., CHUNG, D. H., MAGUIRE, E., LARAMEE, R. S., HAUSER, H., WARD, M., AND CHEN, M. Glyph-based visualization: Foundations, design guidelines, techniques and applications. Eurographics State of the Art Reports (May 2013), 39–63. http://diglib.eg.org/EG/DL/conf/EG2013/stars/039-063.pdf. 8.5.3

[31] BOTSCH, M., AND KOBBELT, L. High-Quality Point-Based Rendering on Modern GPUs. 2003. 1.3.2

[32] BOTSCH, M., KOBBELT, L., PAULY, M., ALLIEZ, P., AND LÉVY, B. Polygon mesh processing. CRC press, 2010. 2.5

[33] BRAATHEN, A., BÆLUM, K., CHRISTIANSEN, H. H., DAHL, T., EIKEN, O., ELVEBAKK, H., HANSEN, F., HANSSEN, T. H., JOCHMANN, M., JOHANSEN, T. A., ET AL. The Longyearbyen CO. Norwegian Journal of Geology (2012). 2, 8.4.4

[34] BRAATHEN, A., TVERANGER, J., FOSSEN, H., SKAR, T., CARDOZO, N., SEMSHAUG, S., BASTESEN, E., AND SVERDRUP, E. Fault facies and its application to sandstone reservoirs. AAPG Bulletin 93, 7 (2009), 891–917. 1.3.1

[35] BUCKLEY, S., SCHWARZ, E., TERLAKY, V., HOWELL, J., AND ARNOTT, R. Terrestrial laser scanning combined with photogrammetry for digital outcrop modelling. Laser scanning (2009), 75–80. 1.2.3, 2.3

[36] BUCKLEY, S., VALLET, J., BRAATHEN, A., AND WHEELER, W. Oblique helicopter-based laser scanning for digital terrain modelling and visualisation of geological outcrops. International Archives of the Photogrammetry, Remote Sensing and Spatial Information Sciences 37, B4 (2008), 493–498. 1.2.3

[37] BUCKLEY, S. J., HOWELL, J. A., ENGE, H. D., AND KURZ, T. H. Terrestrial laser scanning in geology: data acquisition, processing and accuracy considerations. Journal of the Geological Society 165, 3 (2008), 625–638. 1.2.3, 2.1

[38] BUCKLEY, S. J., KURZ, T. H., HOWELL, J. A., AND SCHNEIDER, D. Terrestrial lidar and hyperspectral data fusion products for geological outcrop analysis. Computers & Geosciences 54, 0 (2013), 249 – 258, doi: http://dx.doi.org/10.1016/j.cageo.2013.01.018. 8.3.1, 8.3.1, 8.5.2

[39] BUCKLEY, S. J., RINGDAL, K., DOLVA, B., NAUMANN, N., AND KURZ, T. H. LIME: 3D visualisation and interpretation of virtual geoscience models. In Geophysical Research Abstracts (GRA), vol. 19. European Geoscience Union (EGU), 2017. 3.2, 3.4

[40] BUCKLEY, S. J., SCHWARZ, E., TERLAKY, V., HOWELL, J. A., AND ARNOTT, R. Combining Aerial Photogrammetry and Terrestrial Lidar for Reservoir Analog Modeling. Photogrammetric Engineering & Remote Sensing 76, 8 (2010), 953–963. 1.2.2, 1.2.3

[41] CAERS, J. Geostatistical reservoir modelling using statistical pattern recognition. Journal of Petroleum Science and Engineering 29, 3–4 (2001), 177 – 188, doi: http://dx.doi.org/10.1016/S0920-4105(01)00088-2. Soft Computing and Earth Sciences. 8.5.5

[42] CAERS, J. Geostatistical history matching under training-image based geological model constraints. In SPE annual technical conference and exhibition (2002), Society of Petroleum Engineers. 8.5.5

[43] CAERS, J., AND JOURNEL, A. G. Stochastic reservoir simulation using neural networks trained on outcrop data. In SPE Annual Technical Conference and Exhibition (1998), Society of Petroleum Engineers. 8.5.5, 8.5.5

[44] CAERS, J., AND MA, X. Modeling conditional distributions of facies from seismic using neural nets. Mathematical Geology 34, 2 (2002), 143–167. 8.5.5

[45] CAMP, R. J., AND WHEATON, J. M. Streamlining field data collection with mobile apps. Eos, Transactions American Geophysical Union 95, 49 (2014), 453–454, doi: 10.1002/2014EO490001. 1.4.2

[46] CAUMON, G., COLLON-DROUAILLET, P., LE CARLIER DE VESLUD, C., VISEUR, S., AND SAUSSE, J. Surface-based 3d modeling of geological structures. Mathematical Geosciences 41, 8 (2009), 927–945, doi: 10.1007/s11004-009-9244-2. 2.1, 2.5

[47] CAUMON, G., GRAY, G., ANTOINE, C., AND TITEUX, M. O. Three-dimensional implicit stratigraphic model building from remote sensing data on tetrahedral meshes: Theory and application to a regional model of la popa basin, ne mexico. IEEE Transactions on Geoscience and Remote Sensing 51, 3 (March 2013), 1613–1621, doi: 10.1109/TGRS.2012.2207727. 2.1, 2.5

[48] CAUMON, G., LEPAGE, F., SWORD, C. H., AND MALLET, J.-L. Building and editing a sealed geological model. Mathematical Geology 36, 4 (2004), 405–424, doi: 10.1023/B:MATG.0000029297.18098.8a. 2.1, 2.6

[49] CAUMON, G., LÉVY, B., CASTANIÉ, L., AND PAUL, J.-C. Visualization of grids conforming to geological structures: a topological approach. Computers & Geosciences 31, 6 (2005), 671–680, doi: http://dx.doi.org/10.1016/j.cageo.2005.01.020. 2.1

[50] CAVELIUS, C., BUATOIS, L., VISEUR, S., AND CAUMON, G. Texture mapping of non-orthorectified images onto topographic models. In GOCAD Meeting (2008), vol. 28. 1.4.2, 2, 3.5

[51] CAWOOD, A. J., BOND, C. E., HOWELL, J. A., BUTLER, R. W., AND TOTAKE, Y. LiDAR, UAV or compass-clinometer? accuracy, coverage and the effects on structural models. Journal of Structural Geology 98 (2017), 67 – 82, doi: https://doi.org/10.1016/j.jsg.2017.04.004. 8.2.2

[52] CAZALS, F., GIESEN, J., PAULY, M., AND ZOMORODIAN, A. Conformal alpha shapes. In Point-Based Graphics, 2005. Eurographics/IEEE VGTC Symposium Proceedings (june 2005), pp. 55 – 61. 1.3.2

[53] CHANDLER, J., AND BUCKLEY, S. Structure from motion (SFM) photogrammetry vs terrestrial laser scanning. American Geosciences Institute (AGS), 2016, ch. Chp. 20, Sec. 1. 1.2.3

[54] CHEW, L. P. Constrained delaunay triangulations. In Proceedings of the third annual symposium on Computational geometry (1987), ACM, pp. 215–222. 1

[55] CIGNONI, P., CALLIERI, M., CORSINI, M., DELLEPIANE, M., GANOVELLI, F., AND RANZUGLIA, G. MeshLab: an Open-Source Mesh Processing Tool. In Eurographics Italian Chapter Conference (2008), V. Scarano, R. D. Chiara, and U. Erra, Eds., The Eurographics Association. 2.5

[56] CLEGG, P., BRUCIATELLI, L., DOMINGOS, F., JONES, R., DONATIS, M. D., AND WILSON, R. Digital geological mapping with tablet {PC} and pda: A comparison. Computers & Geosciences 32, 10 (2006), 1682 – 1698, doi: http://dx.doi.org/10.1016/j.cageo.2006.03.007. 1.4.2, 8.2.2

[57] COE, A. Geological Field Techniques. John Wiley & Sons, 2010. 1.3.1

[58] COLOMBERA, L., MOUNTNEY, N. P., AND MCCAFFREY, W. D. A relational database for the digitization of fluvial architecture concepts and example applications. Petroleum Geoscience 18, 1 (2012), 129–140. 1.2.2

[59] COMUNIAN, A., JHA, S. K., GIAMBASTIANI, B. M., MARIETHOZ, G., AND KELLY, B. F. Training images from process-imitating methods. Mathematical Geosciences 46, 2 (2014), 241–260. 1.2.1

[60] COMUNIAN, A., RENARD, P., AND STRAUBHAAR, J. 3d multiple-point statistics simulation using 2d training images. Computers & Geosciences 40, 0 (2012), 49 – 65. 1.2.1

[61] COOK, R. L. Stochastic sampling in computer graphics. ACM Transactions on Graphics (TOG) 5, 1 (1986), 51–72. 8.4.2

[62] CORSINI, M., DELLEPIANE, M., GANOVELLI, F., GHERARDI, R., FUSIELLO, A., AND SCOPIGNO, R. Fully Automatic Registration of Image Sets on Approximate Geometry. International journal of computer vision 102, 1-3 (2013), 91–111. 1.4.2

[63] CORSINI, M., DELLEPIANE, M., PONCHIO, F., AND SCOPIGNO, R. Image-to-geometry registration: a mutual information method exploiting illumination-related geometric properties. In Computer Graphics Forum (2009), vol. 28, Wiley Online Library, pp. 1755–1764. 1.4.2

[64] DE DONATIS, M., BRUCIATELLI, L., AND SUSINI, S. Map it: a gis/gps software solution for digital mapping. In Proceedings of the digital mapping techniques workshop (2005), Citeseer, pp. 2005–1428. 1.4.2

[65] DE FLORIANI, L., KOBBELT, L., AND PUPPO, E. A survey on data structures for level-of-detail models. In Advances in multiresolution for geometric modelling. Springer, 2005, pp. 49–74. 8.3.2

[66] DE FLORIANI, L., AND SPAGNUOLO, M. Shape Analysis and Structuring. Mathematics and Visualization. Springer Berlin Heidelberg, 2007. 1.3.5

[67] DE LEEUW, W. C., AND VAN WIJK, J. J. A probe for local flow field visualization. In Proceedings of the 4th Conference on Visualization '93 (Washington, DC, USA, 1993), VIS '93, IEEE Computer Society, pp. 39–45. 8.5.3

[68] DELAUNAY, B. Sur la sphère vide. Izv. Akad. Nauk SSSR, Otdelenie Matematicheskii i Estestvennyka Nauk 7, 793-800 (1934), 1–2. 1.3.2

[69] DESBRUN, M., MEYER, M., AND ALLIEZ, P. Intrinsic parameterizations of surface meshes. In Computer Graphics Forum (2002), vol. 21, Wiley Online Library, pp. 209–218. 2

[70] DEUTSCH, C., AND TRAN, T. Fluvsim: a program for object-based stochastic modeling of fluvial depositional systems. Computers & Geosciences 28, 4 (2002), 525 – 535, doi: http://dx.doi.org/10.1016/S0098-3004(01)00075-9. 1.2.1

[71] DEUTSCH, C. V., AND JOURNEL, A. G. Geostatistical software library and user's guide. New York 119 (1992), 147. 1.2.1

[72] DEWEZ, T. J., LEROUX, J., AND MORELLI, S. Uav sensing of coastal cliff topography for rock fall hazard applications. In Journées Aléas Gravitaires JAG 2015 (2015). 1.2.3

[73] DEY, T. K., AND GIESEN, J. Detecting undersampling in surface reconstruction. In Proceedings of the seventeenth annual symposium on Computational geometry (New York, NY, USA, 2001), SCG '01, ACM, pp. 257–263. 1.3.2

[74] DEY, T. K., AND GOSWAMI, S. Tight cocone: A water tight surface reconstuctor. In ACM Symposium Solid Modeling Applications (2003), no. 8. 1.3.2

[75] DEY, T. K., AND LEVINE, J. A. Delaunay meshing of piecewise smooth complexes without expensive predicates. Algorithms 2, 4 (2009), 1327–1349, doi: 10.3390/a2041327. 1

[76] DEY, T. K., AND SUN, J. An adaptive mls surface for reconstruction with guarantees. In Proceedings of the third Eurographics symposium on Geometry processing (Aire-la-Ville, Switzerland, Switzerland, 2005), Eurographics Association. 1.3.2

[77] DIELEMAN, S., WILLETT, K. W., AND DAMBRE, J. Rotation-invariant convolutional neural networks for galaxy morphology prediction. Monthly notices of the royal astronomical society 450, 2 (2015), 1441–1459. 8.5.5

[78] DIERSCH, H. FEFLOW: Finite Element Modeling of Flow, Mass and Heat Transport in Porous and Fractured Media. Springer Berlin Heidelberg, 2013. 2.1

[79] DREYER, T., FÄLT, L.-M., HØY, T., KNARUD, R., CUEVAS, J.-L., ET AL. Sedimentary architecture of field analogues for reservoir information (SAFARI): a case study of the fluvial escanilla formation, spanish pyrenees. In The Geological Modeling of Hydrocarbon Reservoirs and Outcrop Analogs (1993), vol. 15, International Association of Sedimentologists – Special Publications, Wiley Online Library, pp. 57–80. 1.2.2, 1.3.1

[80] DÜBEL, S., RÖHLIG, M., TOMINSKI, C., AND SCHUMANN, H. Visualizing 3D Terrain, Geo-Spatial Data, and Uncertainty. Informatics 4, 1 (2017), 1–18, doi: 10.3390/informatics4010006. 1.3.3

[81] EDELSBRUNNER, H., AND MÜCKE, E. P. Three-dimensional alpha shapes. In Proceedings of the 1992 workshop on Volume visualization (New York, NY, USA, 1992), VVS '92, ACM, pp. 75–82. 1.3.2, 2

[82] EFROS, A. A., AND FREEMAN, W. T. Image quilting for texture synthesis and transfer. In Proceedings of the 28th Annual Conference on Computer Graphics and Interactive Techniques (New York, NY, USA, 2001), SIGGRAPH '01, ACM, pp. 341–346. 1.4.1

[83] EIDE, C. H. Shallow-marine facies and virtual outcrop geology: Intra-parasequence variability in ancient shallow-marine environments. Phd thesis, University of Bergen, 2014. 138 p. 1.2.3

[84] EIDE, C. H., HOWELL, J., AND BUCKLEY, S. Distribution of discontinuous mudstone beds within wave-dominated shallow-marine deposits: Star point sandstone and blackhawk formation, eastern utah. AAPG Bulletin 98, 7 (2014), 1401–1429. 1.2.2, 2.1, 3.2, 3.2(a), 3.1, 3.2, 8.1

[85] EIDE, C. H., HOWELL, J. A., AND BUCKLEY, S. J. Sedimentology and reservoir properties of tabular and erosive offshore transition deposits in wave-dominated, shallow-marine strata: Book cliffs, usa. Petroleum Geoscience (2015), 2014–015. 1.4.3

[86] EIDE, C. H., HOWELL, J. A., BUCKLEY, S. J., MARTINIUS, A. W., OFTEDAL, B. T., AND HENSTRA, G. A. Facies model for a coarse-grained, tide-influenced delta: Gule horn formation (early jurassic), jameson land, greenland. Sedimentology (2016). 3.1, 3.2

[87] ENGE, H. D. Deltaic cclinothem - digital data capture, geometries, and reservoir implications. Phd thesis, University of Bergen, 2008. 180 p. 1.2.3

[88] ENGE, H. D., BUCKLEY, S. J., ROTEVATN, A., AND HOWELL, J. A. From outcrop to reservoir simulation model: Workflow and procedures. Geosphere 3, 6 (2007), 469–490. 1.2.2, 2, 2.1, 3.1, 3.2, 8.1

[89] ENGE, H. D., HOWELL, J. A., AND BUCKLEY, S. J. Quantifying clinothem geometry in a forced-regressive river-dominated delta, panther tongue member, utah, usa. Sedimentology 57, 7 (2010), 1750–1770. 3.1, 3.2

[90] ENGEL, J., SCHÖPS, T., AND CREMERS, D. Lsd-slam: Large-scale direct monocular slam. In Computer Vision–ECCV 2014. Springer, 2014, pp. 834–849. 1.4.2

[91] FACHRI, M., TVERANGER, J., BRAATHEN, A., AND RØE, P. Volumetric faults in field-sized reservoir simulation models: A first case study. AAPG Bulletin 100, 5 (2016), 795–817. 1.3.1, 8.4.3

[92] FERSTER, C. J., AND COOPS, N. C. A review of earth observation using mobile personal communication devices. Computers & Geosciences 51 (2013), 339 – 349, doi: http://dx.doi.org/10.1016/j.cageo.2012.09.009. 1.4.2

[93] FISHER, R., BRECKON, T., DAWSON-HOWE, K., FITZGIBBON, A., ROBERTSON, C., TRUCCO, E., AND WILLIAMS, C. Dictionary of Computer Vision and Image Processing. Wiley, 2013. 1.3.4, 1.3.5

[94] FISHMAN, B., AND SCHACHTER, B. Computer display of height fields. Computers & Graphics 5, 2 (1980), 53–60. 2.1

[95] FLAMARY, R. Astronomical image reconstruction with convolutional neural networks. arXiv preprint arXiv:1612.04526 (2016). 8.5.5

[96] FLOATER, M. S., AND HORMANN, K. Surface parameterization: a tutorial and survey. In Advances in multiresolution for geometric modelling. Springer, 2005, pp. 157–186. 2

[97] FREDMAN, N., TVERANGER, J., CARDOZO, N., BRAATHEN, A., SOLENG, H., ROE, P., SKORSTAD, A., AND SYVERSVEEN, A. R. Fault facies modeling: Technique and approach for 3-D conditioning and modeling of faulted grids. AAPG bulletin 92, 11 (2008), 1457–1478. 1.3.1

[98] FRITSCH, D., AND SYLL, M. Photogrammetric 3D reconstruction using mobile imaging. In Proc. Mobile Devices and Multimedia: Enabling Technologies, Algorithms, and Applications (2015), vol. 9411, pp. 94110C–94110C–15. 1.4.2

[99] FUCHS, P. Virtual Reality Headsets - A Theoretical and Pragmatic Approach. CRC Press, 2017. 1.3.3, 8.5.4

[100] FURUKAWA, Y., CURLESS, B., SEITZ, S. M., AND SZELISKI, R. Towards internet-scale multi-view stereo. In Computer Vision and Pattern Recognition (CVPR), 2010 IEEE Conference on (2010), IEEE, pp. 1434–1441. 1.2.3

[101] FURUKAWA, Y., AND PONCE, J. Accurate, dense, and robust multiview stereopsis. IEEE transactions on pattern analysis and machine intelligence 32, 8 (2010), 1362–1376. 1.2.3

[102] GARCÍA, S., PAGÉS, R., BERJÓN, D., AND MORÁN, F. Textured splat-based point clouds for rendering in handheld devices. In Proceedings of the 20th International Conference on 3D Web Technology (New York, NY, USA, 2015), Web3D '15, ACM, pp. 227–230. 1.4.1

[103] GARCÍA-SELLÉS, D., FALIVENE, O., ARBUÉS, P., GRATACOS, O., TAVANI, S., AND MUNOZ, J. Supervised identification and reconstruction of near-planar geological surfaces from terrestrial laser scanning. Computers & Geosciences 37, 10 (2011), 1584 – 1594, doi: http://dx.doi.org/10.1016/j.cageo.2011.03.007. 2.1

[104] GARRO, V., PINTORE, G., GANOVELLI, F., GOBBETTI, E., AND SCOPIGNO, R. Fast metric acquisition with mobile devices. In Proc. 21st International Workshop on Vision, Modeling and Visualization (VMV) (October 2016). To appear. 1.4.2

[105] GAUGLITZ, S., FOSCHINI, L., TURK, M., AND HÖLLERER, T. Efficiently selecting spatially distributed keypoints for visual tracking. In Image Processing (ICIP), 18th IEEE International Conference on (2011), pp. 1869–1872. 1.4.2

[106] GAUGLITZ, S., NUERNBERGER, B., TURK, M., AND HÖLLERER, T. World-stabilized annotations and virtual scene navigation for remote collaboration. In Proceedings of the 27th annual ACM symposium on User interface software and technology (2014), ACM, pp. 449–459. 1.4.2, 2

[107] GEORGE, P., HECHT, F., AND SALTEL, E. Automatic mesh generator with specified boundary. Computer Methods in Applied Mechanics and Engineering 92, 3 (1991), 269 – 288, doi: 10.1016/0045-7825(91)90017-Z. 2.6

[108] GIRARDEAU-MONTAUT, D. CloudCompare-open source project. Open Source Project (2011). 1.2.3, 2.5

[109] GOOGLE. Android - project tango. project website, 2016. https://www.youtube.com/watch?v=3BNOsxMZD14, `https://get.google.com/tango/`. 1.4.2

[110] GOOVAERTS, P. Geostatistics for natural resources evaluation. Oxford University Press on Demand, 1997. 1.2.1

[111] GOPI, M., AND KRISHNAN, S. A fast and efficient projection-based approach for surface reconstruction. In High Performance Computer Graphics, Multimedia and Visualization (2002), pp. 1–12. 2.1, 2.3

[112] GOSWAMI, P., MAKHINYA, M., BÖSCH, J., AND PAJAROLA, R. Scalable parallel out-of-core terrain rendering. In Proceedings Eurographics Symposium on Parallel Graphics and Visualization (2010), pp. 63–71. 1.3.3

[113] GRANSHAW, S. I. Photogrammetric terminology. The Photogrammetric Record 31, 154 (2016), 210–252. 1.3.4, 1.3.4, 1.3.5

[114] GUARDIANO, F. B., AND SRIVASTAVA, R. M. Multivariate geostatistics: beyond bivariate moments. In Geostatistics Troia '92. Springer, 1993, pp. 133–144. 1.2.1

[115] GUEZIEC, A., TAUBIN, G., LAZARUS, F., AND HOM, B. Cutting and stitching: converting sets of polygons to manifold surfaces. IEEE Transactions on Visualization and Computer Graphics 7, 2 (Apr 2001), 136–151, doi: 10.1109/2945.928166. 1.3.2, 2.1, 2.3, 2.3, 2.5

[116] GUTH, P., OERTEL, O., BENARD, G., AND THIBAUD, R. Pocket panorama: 3d gis on a handheld device. In Web Information Systems Engineering Workshops, 2003. Proceedings. Fourth International Conference on (Dec 2003), pp. 100–105. 1.4.2

[117] HAINICH, R., AND BIMBER, O. Displays: Fundamentals & Applications, Second Edition. CRC Press, 2016. 1.3.3, 8.5.4

[118] HALDORSEN, H., AND DAMSLETH, E. Stochastic modeling. Journal of petroleum technology 42, 4 (1990), 404–412. 1.2.1

[119] HANSEN, C., AND JOHNSON, C. Visualization Handbook. Elsevier Science, 2011. 1.3.5

[120] HARTLEY, R., AND ZISSERMAN, A. Multiple View Geometry in Computer Vision. Cambridge University Press, 2003. 1.3.5

[121] HARTSHORNE, R. Algebraic Geometry. Graduate Texts in Mathematics. Springer New York, 2013. 1.3.5, 2.1, 2.3, 2.3

[122] HEMINGWAY, J., AND KNOX, R. O. Lithostratigraphical nomenclature of the Middle Jurassic strata of the Yorkshire Basin of north-east England. In Proceedings of the Yorkshire Geological and Polytechnic Society (1973), vol. 39, Geological Society of London, pp. 527–535. 1.6

[123] HERTZMANN, A., JACOBS, C. E., OLIVER, N., CURLESS, B., AND SALESIN, D. H. Image analogies. In Proceedings of the 28th Annual Conference on Computer Graphics and Interactive Techniques (New York, NY, USA, 2001), SIGGRAPH '01, ACM, pp. 327–340. 1.4.1, 1.12

[124] HILLEN, M. M., GELEYNSE, N., STORMS, J. E., WALSTRA, D. J. R., AND GROENENBERG, R. M. Morphodynamic modelling of wave reworking of an alluvial delta and application of results in the standard reservoir modelling workflow. Special Publication – From Depositional Systems to Sedimentary Successions on the Norwegian Continental Margin 46, 46 (2014), 167–186. 1.2.1

[125] HODGETTS, D. Laser scanning and digital outcrop geology in the petroleum industry: A review. Marine and Petroleum Geology 46, 0 (2013), 335–354, doi: http://dx.doi.org/10.1016/j.marpetgeo.2013.02.014. 1.2.1, 1.2.3, 3.1, 3.2

[126] HODGETTS, D., AND BURNHAM, B. Improving reservoir models through combining digital outcrop data and forward modelling. In 78th EAGE Conference and Exhibition 2016 (2016). 1.2.1

[127] HODGETTS, D., DRINKWATER, N., HODGSON, J., KAVANAGH, J., FLINT, S., KEOGH, K., AND HOWELL, J. Three-dimensional geological models from outcrop data using digital data collection techniques: an example from the tanqua karoo depocentre, south africa. Geological Society, London, Special Publications 239, 1 (2004), 57–75. 1.2.2, 1.4.3, 2.1, 8.2.2

[128] HOLDEN, L., HAUGE, R., SKARE, Ø., AND SKORSTAD, A. Modeling of fluvial reservoirs with object models. Mathematical Geology 30, 5 (1998), 473–496, doi: 10.1023/A:1021769526425. 1.2.1

[129] HOWELL, J. Recent developments in the use of outcrop analogues for building better models of subsurface reservoirs. In Integrated Reservoir Modelling - Are we doing it right? (2012). 1.2.2

[130] HOWELL, J. A., MARTINIUS, A. W., AND GOOD, T. R. The application of outcrop analogues in geological modelling: a review, present status and future outlook. Geological Society, London, Special Publications 387 (2014), SP387–12. 1.2.2, 1.2.2, 1.2.3

[131] HOWELL, J. V. Glossary of geology and related sciences. American Geological Institute, 1960, pp. 207–208. 1.2.2

[132] HU, L., LIU, Y., SCHEEPENS, C., SHULTZ, A., AND THOMPSON, R. Multiple-point simulation with an existing reservoir model as training image. Mathematical Geosciences 46, 2 (2014), 227–240. 1.2.1

[133] HUDSON, R. The Carboniferous Rocks. Proceedings of the Geologists' Association 49, 3 (1938), 306 – 330, doi: http://dx.doi.org/10.1016/S0016-7878(38)80028-6. 1.6

[134] ISSAUTIER, B., VISEUR, S., AUDIGANE, P., AND LE NINDRE, Y.-M. Impacts of fluvial reservoir heterogeneity on connectivity: Implications in estimating geological storage capacity for {CO2}. International Journal of Greenhouse Gas Control 20 (2014), 333 – 349, doi: http://dx.doi.org/10.1016/j.ijggc.2013.11.009. 1.1, 1.2.1, 2, 3.1

[135] JACINTO, H., KÉCHICHIAN, R., DESVIGNES, M., PROST, R., AND VALETTE, S. A web interface for 3d visualization and interactive segmentation of medical images. In Proceedings of the 17th International Conference on 3D Web Technology (2012), ACM, pp. 51–58. 8.3.2

[136] JOHNSTON, S., HOLBROOK, J., AND WARWICK, B. Controlling Factors and Mechanisms in the Formation of a Muddy-Normal Point Bar: A 3-D Architectural-Element Analysis of a Heterolithic Point Bar in Dinosaur Provincial Park, Alberta, Canada. In AAPG Annual Convention and Exhibition (2016). 1.3.1, 1.10

[137] JONES, R., MCCAFFREY, K., CLEGG, P., WILSON, R., HOLLIMAN, N., HOLDSWORTH, R., IMBER, J., AND WAGGOTT, S. Integration of regional to outcrop digital data: 3d visualisation of multi-scale geological models. Computers & Geosciences 35, 1 (2009), 4 – 18. 3D Modeling in Geology. 3.1, 3.2

[138] JONES, R. R., MCCAFFREY, K. J. W., WILSON, R. W., AND HOLDSWORTH, R. E. Digital field data acquisition: towards increased quantification of uncertainty during geological mapping. Geological Society, London, Special Publications 239, 1 (2004), 43–56, doi: 10.1144/GSL.SP.2004.239.01.04. 1.2.2, 2.1

[139] JONES, R. R., PRINGLE, J. K., MCCAFFREY, K. J., IMBER, J., WIGHTMAN, R., GUO, J., AND LONG, J. J. Extending digital outcrop geology into the subsurface. Outcrops Revitalized: Tools, Techniques and Applications: SEPM Society for Sedimentary Geology 10 (2010), 31–50. 2.1, 3.1, 3.2

[140] JONES, R. R., WAWRZYNIEC, T. F., HOLLIMAN, N. S., MCCAFFREY, K. J., IMBER, J., AND HOLDSWORTH, R. E. Describing the dimensionality of geospatial data in the earth sciences—recommendations for nomenclature. Geosphere 4, 2 (2008), 354–359. 2.2, 2.2, 2.2, 2.6

[141] JORDAN, C. Sigmamobile: the bgs digital field mapping system in action: in the united arab emirates. 1.4.2

[142] KAEHLER, A., AND BRADSKI, G. Learning OpenCV 3: Computer Vision in C++ with the OpenCV Library. O'Reilly Media, 2016. 1.3.5, 2.4, 8.2.3

[143] KAZHDAN, M., BOLITHO, M., AND HOPPE, H. Poisson surface reconstruction. In Proceedings of the fourth Eurographics symposium on Geometry processing (Aire-la-Ville, Switzerland, Switzerland, 2006), SGP '06, Eurographics Association, pp. 61–70. 1.3.2

[144] KAZHDAN, M., AND HOPPE, H. Screened poisson surface reconstruction. ACM Transactions on Graphics (TOG) 32, 3 (2013), 29. 2.5, 8.5.2

[145] KEHL, C. Distributed Rendering and Collaborative User Navigation- and Scene Manipulation. In 3D-NordOst (December 2014), L. Paul, G. Stanke, N. Heuwold, and M. Pochanke, Eds., vol. 17, Gesellschaft zur Foerderung angewandter Informatik, pp. 25–34. Application-oriented Workshop about the Acquisition, Modelling, Processing and Analysis of 3D data. 1.4.2, 8.5.4

[146] KEHL, C., BUCKLEY, S. J., AND HOWELL, J. A. Image-to-Geometry Registration on Mobile Devices - An Algorithmic Assessment. In Proceedings of the 3D-NordOst workshop (December 2015), vol. 18, GFaI, pp. 17–26. ISBN 978-3-942709-14-9. 1.4.2

[147] KEHL, C., AND DE HAAN, G. Interactive Simulation and Visualisation of Realistic Flooding Scenarios. In Intelligent Systems for Crisis Management (2012). 8.3.2, 8.4.4

[148] KEHL, C., MALAN, D. F., AND EISEMANN, E. Conformal multi-material mesh generation from labelled medical volumes. In 3D-NordOst (December 2012), L. Paul, G. Stanke, N. Heuwold, and M. Pochanke, Eds., vol. 15, Gesellschaft zur Förderung angewandter Informatik, pp. 47–56. Application-oriented Workshop about the Acquisition, Modelling, Processing and Analysis of 3D data. 2.5

[149] KEHL, C., TUTENEL, T., AND EISEMANN, E. Smooth, Interactive Rendering Techniques on Large-Scale, Geospatial Data in Flood Visualisation. In Information and Communication Technologie (ICT) Open (2013). 8.4.4

[150] KEIM, D., KOHLHAMMER, J., ELLIS, G., AND MANSMANN, F. Mastering the information age solving problems with visual analytics. Eurographics Association, 2010. 1.3.5

[151] KENNELLY, P., AND KIMERLING, A. Non-photorealistic rendering and terrain representation. Cartographic Perspectives 0, 54 (2006). 1.3.3

[152] KESSENICH, J., SELLERS, G., AND SHREINER, D. OpenGL Programming Guide: The Official Guide to Learning OpenGL, Version 4.5 with SPIR-V. OpenGL. Pearson Education, 2016. 1.3.3, 1.3.5, 2

[153] KIL, Y. J., AND AMENTA, N. GPU-assisted surface reconstruction on locally-uniform samples. In Meshing roundtable (2008), pp. 369–385. 2.3, 2.4

[154] KOLTERMANN, C. E., AND GORELICK, S. M. Heterogeneity in sedimentary deposits: A review of structure-imitating, process-imitating, and descriptive approaches. Water Resources Research 32, 9 (1996), 2617–2658. 1.2.1, 1.2.1

[155] KOSCHIER, D., LIPPONER, S., AND BENDER, J. Adaptive tetrahedral meshes for brittle fracture simulation. In Proceedings of the ACM SIGGRAPH/Eurographics Symposium on Computer Animation (Aire-la-Ville, Switzerland, Switzerland, 2014), SCA '14, Eurographics Association, pp. 57–66. 2.1

[156] KRAUS, K. Photogrammetry: Geometry from Images and Laser Scans. No. v. 1 in de Gruyter Textbook. Bod Third Party Titles, 2007. 1.3.4, 1.3.5

[157] KRIGE, D. A statistical approach to some mine valuations and allied problems at the Witwatersrand. PhD thesis, University of Witwatersrand, 1951. 2.1

[158] KRIZHEVSKY, A., SUTSKEVER, I., AND HINTON, G. E. ImageNet classification with deep convolutional neural networks. In Advances in neural information processing systems (2012), pp. 1097–1105. 8.5.5, 8.5.5, E

[159] KRÖHNERT, M. Automatic Waterline Extraction from Smartphone Images. ISPRS-International Archives of the Photogrammetry, Remote Sensing and Spatial Information Sciences (2016), 857–863. 1.4.2

[160] KUDELSKI, D., MARI, J.-L., AND VISEUR, S. 3d feature line detection based on vertex labeling and 2d skeletonization. In Shape Modeling International Conference (SMI), 2010 (2010), IEEE, pp. 246–250. 8.5.1

[161] KUDELSKI, D., VISEUR, S., SCROFANI, G., AND MARI, J.-L. Feature line extraction on meshes through vertex marking and 2d topological operators. International Journal of Image and Graphics 11, 04 (2011), 531–548, doi: 10.1142/S0219467811004226. 8.5.1, 8.10

[162] KURZ, T. H., BUCKLEY, S. J., AND HOWELL, J. A. Close-range hyperspectral imaging for geological field studies: workflow and methods. International Journal of Remote Sensing 34, 5 (2013), 1798–1822, doi: 10.1080/01431161.2012.727039. 8.5.2

[163] KURZ, T. H., BUCKLEY, S. J., HOWELL, J. A., AND SCHNEIDER, D. Integration of panoramic hyperspectral imaging with terrestrial lidar data. The Photogrammetric Record 26, 134 (2011), 212–228, doi: 10.1111/j.1477-9730.2011.00632.x. 2.1, 8.3.1

[164] KWATRA, V., ESSA, I., BOBICK, A., AND KWATRA, N. Texture optimization for example-based synthesis. In ACM SIGGRAPH 2005 Papers (New York, NY, USA, 2005), SIGGRAPH '05, ACM, pp. 795–802. 1.4.1

[165] LABOURDETTE, R., AND JONES, R. R. Characterization of fluvial architectural elements using a three-dimensional outcrop data set: Escanilla braided system, south-central pyrenees, spain. Geosphere 3, 6 (2007), 422–434. 1.2.2, 1.2.3, 3.1, 3.2

[166] LAGAE, A., AND DUTRÉ, P. A comparison of methods for generating poisson disk distributions. Computer Graphics Forum 27, 1 (2008), 114–129, doi: 10.1111/j.1467-8659.2007.01100.x. 8.4.2

[167] LALLIER, F., CAUMON, G., BORGOMANO, J., VISEUR, S., FOURNIER, F., ANTOINE, C., AND GENTILHOMME, T. Relevance of the stochastic stratigraphic well correlation approach for the study of complex carbonate settings: Application to the malampaya buildup (offshore palawan, philippines). Geological Society, London, Special Publications 370, 1 (2012), 265–275. 3.1

[168] LANNUTTI, E., LENZANO, M., TOTH, C., LENZANO, L., AND RIVERA, A. Optical Flow Applied to Time-Lapse Image Series to Estimate Glacier Motion in the Southern Patagonia Ice Field. ISPRS-International Archives of the Photogrammetry, Remote Sensing and Spatial Information Sciences (2016), 503–509. 8.4.4

[169] LECOMTE, I., LAVADERA, P. L., BOTTER, C., ANELL, I., BUCKLEY, S. J., EIDE, C. H., GRIPPA, A., MASCOLO, V., AND KJOBERG, S. 2 (3) d convolution modelling of complex geological targets beyond–1d convolution. First Break 34, 5 (2016), 99–107. 3.2

[170] LECUN, Y., BOTTOU, L., BENGIO, Y., AND HAFFNER, P. Gradient-based learning applied to document recognition. Proceedings of the IEEE 86, 11 (1998), 2278–2324. 8.5.5, 8.5.5, E

[171] LECUN, Y. A., BOTTOU, L., ORR, G. B., AND MÜLLER, K.-R. Efficient backprop. In Neural networks: Tricks of the trade. Springer, 2012, pp. 9–48. 8.5.5

[172] LEFEBVRE, S., HORNUS, S., AND NEYRET, F. Texture sprites: texture elements splatted on surfaces. In Proceedings of the 2005 symposium on Interactive 3D graphics and games (New York, NY, USA, 2005), I3D '05, ACM, pp. 163–170. 1.3.2

[173] LESKENS, J. G., KEHL, C., TUTENEL, T., KOL, T., DE HAAN, G., STELLING, G., AND EISEMANN, E. An interactive simulation and visualization tool for flood analysis usable for practitioners. Mitigation and Adaptation Strategies for Global Change (2015), 1–18. 8.4.4

[174] LESSER, G., ROELVINK, J., VAN KESTER, J., AND STELLING, G. Development and validation of a three-dimensional morphological model. Coastal engineering 51, 8 (2004), 883–915. 1.2.1

[175] LEVOY, M. Experimental platforms for computational photography. IEEE Computer Graphics and Applications 30, 5 (Sept 2010), 81–87, doi: 10.1109/MCG.2010.85. 1.2.3

[176] LÉVY, B. Constrained texture mapping for polygonal meshes. In Proceedings of the 28th Annual Conference on Computer Graphics and Interactive Techniques (New York, NY, USA, 2001), SIGGRAPH '01, ACM, pp. 417–424. 2.4, 2

[177] LÉVY, B., PETITJEAN, S., RAY, N., AND MAILLOT, J. Least squares conformal maps for automatic texture atlas generation. In ACM Transactions on Graphics (TOG) (2002), vol. 21, ACM, pp. 362–371. 2

[178] LEWIS, J.-P. Texture synthesis for digital painting. SIGGRAPH Comput. Graph. 18, 3 (Jan. 1984), 245–252, doi: 10.1145/964965.808605. 1.4.1

[179] LIDAL, E., PATEL, D., BENDIKSEN, M., LANGELAND, T., AND VIOLA, I. Rapid sketch-based 3d modeling of geology. In Workshop on Visualisation in Environmental Science (2013), pp. 1–5. 8.4.1

[180] LIDAL, E. M., HAUSER, H., AND VIOLA, I. Geological storytelling: graphically exploring and communicating geological sketches. In Proceedings of the International Symposium on Sketch-Based Interfaces and Modeling (2012), Eurographics Association, pp. 11–20. 1.4.2

[181] LIDAL, E. M., NATALI, M., PATEL, D., HAUSER, H., AND VIOLA, I. Geological storytelling. Computers & graphics 37, 5 (2013), 445–459. 1.4.2

[182] LIEPA, P. Filling holes in meshes. In Proceedings of the 2003 Eurographics/ACM SIGGRAPH symposium on Geometry processing (2003), Eurographics Association, pp. 200–205. 2.5

[183] LINDER, W. Digital Photogrammetry: A Practical Course. Springer Berlin Heidelberg, 2009. 1.3.5

[184] LOCHBÜHLER, T., PIROT, G., STRAUBHAAR, J., AND LINDE, N. Conditioning of multiple-point statistics facies simulations to tomographic images. Mathematical Geosciences 46, 5 (2014), 625–645. 1.2.1, 2.6

[185] LOPEZ, S., COJAN, I., RIVOIRARD, J., AND GALLI, A. Process-based stochastic modelling: meandering channelized reservoirs. Analogue Numer Model Sediment Syst: From Understand Predict (Special Publ. 40 of the IAS) 40 (2009). 1.2.1

[186] LUEBKE, D. P. Level of Detail for 3D Graphics. Morgan Kaufmann, 2003. 8.3.2

[187] MAERTEN, L., POLLARD, D. D., AND MAERTEN, F. Digital mapping of three-dimensional structures of the chimney rock fault system, central utah. Journal of Structural Geology 23, 4 (2001), 585 – 592, doi: http://dx.doi.org/10.1016/S0191-8141(00)00142-5. 8.2.2

[188] MALLET, J. GOCAD: a computer aided design program for geological applications. In Three-dimensional modeling with geoscientific information systems. Springer, 1992, pp. 123–141. 2.1

[189] MALLET, J. Geomodeling. Applied Geostatistics. Oxford University Press, 2002. 1.1, 1.2.1

[190] MALLET, J.-L. Discrete smooth interpolation. ACM Trans. Graph. 8, 2 (1989), 121–144, doi: 10.1145/62054.62057. 2.1

[191] MALLET, J.-L. Discrete smooth interpolation in geometric modelling. Computer-Aided Design 24, 4 (1992), 178 – 191, doi: http://dx.doi.org/10.1016/0010-4485(92)90054-E. 2.1

[192] MALOMO, L., CIGNONI, P., AND SCOPIGNO, R. Generalized trackball for surfing over surfaces. In STAG: Smart Tools and Apps for Graphics (2016), Eurographics. 1.4.1, 8.5.1

[193] MARSCHNER, S., AND SHIRLEY, P. Fundamentals of Computer Graphics, Fourth Edition. CRC Press, 2015. 1.3.5

[194] MARSHALL, R., WILSON, R., AND CARLSON, W. Procedure models for generating three-dimensional terrain. In ACM SIGGRAPH Computer Graphics (1980), vol. 14, ACM, pp. 154–162. 2.1

[195] MARTINEZ, P., HARBAUGH, J., AND MERRIAM, D. Simulating Nearshore Environments. Computer Methods in the Geosciences. Elsevier Science, 1993. 1.2.1

[196] MARTINEZ, P. A. Wave: Program for simulating onshore-offshore transport in two dimensions using the macintosh computer. Computers & Geosciences 13, 5 (1987), 513 – 540, doi: http://dx.doi.org/10.1016/0098-3004(87)90053-7. 1.2.1

[197] MATHERON, G., BEUCHER, H., DE FOUQUET, C., GALLI, A., GUERILLOT, D., RAVENNE, C., ET AL. Conditional simulation of the geometry of fluvio-deltaic reservoirs. In SPE Annual Technical Conference and Exhibition (1987), Society of Petroleum Engineers. 1.2.1

[198] MCCAFFREY, K., HODGETTS, D., HOWELL, J., HUNT, D., IMBER, J., JONES, R., TOMASSO, M., THURMOND, J., AND VISEUR, S. Virtual fieldtrips for petroleum geoscientists. In Geological Society, London, Petroleum Geology Conference series (2010), vol. 7, Geological Society of London, pp. 19–26. 1.4.2

[199] MCCAFFREY, K., JONES, R., HOLDSWORTH, R., WILSON, R., CLEGG, P., IMBER, J., HOLLIMAN, N., AND TRINKS, I. Unlocking the spatial dimension: digital technologies and the future of geoscience fieldwork. Journal of the Geological Society 162, 6 (2005), 927–938. 1.2.2, 1.2.3, 1.4.2, 3.1, 3.2

[200] MCGLONE, J., MIKHAIL, E., BETHEL, J., FOR PHOTOGRAMMETRY, A. S., SENSING, R., AND MULLEN, R. Manual of Photogrammetry. American Society for Photogrammetry and Remote Sensing, 2004. 1.3.5

[201] MEYER, M., KIRBY, R., AND WHITAKER, R. Topology, accuracy, and quality of isosurface meshes using dynamic particles. Visualization and Computer Graphics, IEEE Transactions on 13, 6 (nov.-dec. 2007), 1704 –1711, doi: 10.1109/TVCG.2007.70604. 2.1, 2.3, 2.6

[202] MEYER, M., WHITAKER, R., KIRBY, R. M., LEDERGERBER, C., AND PFISTER, H. Particle-based sampling and meshing of surfaces in multimaterial volumes. IEEE Transactions on Visualization and Computer Graphics 14, 6 (2008), 1539–1546, doi: 10.1109/TVCG.2008.154. 2.5

[203] MIALL, A. The Geology of Fluvial Deposits. Springer Verlag, New York, 1996. 1.2.1, 1.2.2

[204] MIALL, A. D. Architectural-element analysis: a new method of facies analysis applied to fluvial deposits. Earth Science Reviews 22 (1985), 26–308. 1.3.1

[205] MICHAEL, H., LI, H., BOUCHER, A., SUN, T., CAERS, J., AND GORELICK, S. Combining geologic-process models and geostatistics for conditional simulation of 3-d subsurface heterogeneity. Water Resources Research 46, 5 (2010). 1.2.1

[206] MIDDLETON, G., FAIRBRIDGE, R., AND BOURGEOIS, J. Facies. Encyclopedia of sedimentology (1978), 323–325. 1.3.1

[207] MILLS, J. P., BUCKLEY, S. J., MITCHELL, H. L., CLARKE, P. J., AND EDWARDS, S. J. A geomatics data integration technique for coastal change monitoring. Earth Surface Processes and Landforms 30, 6 (2005), 651–664, doi: 10.1002/esp.1165. paper on Simon's PhD thesis. 8.4.4

[208] MINISINI, D., WANG, M., BERGMAN, S. C., AND AIKEN, C. Geological data extraction from lidar 3-d photorealistic models: A case study in an organic-rich mudstone, eagle ford formation, texas. Geosphere 10, 3 (2014), 610–626. 2.1

[209] MJØS, R., AND PRESTHOLM, E. The geometry and organization of fluviodeltaic channel sandstones in the jurassic saltwick formation, yorkshire, england. Sedimentology 40, 5 (1993), 919–935. 1.6

[210] MORRIS, T. Computer Vision and Image Processing. Cornerstones of computing. Palgrave Macmillan, 2004. 1.3.5

[211] MUNSHI, A., GINSBURG, D., AND SHREINER, D. OpenGL ES 2.0 programming guide. Pearson Education, 2008. 1.4.1

[212] MUNZNER, T. A nested model for visualization design and validation. IEEE transactions on visualization and computer graphics 15, 6 (2009). 8.5.4

[213] MUNZNER, T. Visualization Analysis and Design. AK Peters Visualization Series. CRC Press, 2014. 1.3.3, 1.3.5, 8.5.3

[214] NATALI, M., LIDAL, E. M., PARULEK, J., VIOLA, I., AND PATEL, D. Modeling terrains and subsurface geology. In Proceedings of EuroGraphics (2013), pp. 155–173. 1.3.3

[215] NGUYEN, H. GPU Gems 3, first ed. Addison-Wesley Professional, 2007. 1.3.5, 2.1

[216] NICK, H. M., AND MATTHÄI, S. K. Comparison of three fe-fv numerical schemes for single- and two-phase flow simulation of fractured porous media. Transport in Porous Media 90, 2 (2011), 421–444, doi: 10.1007/s11242-011-9793-y. 2.1, 8.5.2

[217] NOAD, J. The (forgotten?) art of geological field sketches. In AAPG Annual Convention and Exhibition (2016). 8.5.3, 8.14(b)

[218] NOVAKOVA, L., AND PAVLIS, T. L. Assessment of the precision of smart phones and tablets for measurement of planar orientations: A case study. Journal of Structural Geology 97 (2017), 93 – 103, doi: https://doi.org/10.1016/j.jsg.2017.02.015. 8.2.2

[219] NUERNBERGER, B., LIEN, K.-C., GRINTA, L., SWEENEY, C., TURK, M., AND HÖLLERER, T. Multi-view gesture annotations in image-based 3d reconstructed scenes. In Proceedings of the 22nd ACM Conference on Virtual Reality Software and Technology (2016), ACM, pp. 129–138. 1.4.2, 2

[220] NYBERG, B., BUCKLEY, S. J., HOWELL, J. A., AND NANSON, R. A. Geometric attribute and shape characterization of modern depositional elements: A quantitative {GIS} method for empirical analysis. Computers & Geosciences 82 (2015), 191 – 204, doi: http://dx.doi.org/10.1016/j.cageo.2015.06.003. 8.5.5

[221] NYBERG, B. B. Global Characterization of Modern Depositional Environments for Reservoir Analogues. Phd thesis, University of Bergen, 2015. 161 p. 1.2.3, 8.5.5

[222] OGATA, K., SENGER, K., BRAATHEN, A., TVERANGER, J., AND OLAUSSEN, S. The importance of natural fractures in a tight reservoir for potential co2 storage: a case study of the upper triassic–middle jurassic kapp toscana group (spitsbergen, arctic norway). Geological Society, London, Special Publications 374, 1 (2014), 395–415. 1.1, 8.4.4

[223] OGG, J. G., AGTERBERG, F., AND GRADSTEIN, F. A geologic time scale 2004. In Abstracts with Programs-Geological Society of America (2004), vol. 36, p. 74. 8.5.3

[224] OLARIU, M., AIKEN, C., BHATTACHARYA, J., AND XU, X. Interpretation of channelized architecture using three-dimensional photo real models, pennsylvanian deep-water deposits at big rock quarry, arkansas. Marine and Petroleum Geology 28, 6 (2011), 1157–1170. 1.4.3, 2.1, 3.2, 3.3, 3.3, 3.1, 3.2, 3.4

[225] O'ROURKE, J. Computational geometry in C. Cambridge university press, 1998. 1.3.5, 2.2, 1

[226] ORTNER, T., SORGER, J., PIRINGER, H., HESINA, G., AND GRÖLLER, E. Visual analytics and rendering for tunnel crack analysis. The Visual Computer 32, 6 (2016), 859–869, doi: 10.1007/s00371-016-1257-5. 8.5.4

[227] PARISI, T. Learning Virtual Reality: Developing Immersive Experiences and Applications for Desktop, Web, and Mobile. O'Reilly Media, 2015. 8.5.4

[228] PARKER, J. Algorithms for Image Processing and Computer Vision. EBL-Schweitzer. Wiley, 2010. 1.3.5

[229] PELLERIN, J., LÉVY, B., AND CAUMON, G. A voronoi-based hybrid meshing method. In International Meshing Roundtable (Research Note) (2012). 2.1, 8.5.2

[230] PERRIN, M., ZHU, B., RAINAUD, J.-F., AND SCHNEIDER, S. Knowledge-driven applications for geological modeling. Journal of Petroleum Science and Engineering 47, 1–2 (2005), 89 – 104, doi: http://dx.doi.org/10.1016/j.petrol.2004.11.010. Intelligent Computing in Petroleum Engineering. 1.2.1

[231] PETERSEN, K., NIELSEN, M., DIAO, P., KARSSEMEIJER, N., AND LILLHOLM, M. Breast Tissue Segmentation and Mammographic Risk Scoring Using Deep Learning. Springer International Publishing, Cham, 2014, pp. 88–94. 8.5.5

[232] PICKEL, A., FRECHETTE, J., COMUNIAN, A., AND WEISSMANN, G. Building a training image with digital outcrop models. Journal of Hydrology 531, Part 1 (2015), 53 – 61. Groundwater flow and transport in aquifers: Insights from modeling and characterization at the field scale. 1.2.1

[233] PIETRONI, N., TARINI, M., AND CIGNONI, P. Almost isometric mesh parameterization through abstract domains. IEEE Transactions on Visualization and Computer Graphics 16, 4 (2010), 621–635. 2, 5

[234] PINTORE, G., GANOVELLI, F., GOBBETTI, E., AND SCOPIGNO, R. Mobile mapping and visualization of indoor structures to simplify scene understanding and location awareness. In Proc. Fourth International Workshop on Assistive Computer Vision and Robotics (ACVR) (October 2016). To appear. 1.4.1, 8.5.1

[235] PINTUS, R., GOBBETTI, E., CALLIERI, M., AND DELLEPIANE, M. Techniques for Seamless Color Registration and Mapping on Dense 3D Models. Springer International Publishing, Cham, 2017, pp. 355–376. 1.4.2

[236] PONCHIO, F., AND DELLEPIANE, M. Multiresolution and fast decompression for optimal web-based rendering. Graphical Models 88 (2016), 1 – 11, doi: http://dx.doi.org/10.1016/j.gmod.2016.09.002. 1.4.1

[237] PRINGLE, J., HOWELL, J., HODGETTS, D., WESTERMAN, A., AND HODGSON, D. Virtual outcrop models of petroleum reservoir analogues: a review of the current state-of-the-art. First break 24, 3 (2006). Mam tor and Alport Castles. 1.6

[238] PRINGLE, J., WESTERMAN, A., CLARK, J., DRINKWATER, N., AND GARDINER, A. 3d high-resolution digital models of outcrop analogue study sites to constrain reservoir model uncertainty: an example from alport castles, derbyshire, uk. Petroleum Geoscience 10, 4 (2004), 343–352. 3.1, 3.2

[239] PRINGLE, J., WESTERMAN, R., GARDINER, A., ET AL. Virtual geological outcrops-fieldwork and analysis made less exhaustive? Geology Today 20, 2 (2004), 64–69. 1.2.3

[240] QU, D., RØE, P., AND TVERANGER, J. A method for generating volumetric fault zone grids for pillar gridded reservoir models. Computers & Geosciences 81 (2015), 28 – 37, doi: http://dx.doi.org/10.1016/j.cageo.2015.04.009. 1.3.1, 8.4.3

[241] QU, D., AND TVERANGER, J. Incorporation of deformation band fault damage zones in reservoir models. AAPG Bulletin 100, 3 (2016), 423–443. 1.3.1, 8.4.3

[242] QUAN, L. Image-Based Modeling. Springer US, 2010. 1.3.5

[243] RANZUGLIA, G., CALLIERI, M., DELLEPIANE, M., CIGNONI, P., AND SCOPIGNO, R. Meshlab as a complete tool for the integration of photos and color with high resolution 3d geometry data. In CAA 2012 Conference Proceedings (2013), Pallas Publications - Amsterdam University Press (AUP), pp. 406–416. 2.5

[244] RARITY, F., VAN LANEN, X., HODGETTS, D., GAWTHORPE, R., WILSON, P., FABUEL-PEREZ, I., AND REDFERN, J. Lidar-based digital outcrops for sedimentological analysis: workflows and techniques. Geological Society, London, Special Publications 387, 1 (2014), 153–183. 1.2.2, 1.2.3, 2.1, 2.2, 3.2, 3.1(a), 3.1, 3.2

[245] REY, J., GALEOTTI, S., ET AL. Stratigraphy: terminology and practice. Editions Technip, 2008. 1.3.1

[246] RICHET, R., BORGOMANO, J., ADAMS, E. W., MASSE, J.-P., AND VISEUR, S. Numerical outcrop geology applied to stratigraphical modeling of ancient carbonate platforms: the lower cretaceous vercors carbonate platform (se france). Outcrops revitalized, Tools, Techniques and Applications. OJ Martinsen, A. Pulham, P. Haughton and M. Sullivan (Eds)., SEPM Spec. Publ 10 (2011), 195–210. 1.2.2, 1.2.3, 1.4.3, 2.1, 3.2, 3.1(b), 3.1, 3.2

[247] RINGROSE, P., AND BENTLEY, M. Reservoir Model Design: A Practitioner's Guide. Springer Netherlands, 2014. 1.1, 1.2, 1.2.1, 1.2.1

[248] RINGROSE, P. S., ROBERTS, D. M., GIBSON-POOLE, C. M., BOND, C., WIGHTMAN, R., TAYLOR, M., RAIKES, S., IDING, M., AND ØSTMO, S. Characterisation of the Krechba CO2 storage site: Critical elements controlling injection performance. Energy Procedia 4 (2011), 4672–4679. 1.1

[249] RIPOLLES, O., CHOVER, M., GUMBAU, J., RAMOS, F., AND PUIG-CENTELLES, A. Rendering continuous level-of-detail meshes by masking strips. Graphical Models 71, 5 (2009), 184–195. 8.3.2

[250] RITTERSBACHER, A. Fluvial facies and virtual outcrop geology. Phd thesis, University of Bergen, 2013. 185 p. 1.2.3

[251] RITTERSBACHER, A., BUCKLEY, S. J., HOWELL, J. A., HAMPSON, G. J., AND VALLET, J. Helicopter-based laser scanning: a method for quantitative analysis of large-scale sedimentary architecture. Geological Society, London, Special Publications 387 (2013), SP387–3. 1.4.3

[252] RITTERSBACHER, A., HOWELL, J. A., AND BUCKLEY, S. J. Analysis of fluvial architecture in the blackhawk formation, wasatch plateau, utah, u.s.a., using large 3d photorealistic models. Journal of Sedimentary Research 84, 2 (2014), 72–87. 1.2.2, 2.1, 3.2, 3.2(b), 3.1, 3.2, 8.1

[253] RODRÍGUEZ, M. B., AGUS, M., MARTON, F., AND GOBBETTI, E. HuMoRS: Huge Models Mobile Rendering System. In Proceedings of the Nineteenth International ACM Conference on 3D Web Technologies (New York, NY, USA, 2014), Web3D '14, ACM, pp. 7–15. 1.4.1

[254] RODRÍGUEZ, M. B., GOBBETTI, E., MARTON, F., AND TINTI, A. Coarse-grained multiresolution structures for mobile exploration of gigantic surface models. In Proc. SIGGRAPH Asia Symposium on Mobile Graphics and Interactive Applications (November 2013). To appear. 8.3.2

[255] ROYER, J. J., MEJIA, P., CAUMON, G., AND COLLON, P. 3D and 4D Geomodelling Applied to Mineral Resources Exploration – An Introduction. Springer International Publishing, 2015, pp. 73–89. 2, 2.1

[256] RUIU, J., CAUMON, G., AND VISEUR, S. Semiautomatic interpretation of 3d sedimentological structures on geologic images: An object-based approach. Interpretation 3, 3 (2015), SX63–SX74. 8.5.5

[257] RUSINKIEWICZ, S., AND LEVOY, M. Qsplat: a multiresolution point rendering system for large meshes. In Proceedings of the 27th annual conference on Computer graphics and interactive techniques (New York, NY, USA, 2000), SIGGRAPH '00, ACM Press/Addison-Wesley Publishing Co., pp. 343–352. 1.3.2

[258] SAINI-EIDUKAT, B., SCHWERT, D. P., AND SLATOR, B. M. Geology explorer: virtual geologic mapping and interpretation. Computers & Geosciences 28, 10 (2002), 1167 – 1176, doi: http://dx.doi.org/10.1016/S0098-3004(02)00036-5. Shareware and freeware in the Geosciences II. A special issue in honour of John Butler. 2.1

[259] SAMSONOV, T. Morphometric mapping of topography by flowline hachures. The Cartographic Journal 51, 1 (2014), 63–74. 8.5.3, 8.16(c)

[260] SCHUELLER, S., BRAATHEN, A., FOSSEN, H., AND TVERANGER, J. Spatial distribution of deformation bands in damage zones of extensional faults in porous sandstones: Statistical analysis of field data. Journal of Structural Geology 52 (2013), 148–162. 8.4.3

[261] SEMMO, A., DÖLLNER, J., AND SCHLEGEL, F. Becasso: Image stylization by interactive oil paint filtering on mobile devices. In ACM SIGGRAPH 2016 Appy Hour (New York, NY, USA, 2016), SIGGRAPH '16, ACM, pp. 6:1–6:1. 1.4.1

[262] SEMMO, A., HILDEBRANDT, D., TRAPP, M., AND DÖLLNER, J. Concepts for cartography-oriented visualization of virtual 3d city models. Photogrammetrie - Fernerkundung - Geoinformation (PFG), 4 (2012), 455–465, doi: 10.1127/1432-8364/2012/0131. 8.5.3, 8.16(b)

[263] SEMMO, A., KYPRIANIDIS, J. E., TRAPP, M., AND DÖLLNER, J. Real-time rendering of water surfaces with cartography-oriented design. In Proceedings of the Symposium on Computational Aesthetics (2013), ACM, pp. 5–14. 8.5.3, 8.16(a)

[264] SEMMO, A., TRAPP, M., JOBST, M., AND DÖLLNER, J. Cartography-oriented design of 3d geospatial information visualization – overview and techniques. The Cartographic Journal 52, 2 (2015), 95–106, doi: 10.1080/00087041.2015.1119462. 8.5.3

[265] SENGER, K., ROY, S., BRAATHEN, A., BUCKLEY, S. J., BÆLUM, K., GERNIGON, L., MJELDE, R., NOORMETS, R., OGATA, K., OLAUSSEN, S., ET AL. Geometries of doleritic intrusions in central spitsbergen, svalbard: an integrated study of an onshore-offshore magmatic province with implications for co2 sequestration. Geological controls on fluid flow and seepage in western Svalbard fjords, Norway. An integrated marine acoustic study (2013). 1.4.3, 3.1, 8.4.4

[266] SHARF, A., LEWINER, T., SHAMIR, A., KOBBELT, L., AND COHEN–OR, D. Competing fronts for coarse–to–fine surface reconstruction. Computer Graphics Forum 25, 3 (2006), 389–398, doi: 10.1111/j.1467-8659.2006.00958.x. 2.6

[267] SHEWCHUK, J. R. Triangle: Engineering a 2D Quality Mesh Generator and Delaunay Triangulator. In Applied Computational Geometry: Towards Geometric Engineering, M. C. Lin and D. Manocha, Eds., vol. 1148 of Lecture Notes in Computer Science. Springer-Verlag, May 1996, pp. 203–222. From the First ACM Workshop on Applied Computational Geometry. 1

[268] SHEWCHUK, J. R. What is a good linear element? - interpolation, conditioning, and quality measures. In In 11th International Meshing Roundtable (2002), pp. 115–126. 2.1

[269] SHEWCHUK, J. R. General-dimensional constrained delaunay and constrained regular triangulations, i: Combinatorial properties. Discrete & Computational Geometry 39, 1-3 (2008), 580–637. 2.6, 1

[270] SHEWCHUK, J. R., AND SI, H. Higher-quality tetrahedral mesh generation for domains with small angles by constrained delaunay refinement. In Proceedings of the Thirtieth Annual Symposium on Computational Geometry (New York, NY, USA, 2014), SOCG'14, ACM, pp. 290:290–290:299. 2.5

[271] SIMA, A., BUCKLEY, S. J., KURZ, T. H., AND SCHNEIDER, D. Semi-automatic integration of panoramic hyperspectral imagery with photorealistic lidar models. Photogrammetrie-Fernerkundung-Geoinformation 2012, 4 (2012), 443–454. 8.3.1

[272] SIMA, A., BUCKLEY, S. J., SCHNEIDER, D., AND HOWELL, J. A. An improved workflow for image-and laser-based virtual geological outcrop modelling. IAPRS XXXVIII (2013), 115–120. 1.2.3

[273] SIMA, A. A. An Improved Workflow for Image- and Laser-based Virtual Geological Outcrop Modellin Phd thesis, University of Bergen, 2013. 180p. 1.2.3

[274] SIMA, A. A., BONAVENTURA, X., FEIXAS, M., SBERT, M., HOWELL, J. A., VIOLA, I., AND BUCKLEY, S. J. Computer-aided image geometry analysis and subset selection for optimizing texture quality in photorealistic models. Computers & Geosciences 52, 0 (2013), 281 – 291, doi: http://dx.doi.org/10.1016/j.cageo.2012.11.004. 1.2.3

[275] SIMA, A. A., BUCKLEY, S. J., KURZ, T. H., AND SCHNEIDER, D. Semi-automated registration of close-range hyperspectral scans using oriented digital camera imagery and a 3d model. The Photogrammetric Record 29, 145 (2014), 10–29, doi: 10.1111/phor.12049. 2.1

[276] SIMA, A. A., BUCKLEY, S. J., AND VIOLA, I. An interactive tool for analysis and optimization of texture parameters in photorealistic virtual 3d models. ISPRS Annals of Photogrammetry, Remote Sensing and Spatial Information Sciences I-2 (2012), 165–170, doi: 10.5194/isprsannals-I-2-165-2012. 1.2.3

[277] SNAVELY, N., SEITZ, S. M., AND SZELISKI, R. Photo tourism: exploring photo collections in 3d. ACM transactions on graphics (TOG) 25, 3 (2006), 835–846. 1.2.3, 2.1

[278] SOLTAN, R., MOUNTNEY, N., MCCAFFREY, W., AND PATON, D. Reconstruction of channel and barform architecture in a pennsylvanian fluvio-deltaic succession: Brimham grit, northern england. AAPG Search and Discovery 50884 (October 2013), 1 – 4. (c) 2013, AAPG. Reproduced with permission from the publisher. 1.6

[279] SOLTAN, R., AND MOUNTNEY, N. P. Interpreting complex fluvial channel and barform architecture: Carboniferous central pennine province, northern england. Sedimentology 63, 1 (2016), 207–252, doi: 10.1111/sed.12224. 1.6

[280] SOUTHERN, S. J., MOUNTNEY, N. P., AND PRINGLE, J. K. The carboniferous southern pennine basin, uk. Geology Today 30, 2 (2014), 71–78, doi: 10.1111/gto.12044. Alport Castles and Mam Tor. 1.6

[281] SPENCE, R. Information Visualization: An Introduction. Springer International Publishing, 2014. 1.3.5

[282] STOYAN, D., KENDALL, W. S., AND MECKE, J. Stochastic Geometry and its Applications. Wiley, 1987, p. 283pp. 1.2.1

[283] STRÉBELLE, S. Sequential simulation drawing structures from training images. PhD thesis, Stanford University, California, 2000. 1.2.1

[284] STREBELLE, S. Conditional simulation of complex geological structures using multiple-point statistics. Mathematical Geology 34, 1 (2002), 1–21. 1.2.1

[285] STREBELLE, S. Integration of sequence stratigraphy concepts into multiple-point geostatistical models. In Proceedings of IAMG (2003), Citeseer, pp. 7–12. 1.2.1

[286] STREBELLE, S. Multiple-point geostatistics: from theory to practice. In Expanded Abstract Collection from Ninth International Geostatistics Congress (Oslo, Norway, 2012), Chevron, Norwegian Computing Center, p. 65. 1.2.1

[287] STREBELLE, S. B., AND JOURNEL, A. G. Reservoir modeling using multiple-point statistics. In SPE Annual Technical Conference and Exhibition (2001), Society of Petroleum Engineers. 1.2.1

[288] STRUGAR, F. Continuous distance-dependent level of detail for rendering heightmaps. Journal of Graphics, GPU, and Game Tools 14, 4 (2009), 57–74, doi: 10.1080/2151237X.2009.10129287. 8.3.2

[289] SWEENEY, C., FLYNN, J., NUERNBERGER, B., TURK, M., AND HOLLERER, T. Efficient computation of absolute pose for gravity-aware augmented reality. In Mixed and Augmented Reality (ISMAR), 2015 IEEE International Symposium on (Sept 2015), pp. 19–24. 1.4.2, 2

[290] TANSKANEN, P., KOLEV, K., MEIER, L., CAMPOSECO, F., SAURER, O., AND POLLEFEYS, M. Live metric 3d reconstruction on mobile phones. In Computer Vision (ICCV), 2013 IEEE International Conference on (2013), IEEE, pp. 65–72. 1.4.2

[291] TJELMELAND, H., AND HOLDEN, L. Semi-markov random fields. In Geostatistics Troia'92. Springer, 1993, pp. 479–491. 1.2.1

[292] TRAXLER, C., HESINA, G., BARNES, R., GUPTA, S., AND PAAR, G. The PRoViDE framework for the quantitative geologic analysis of reconstructed Martian terrain and outcrops. In EGU General Assembly Conference Abstracts (2016), vol. 18 of EGU General Assembly Conference Abstracts, p. 7196. 8.5.4

[293] TRINKS, I., CLEGG, P., MCCAFFREY, K., JONES, R., HOBBS, R., HOLDSWORTH, B., HOLLIMAN, N., IMBER, J., WAGGOTT, S., AND WILSON, R. Mapping and analysing virtual outcrops. Visual Geosciences 10, 1 (2005), 13–19. 2.1, 3.1, 3.2

[294] TVERANGER, J., AAANONSEN, S., BRAATHEN, A., ESPEDAL, M., FOSSEN, H., HESTHAMMER, J., HOWELL, J., PETTERSEN, Ø., SKORSTAD, A., AND SKAR, T. The fault facies project–3d modelling of faults and tectonic impact in petroleum reservoirs. In Abstracts and Proceeding of the Geological Society of Norway (2005), vol. 1, pp. 121–122. 1.3.1

[295] TVERANGER, J., BRAATHEN, A., SKAR, T., AND SKAUGE, A. Centre for integrated petroleum research – research activities with emphasis on fluid flow in fault zones. Norwegian Journal of Geology 85, 1-2 (2005), 63–71. 8.4.3, 8.4.3

[296] VALLET, J., AND SKALOUD, J. Development and experiences with a fully-digital handheld mapping system operated from a helicopter. The International Archives of the Photogrammetry, Remote Sensing and Spatial Information Sciences, Istanbul 35, Part B (2004). 1.2.3

[297] VAN DAMME, T. Computer vision photogrammetry for underwater archaeological site recording in a low-visibility environment. ISPRS-International Archives of the Photogrammetry, Remote Sensing and Spatial Information Sciences 1 (2015), 231–238. 1.4.2

[298] VARADHAN, G., AND MANOCHA, D. Out-of-core rendering of massive geometric environments. In Visualization, 2002. VIS 2002. IEEE (Nov 2002), pp. 69–76. 8.3.2

[299] VERWER, K., ADAMS, D., AND KENTER, J. Digital outcrop models: technology and applications. First break 25, 8 (2007), 57–63. 2.1

[300] VERWER, K., KENTER, J. A., MAATHUIS, B., AND DELLA PORTA, G. Stratal patterns and lithofacies of an intact seismic-scale carboniferous carbonate platform (asturias, northwestern spain): a virtual outcrop model. Geological Society, London, Special Publications 239, 1 (2004), 29–41. 2.1

[301] VISEUR, S., RICHET, R., BORGOMANO, J., AND ADAMS, E. Semi-automated detections of geological features from dom–the gresse-en-vercors cliff. In 69th EAGE Conference and Exhibition incorporating SPE EUROPEC 2007 (2007). 2.1

[302] VISEUR, S., ROUDAUT, R., BERTOZZI, R., CASTELLI, M., AND MARI, J.-L. 3d interactive geological interpretations on digital outcrops using a touch pad. In Vertical Geology Conference (VGC) (2014). 1.4.2, 1.15, 1, 8.5.1

[303] VIVONI, E. R., AND CAMILLI, R. Real-time streaming of environmental field data. Computers & Geosciences 29, 4 (2003), 457 – 468, doi: http://dx.doi.org/10.1016/S0098-3004(03)00022-0. 1.4.2

[304] WALKER, J. D., BLACK, R. A., LINN, J. K., THOMAS, A., WISEMAN, R., AND D'ATTILIO, M. Development of geographic information systems-oriented databases for integrated geological and geophysical applications. GSA TODAY 6, 3 (1996), 1–6. 1.2.2

[305] WALTHAM, A., AND DIXON, N. Movement of the mam tor landslide, derbyshire, uk. Quarterly Journal of Engineering Geology and Hydrogeology 33, 2 (2000), 105–123. Mam Tor. 1.6

[306] WANG, R., AND QIAN, X. OpenSceneGraph 3 Cookbook. Community experience distilled. Packt Pub./Open Source, 2012. 8.2.3

[307] WATERS, C., AND DAVIES, S. Carboniferous: Extensional Basins, Advancing Deltas and Coal Swamp Geological Society of London, 2006. 1.6

[308] WATT, A. 3D Computer Graphics, 3rd ed., vol. 1 of 3D Computer Graphics. Addison-Wesley, 2000. 1.3.3, 1.3.5, 3.2

[309] WEI, L.-Y., AND LEVOY, M. Fast texture synthesis using tree-structured vector quantization. In Proceedings of the 27th Annual Conference on Computer Graphics and Interactive Techniques (New York, NY, USA, 2000), SIGGRAPH '00, ACM Press/Addison-Wesley Publishing Co., pp. 479–488. 1.4.1

[310] WENG, Y.-H., SUN, F.-S., AND GRIGSBY, J. D. Geotools: An android phone application in geology. Computers & Geosciences 44, 0 (2012), 24 – 30, doi: http://dx.doi.org/10.1016/j.cageo.2012.02.027. 1.4.2

[311] WEYAND, T., KOSTRIKOV, I., AND PHILBIN, J. Planet-photo geolocation with convolutional neural networks. In European Conference on Computer Vision (2016), Springer, pp. 37–55. 8.5.5

[312] WILSON, P., HODGETTS, D., RARITY, F., GAWTHORPE, R. L., AND SHARP, I. R. Structural geology and 4D evolution of a half-graben: New digital outcrop modelling techniques applied to the Nukhul half-graben, Suez Rift, Egypt. Journal of Structural Geology 31, 3 (2009), 328–345. 1.2.2, 2.1, 2.2, 3.1, 3.2

[313] WOLNIEWICZ, P. Sedmob: A mobile application for creating sedimentary logs in the field. Computers & Geosciences 66, 0 (2014), 211 – 218. 1.4.2

[314] WU, C. Towards linear-time incremental structure from motion. In 3DTV-Conference, 2013 International Conference on (2013), IEEE, pp. 127–134. 1.2.3

[315] XU, H., AND BARBIČ, J. Signed distance fields for polygon soup meshes. In Proceedings of Graphics Interface 2014 (Toronto, Ont., Canada, Canada, 2014), GI '14, Canadian Information Processing Society, pp. 35–41. 1.3.2, 2.3, 2.3

[316] XU, X., AIKEN, C. L., AND NIELSEN, K. C. Real time and the virtual outcrop improve geological field mapping. Eos, Transactions American Geophysical Union 80, 29 (1999), 317–324. 1.2.3, 2.1

[317] YU, L., EFSTATHIOU, K., ISENBERG, P., AND ISENBERG, T. Cast: Effective and efficient user interaction for context-aware selection in 3d particle clouds. IEEE Transactions on Visualization and Computer Graphics 22, 1 (Jan 2016), 886–895, doi: 10.1109/TVCG.2015.2467202. 1.4.1, 8.5.1

[318] ZENG, K., ZHAO, M., XIONG, C., AND ZHU, S.-C. From image parsing to painterly rendering. ACM Trans. Graph. 29, 1 (Dec. 2009), 2:1–2:11, doi: 10.1145/1640443.1640445. 1.4.1

[319] ÁLVAREZ MENÉNDEZ, L., DE COS JUEZ, F., LASHERAS, F. S., AND ÁLVAREZ RIESGO, J. Artificial neural networks applied to cancer detection in a breast screening programme. Mathematical and Computer Modelling 52, 7–8 (2010), 983 – 991, doi: http://dx.doi.org/10.1016/j.mcm.2010.03.019. Mathematical Models in Medicine, Business & Engineering 2009. 8.5.5

Glossary

ACE Annual Convention and Exhibition. iii

AI artificial intelligence. 191–194

ANN artificial neural network. 191, 192

AR augmented reality. 10, 16, 20, 21, 23, 190

BGS British Geological Survey. 21

BLAS basic linear algebra subprograms. 165

BRGM Bureau de Recherches Géologiques et Minières. 21

CAD computer-aided design. 37

CAVE cave automatic virtual environment. 187

CFD computational fluid dynamics. 4

CG computer graphics. 10, 13–16, 20, 36, 50

CGAL Computational Geometry Algorithms Library. 48, 50

CGI computer-generated imagery. 10, 20, 36, 188

CNN convolutional neural network. 191, 193

CPU central processing unit. 26

CT computed tomography. 4, 50, 51

CV computer vision. 10, 17, 23

DCT discrete cosine transform. 162

DEM digital elevation model. 6, 7, 18, 21, 36, 37, 51, 164

dGPS differential GPS. 164, 189

DOM digital outcrop model. 6–8, 12, 14–16, 24–28, 30, 32, 33, 35–37, 40, 41, 48–51, 54–58, 62, 159–163, 165–168, 171, 173, 176–185, 187, 189, 190, 193, 231, 233

DRAM dynamic RAM. 162

DSI Discrete Smooth Interpolation. 37

DSLR digital single lens reflex. 8, 42, 181

DSM digital surface model. 36, 37

DTM digital terrain model. 14, 36, 37, 51

ES Embedded Systems. 20

FEA finite-element analysis. 37, 48

GIS geographic information system. 14, 18, 20, 36

GML Geography Markup Language. 161, 167, 231

GNSS global navigation satellite system. 21, 163, 164

GPS global positioning system. 163, 164, 170

GPU graphics processing unit. 26, 161, 162

GRIT Geological Registration and Interpretation Toolset. 159, 161, 163, 167–170, 174, 176

GUI graphical user interface. 160

HCI human-computer interaction. 160

KML Keyhole Markup Language. 161

LAPACK linear algebra package. 165

lidar light detection and range. 7, 13, 27, 35, 36, 39, 48, 55, 163, 174, 180

LIME Lidar Interpretation Mapping Environment. 57, 62, 160, 170, 193, 231

LoD Level-of-Detail. 167

MPS Multiple point statistics. 4–6, 27, 33, 54, 161, 165, 170, 171, 193, 233

NN neural network. 191–194

NPR non-photorealistic rendering. 177

OGC Open Geospatial Consortium. 161, 231

OSM Open Street Map. 21

PBR Point-based rendering. 19

PGS plurigaussian simulation. 4

PLC piecewise-linear complex. 40, 41, 48, 49, 62, 177

PLS piecewise-linear simplex. 40

RAM random access memory. 163

SfM structure from motion. 7, 23, 27, 35, 36, 164, 174, 181

SGD stochastic gradient descent. 192

SGS sequential gaussian simulation. 4

SIS sequential indicator simulation. 4

SLAM simultaneous localisation and mapping. 23, 25

SRAM static memory. 163

SVG Scalable Vector Graphics. 161

TGS truncated gaussian simulation. 4

THMC thermal, hydraulic, mechanical and chemical. 37, 181

TI training image. 3–6, 27, 33, 54, 161, 170, 193

TIN triangulated irregular network. 6, 14, 37, 57, 183, 184

TLS terrestrial laser scanning. 7, 8, 27

UAV unmanned aerial vehicle. 7, 174

VGI Volunteered Geographic Information. 24

VR virtual reality. 10, 16, 20, 21, 23, 164, 187–191

VRGS Virtual Reality Geological Studio. 62, 193

XML Extensible Markup Language. 161